ÉCOLE DE TECHNOLOGIE SUPÉRIEURE
UNIVERSITÉ DU QUÉBEC

THESIS PRESENTED TO
ÉCOLE DE TECHNOLOGIE SUPÉRIEURE

IN PARTIAL FULFILLMENT OF THE REQUIREMENTS FOR
A MASTER'S DEGREE IN ELECTRICAL ENGINEERING
M. Eng.

BY
Dominique RIVARD

MULTI-FEATURE APPROACH FOR WRITER-INDEPENDENT OFFLINE SIGNATURE VERIFICATION

MONTREAL, OCTOBER 20, 2010

BOARD OF EXAMINERS

THIS THESIS HAS BEEN EVALUATED

BY THE FOLLOWING BOARD OF EXAMINERS

M. Robert Sabourin, Thesis Supervisor
Département de génie de la production automatisée à l'École de technologie supérieure

M. Eric Granger, Thesis Co-supervisor
Département de génie de la production automatisée à l'École de technologie supérieure

M. Jean-Marc Robert, President of the Board of Examiners
Département de génie logiciel et des TI à l'École de technologie supérieure

M. Richard Lepage
Département de génie de la production automatisée à l'École de technologie supérieure

THIS THESIS HAS BEEN PRESENTED AND DEFENDED

BEFORE A BOARD OF EXAMINERS AND PUBLIC

OCTOBER 6, 2010

AT ÉCOLE DE TECHNOLOGIE SUPÉRIEURE

ACKNOWLEDGMENTS

I would like to extend my sincere gratitude to Dr. Robert Sabourin and Dr. Eric Granger for supervising my work over these last years.

My thanks go to all the friends at LIVIA for their help and friendship that enriched my study these years.

I would like to thank the members of my examining committee: Dr. Jean-Marc Robert and Dr. Richard Lepage. Their comments helped to improve the quality of the final version of this thesis.

Special thanks to my parents, Jacqueline and Pierre Rivard, for their love and guidance.

Most of all, thanks to my wife, Audrée Gagné, for her unfailing support that gave me peace and strength all the way through. This work is dedicated to her and to our son Luca.

This research has been financially supported by Banctec Canada and by research grants from *Fonds de recherche sur la nature et les technologies* and *École de technologie supérieure*.

FUSION AU NIVEAU DES CARACTÉRISTIQUES POUR LA VÉRIFICATION DES SIGNATURES MANUSCRITES DANS UN CONTEXTE INDÉPENDANT DU SCRIPTEUR

Dominique RIVARD

RÉSUMÉ

Les principales difficultés rencontrées en vérification des signatures manuscrites statiques sont la grande quantité d'utilisateurs, la grande quantité de caractéristiques, le nombre limité de signatures de référence disponibles pour l'apprentissage, la grande variabilité naturelle des signatures et l'absence de faux en guise de contre-exemples d'apprentissage. Cette recherche présente premièrement une revue de littérature des techniques utilisées pour la vérification des signatures manuscrites statiques, en portant une attention particulière à l'extraction de caractéristiques et aux stratégies de vérification. L'objectif est de présenter les progrès les plus importants, ainsi que les défis de ce domaine. Un intérêt particulier est porté aux techniques qui permettent de concevoir un système de vérification de signatures avec un nombre limité de données. Ensuite est présenté un nouveau système de vérification des signatures statiques basé sur plusieurs techniques d'extraction de caractéristiques, la transformation dichotomique et la sélection de caractéristiques par *boosting*. L'utilisation de plusieurs techniques d'extraction de caractéristiques augmente la diversité de l'information extraite des signatures, produisant ainsi des caractéristiques pouvant atténuer la variabilité naturelle des signatures alors que la transformation dichotomique permet une classification indépendante du scripteur, ce qui insensibilise le système de vérification par rapport à l'impact du nombre très grand de scripteurs. Finalement, la sélection de caractéristiques par *boosting* permet la construction d'un système de vérification rapide en sélectionnant les caractéristiques *lors* de son apprentissage. Ainsi, le système proposé offre un contexte pratique pour l'exploration et l'apprentissage de problèmes composés de nombre important de caractéristiques potentielles. Une étude comparative avec les résultats publiés dans la littérature confirme la viabilité du système proposé, même lorsqu'*une seule* signature de référence est disponible. Le système proposé offre une solution efficace à un grand nombre de problèmes (par exemple, en vérification biométrique) où le nombre d'exemples est limité lors de l'apprentissage, où de nouveaux exemples peuvent survenir en cours d'utilisation, où les classes sont nombreuses et où peu, sinon aucun, contre-exemple n'est disponible.

Mots-clés : vérification des signatures statiques, extraction de caractéristiques multi-échelles, sélection de caractéristiques par boosting, vérification indépendante du scripteur

MULTI-FEATURE APPROACH FOR WRITER-INDEPENDENT OFFLINE SIGNATURE VERIFICATION

Dominique RIVARD

ABSTRACT

Some of the fundamental problems facing handwritten signature verification are the large number of users, the large number of features, the limited number of reference signatures for training, the high intra-personal variability of the signatures and the unavailability of forgeries as counterexamples. This research first presents a survey of offline signature verification techniques, focusing on the feature extraction and verification strategies. The goal is to present the most important advances, as well as the current challenges in this field. Of particular interest are the techniques that allow for designing a signature verification system based on a limited amount of data. Next is presented a novel offline signature verification system based on multiple feature extraction techniques, dichotomy transformation and boosting feature selection. Using multiple feature extraction techniques increases the diversity of information extracted from the signature, thereby producing features that mitigate intra-personal variability, while dichotomy transformation ensures writer-independent classification, thus relieving the verification system from the burden of a large number of users. Finally, using boosting feature selection allows for a low cost writer-independent verification system that selects features *while* learning. As such, the proposed system provides a practical framework to explore and learn from problems with numerous potential features. Comparison of simulation results from systems found in literature confirms the viability of the proposed system, even when only *a single* reference signature is available. The proposed system provides an efficient solution to a wide range problems (eg. biometric authentication) with limited training samples, new training samples emerging during operations, numerous classes, and few or no counterexamples.

Keywords: offline signature verification, multi-scale feature extraction, boosting feature selection, writer-independent verification

TABLE OF CONTENT

Page

LIST OF TABLES

Page

LIST OF FIGURES

Page

LIST OF SYMBOLS

$\delta\,(m,n)$	Euclidian distance from the center of the filter
ω_k	Class k
$\omega_{\oplus}$	*Within* class
$\omega_{\ominus}$	*Between* class
Φ	Number of quantization ranges
$\boldsymbol{\mu}$	Mean parameter of gaussian distribution
$\boldsymbol{\Sigma}$	Variance parameter of gaussian distribution
ρ_t^{left}	Weighted mean of the response for the left leave of decision stump t
ρ_t^{right}	Weighted mean of the response for the right leave of decision stump t
τ_t	Splitting threshold of decision stump t
AER	Average Error Rate
AUC	Arear Under and ROC Curve
$\mathrm{ang}(m,n)$	Direction of the gradient vector at pixel (m,n)
$\mathbf{B}^{\text{horz}}$	Set of bits on the Extended Shadow Code horizontal bars
$\mathbf{B}^{\text{main}}$	Set of bits on the Extended Shadow Code main diagonal bar
$\mathbf{B}^{\text{seco}}$	Set of bits on the Extended Shadow Code secondary diagonal bar
$\mathbf{B}^{\text{vert}}$	Set of bits on the Extended Shadow Code vertical bars
$C_{i,j}$	Individual cell of an image segmentation grid
DPDF	Directional PDF (Probability Density Function)

D	Number of dimensions
$\mathcal{D}$	Development database of signatures
d_t	Splitting dimension of decision stump t
EER	Equal Error Rate
ESC	Extended Shadow Code
$\mathcal{E}$	Exploitation database of signatures
FAR	False Acceptation Rate
FRR	False Rejection Rate
$F(\mathbf{u})$	Confidence score of the committee for sample $\mathbf{u}$
$f_t(\mathbf{u})$	Confidence score of a decision stump for sample $\mathbf{u}$
$g(\cdot)$	Fusion function
G_m	Vertical component of a Sobel filter
G_n	Horizontal component of a Sobel filter
G_{LPF}	Gaussian lowpass filter
$\mathcal{H}$	Hold-out set
H	Number of samples in the hold-out set
$\mathcal{I}$	Set of horizontal scales
$\mathcal{J}$	Set of vertical scales
K	Number of classes (writers)
$\mathcal{L}$	Learning set

L	Number of samples in the learning set
M'	Height of a grid cell in pixels
M	Height of an image in pixels
$\mathrm{mag}(m,n)$	Magnitude of the gradient vector at pixel (m,n)
N'	Width of a cell in pixels
N	Width of an image in pixels
N_s	Number of support vectors
O	Number of bits on the Extended Shadow Code diagonals
$\mathcal{Q}$	Set of questioned signatures
Q	Number of samples in the questioned set
$\mathrm{qnt}(m,n)$	Quantization of the direction of the gradient vector at pixel (m,n)
$\mathcal{R}$	set of reference signatures
ROC	Receiver Operating Characteristics
R	Number of samples in the reference set
$S\,(m,n)$	Pixel (m,n) of a signature image
S_q	Questioned signature
S_r	Reference signature
T	Number of decision stumps in a committee
$T_{\mathcal{H}}$	Early stopping criterion
$T_{\mathcal{L}}$	Maximum iteration stopping criterion

t_{test}^{wc}	Worst case time to classify an input vector
t_{sort}^{wc}	Worst case time to perform a quick sort
t_{sort}^{ave}	Average case time to perform a quick sort
t_{stump}^{wc}	Worst case time to train a decision stump
t_{AUC}^{wc}	Worst case time to compute the AUC
t_{GAB}^{wc}	Worst case time to train a committee
t_1	Time taken for a simple operation
t_2	Time taken for a complex operation
$\mathbf{u}_i$	Distance vector of sample i
v_i	Distance label of sample i
$\mathbf{x}_i$	Feature vector of sample i
$\mathbf{x}^{\text{ESC}}$	Extended Shadow Code feature vector
x^{horz}	Horizontal feature extracted from an Extended Shadow Code cell
x^{main}	Main diagonal feature extracted from an Extended Shadow Code cell
x^{seco}	Secondary diagonal feature extracted from an Extended Shadow Code cell
x^{vert}	Vertical feature extracted from an Extended Shadow Code cell
y_i	Feature label of sample i

INTRODUCTION

Although biometrics has emerged from its extensive use in law enforcement and forensic sciences, it is increasingly being adopted in a wide variety of civilian applications to ensure security and privacy (Prabhakar et al., 2007). Biometric systems perform the recognition of individuals based on their physiological or behavioral characteristics. Physiological characteristics consist of biological traits such as face and fingerprint, while behavioral traits consider behavioral patterns like voice print and handwritten signature. Further, biometric traits are intrinsic to a person, and as such cannot be lost, stolen or forgotten as with security tokens and secret knowledge (Jain et al., 2004).

Biometric systems provide three recognition functions: identification, screening and verification. Identification seeks to establish a person's identity by matching his biometric sample against all user templates in the system database. Screening discreetly determines if the biometric sample of an individual, whose enrollment procedure is not typically well-defined, matches the system's watchlist of identities. Finally, verification authenticates the claimed identity of an individual by comparing his biometric sample to his template stored in the system database (Jain et al., 2006). Further, a biometric system should also address practical issues such as performance, acceptability and circumvention. In other words, its design has to maximize recognition accuracy and speed while minimizing the use of resources. Also, it has to rely on a biometric trait accepted by the users and it must be resistant to fraudulent methods (Jain et al., 2004).

Among the numerous biometric traits considered so far, handwritten signatures have long been established as one of the most widespread means for authenticating a person's identity by administrative and financial institutions. Furthermore, the procedure for acquisition of signature samples is familiar and non-invasive (Fairhurst, 1997).

Features extracted from handwritten signatures are broadly divided into two categories, static and dynamic, according to the basis of the acquisition method. Static features are extracted by offline acquisition device after the writing process has been completed, while dynamic features

are extracted by online acquisition device during the writing process. By extension, automatic signature verification systems are either referred to as offline or online.

Problem Statement

Some of the fundamental problems facing handwritten signature verification are the large number of users, the large number of features, the limited number of reference signatures for training, the high intra-personal variability of the signatures and the unavailability of forgeries as counterexamples.

A forgery occurs when a forger attempts to reproduce signatures to bypass the verification system. Forgeries are usually divided into three types, namely random, simple and skilled. The random forgery occurs when the forger does not know both the writer's name and the signature's morphology. It can also happen when a genuine signature presented to the system is mislabeled to another user. When the forger knows the writer's name but not the signature's morphology, the forger can only produce a simple forgery using a style of writing of his liking. The skilled forgery occurs when the forger has access to a sample to produce a reasonable imitation of the genuine signature. Clearly, when enrolling a new writer, only genuine signatures and no forgeries are provided, hence the unavailability of forgeries as counterexamples to train the verification system.

Since no single biometric trait, sensor or sampling can guarantee perfect authentication by itself, some authors advocate the use of multiple feature extraction techniques (Jain et al., 2004). Verification systems based on multiple feature extraction techniques can be used to diversify the information extracted from a given biometric trait and thus lead to improvement in recognition rate. In this respect, handwritten signature is a promising candidate since diverse feature extraction techniques have been proposed in literature (Batista et al., 2008), (Impedovo and Pirlo, 2008). In addition, extracting different feature types at multiple scales from a signature sample may uncover information that might go undetected using a single scale, thereby producing features that mitigate intra-personal variability, and thus improve accuracy.

Authors have described two approaches for offline signature verification: writer-dependent and writer-independent. The former models the signature of a specific individual from his samples, thus a specialized classifier is built for each writer. The latter uses a classifier to match the input questioned signature to one (or more) reference signatures, and therefore a single classifier is needed for all writers (Srihari et al., 2004b). Automatic signature verification systems proposed in the literature are mainly writer-dependent. However, as with most biometric applications, the performance of signature verification systems degrades due to the large number of users and limited number of reference signatures per person. For instance, in verification of bank check signatures, the number of bank customers can easily reach the tens of thousands. In most cases, sampling a sufficient number of samples from each writer is not practical and is limited to 4-6 signatures in general (Oliveira et al., 2007).

In contrast, the writer-independent approach alleviates both these problems. Input feature vectors are transformed into a distance space to construct one single classifier. Thus the number of users is of little consequence to a writer-independent approach since only a single, two-class classifier is needed to authenticate the signature of all writers. To tackle the lack of genuine signatures, the writer-independent classifier can be built from a sufficient set of signatures collected beforehand. The writers composing this learning set do not need to be the system users since the classifier is writer-independent. However, the underlying hypothesis is that their signatures are representative of those of the legitimate users of the signature verification system.

Proposed approach

This research presents a novel writer-independent offline signature verification system based on multiple feature extraction techniques, dichotomy transformation and Boosting Feature Selection. The multiscale approach implies that the representation and analysis of signature images is performed on more than one scale, and is achieved by extracting features at multiple grid scales using two well-known and complementary grid-based feature extraction techniques, namely Extended Shadow Code (Sabourin and Genest, 1994) and Directional Probability Density Functions (Drouhard et al., 1996). While the Extended Shadow Code extracts information

about the spatial distribution of the signature, Directional Probability Density Functions extracts information about the orientation of the strokes. In this research, both feature extraction techniques are shown to be complementary, and once combined into a single feature set, they provide a powerful spatio-directional representation of the signature.

Using multiple scales and features results in a large number of features per sample per writer, and therefore requires the classifier to provide a high level of performance in very high dimensional spaces. The Boosting Feature Selection algorithm is employed in this research because it is known to efficiently select a small subset of discriminant features from the very large set of potential features *while* building the classifier (Tieu and Viola, 2004). In this research, signature verification is performed in a writer-independent framework derived from a forensic document examination approach (Santos et al., 2004) and compared to the performance of state-of-the-art results on a database composed of 168 writers. Writer-independence is achieved by the verification system by using the dissimilarity between the questioned signatures and the reference signatures.

Organization of the thesis

The thesis is organized as follows. Chapter 1 presents a survey of the most important techniques used for feature extraction and verification in the field of offline signature verification. A survey of related writer-independent signature verification systems is provided in Chapter 2 before presenting the proposed framework in Chapter 3. In Chapter 4, the experimental methodology, including data and performance metrics are defined. In Chapter 5, simulation results are presented and discussed.

CHAPTER 1

STATE OF THE ART IN OFFLINE SIGNATURE VERIFICATION

The handwritten signature has always been one of the most simple and accepted way to authenticate an official document. It is easy to obtain, results from a spontaneous gesture and it is unique to each individual (Abdelghani and Amara, 2006). Automatic signature verification can, therefore, be applied in all situations where handwritten signatures are currently used, such as cashing a check, signing a credit card transaction and authenticating a document (Griess and Jain, 2002).

The goal of a signature verification system is to verify the identity of an individual based on an analysis of his or her signature through a process that discriminates a genuine signature from a forgery (Plamondon, 1994). Figure 1.1 shows an example of a generic signature verification system. The process follows the classical pattern recognition model steps, that is, data acquisition, preprocessing, feature extraction, classification (which is generally called "verification" in the signature verification field) and decision.

Depending on the data acquisition mechanism, the process of signature verification can be classified as online or offline. In the online (or dynamic) approach, specialized hardware (such as a digitizing tablet or a pressure sensitive pen) is used in order to capture the pen movements over the paper at the time of the writing. In this case, a signature can be viewed as a space-time variant curve that can be analyzed in terms of its curvilinear displacement, its angular displacement and the torsion of its trajectory (Plamondon and Lorette, 1989). On the other hand, in the offline (or static) approach, the signature is available on a sheet of paper, which is later scanned in order to obtain a digital representation composed of $M \times N$ pixels. Hence, the signature image is considered as a discrete 2D function $f(x, y)$, where $x = 0, 1, 2, \ldots, M$ and $y = 0, 1, 2, \ldots, N$ denote the spatial coordinates. The value of f in any (x, y) corresponds to the grey level (generally a value from 0 to 255) in that point (Gonzalez and Woods, 2002).

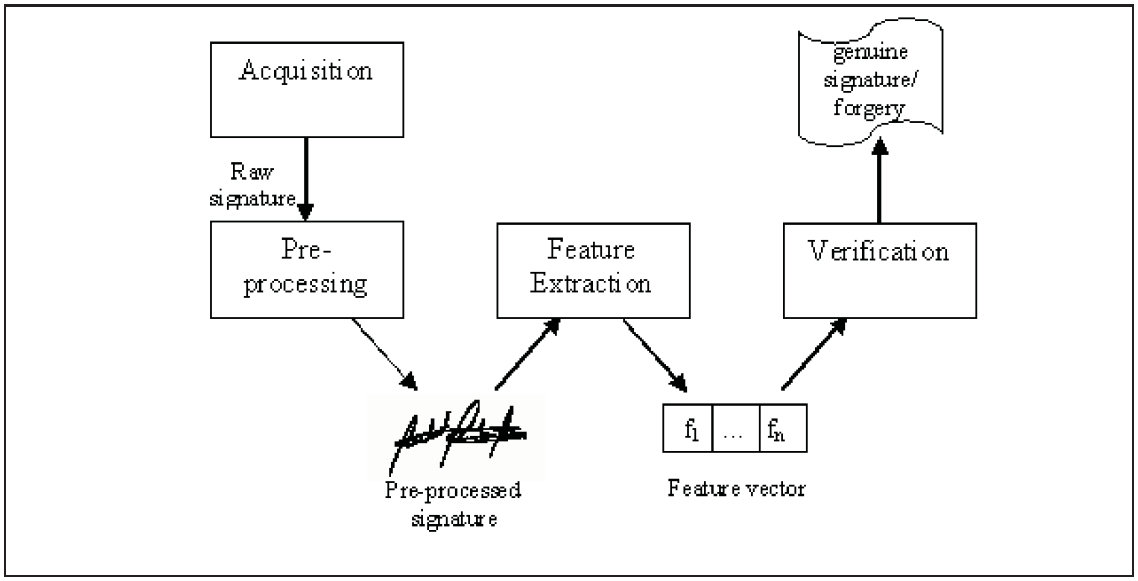

Figure 1.1 : Block diagram of a generic signature verification system.

Over the last two decades, and with the renewed interest in biometrics caused by the tragic events of 9/11, several innovative approaches for offline signature verification have been introduced in literature. Therefore, this chapter presents a survey of offline signature verification techniques, focusing on the feature extraction and verification strategies. The goal is to present the most important advances, as well as the current challenges in this field. Of particular interest are the techniques that allow for designing a signature verification system based on a limited amount of data.

In the next sections, the types of signatures and forgeries are defined. Next, a literature review of the feature extraction techniques and verification strategies proposed in this field is presented. Then some strategies used to face the problem of a limited amount of data are discussed.

1.1 Signatures and Forgeries Types

The signature verification is directly related to the alphabet (Roman, Chinese, Arabic, etc.) and the form of writing of each region (Justino, 2001). The occidental signatures can be classified

in two main styles: cursive or graphical, as shown in Figure 1.2 . With cursive signatures, the author writes his or her name in a legible way, while the graphical signatures contain complex patterns which are very difficult to interpret as a set of characters.

Figure 1.2 : Examples of (a) (b) cursive and (c) graphical signatures.

According to Coetzer *et al.* (Coetzer et al., 2004), the forged signatures can be classified in three basic types:

1) *Random forgery,* the forger has no access to the genuine signature (not even the author's name) and reproduces a random one. A random forgery may also include the forger's own signature;

2) *Simple forgery,* the forger knows the author's name, but has no access to a sample of the signature. Thus, the forger reproduces the signature in his own style;

3) *Skilled forgery,* the forger has access to one or more samples of the genuine signature and is able to reproduce it. Skilled forgeries can be even subdivided according to the level of the forger's skill. Figure 1.3 presents examples of the mentioned types of forgeries.

Figure 1.3 : Examples of (a) genuine signature, (b) random forgery, (c) simple forgery and (d) skilled forgery.

Generally, only random forgeries are used to train the classification module of a signature verification system. The reason is that, in practice, it is rarely possible to obtain samples of forgeries; and for example, when dealing with banking applications, it becomes impracticable (Oliveira et al., 2007). On the other hand, all the types of forgeries are used to evaluate the system's performance.

1.2 Feature Extraction Techniques

Feature extraction is essential to the success of a signature verification system. In an offline environment, the signatures are acquired from a medium, usually paper, and preprocessed before the feature extraction begins. Offline feature extraction is a fundamental problem because of handwritten signatures variability and the lack of dynamic information about the signing process. An ideal feature extraction technique extracts a minimal feature set that maximizes interpersonal distance between signature examples of different persons, while minimizing intrapersonal distance for those belonging to the same person.

There are two classes of features used in offline signature verification:

1) *Static*, related to the signature shape;

2) *Pseudo-dynamic*, related to the dynamics of the writing.

These features can be extracted locally, if the signature is viewed as a set of segmented regions, or globally, if the signature is viewed as a whole. It is important to note that techniques used to extract global features can also be applied to specific regions of the signature in order to produce local features. In the same way, a local technique can be applied to the whole image to produce global features. Figure 1.4 presents a taxonomy of the categories of features used signature verification.

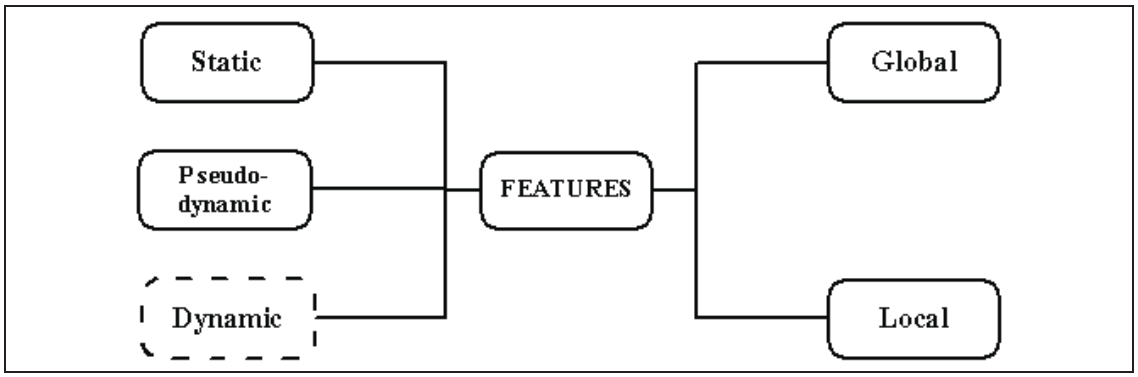

Figure 1.4 : A taxonomy of feature types used in signature verification. The dynamic features are represented but are only used in online approaches.

Moreover, the local features can be described as contextual and non-contextual. If the signature segmentation is performed in order to interpret the text (for example, bars of "t" and dots of "i"), the analysis is considered contextual (Chuang, 1977). This type of analysis is not popular for two reasons:

1) It requires a complex segmentation process;

2) It is not suitable to deal with graphical signatures.

On the other hand, if the signature is viewed as a drawing composed of line segments (as it occurs in the majority of the literature), the analysis is considered non-contextual.

Before describing the most important features extraction techniques in the field of offline signature verification, signature representation is discussed.

1.2.1 Signature Representations

Some techniques transform the signature image into another representation before extracting the features. Offline signature verification literature is quite extensive about signature representations.

Box and convex hull representations have been used to represent signatures (Frias-Martinez et al., 2006). The box representation is composed of the smallest rectangle fitting the signature. Its perimeter, area and perimeter/area ratio can be used as features. The convex hull representation is composed of the smallest convex hull fitting the signature. Its area, roundness, compactness and also the length and orientation of its maximum axis can be used as features. The skeleton of the signature, its outline, directional frontiers and ink distributions have also been used has signature representations (Huang and Yan, 1997). The skeleton (or core) representation is the pixel wide strokes resulting from the application of a thinning algorithm to a signature image. The skeleton can be used to identify the signature edge points (1-neighbor pixels) that mark the beginning and ending of strokes (Ozgunduz et al., 2005). Further, pseudo-Zernike moments have also been extracted from this kind of representation (Wen-Ming et al., 2004).

The outline representation is composed of every black pixel adjacent to at least one white pixel. Directional frontiers (also called shadow images) are obtained when keeping only the black pixels touching a white pixel in a given direction (and there are 8 possible directions). To perform ink distribution representations, a virtual grid is superposed over the signature image. The cells containing more than 50% of black pixels are completely filled while the others are emptied. Depending on the grid scale, the ink distributions can be coarser or more detailed.

The number of filled cells can also be used as a global feature. Upper and lower envelopes (or profiles) are also found in the literature. The upper envelope is obtained by selecting column-wise the upper pixels of a signature image, while the lower envelope is achieved by selecting the lower pixels, as illustrated by Figure 1.5 . As global features, the numbers of turns and gaps in these representations have been extracted (Ramesh and Murty, 1999).

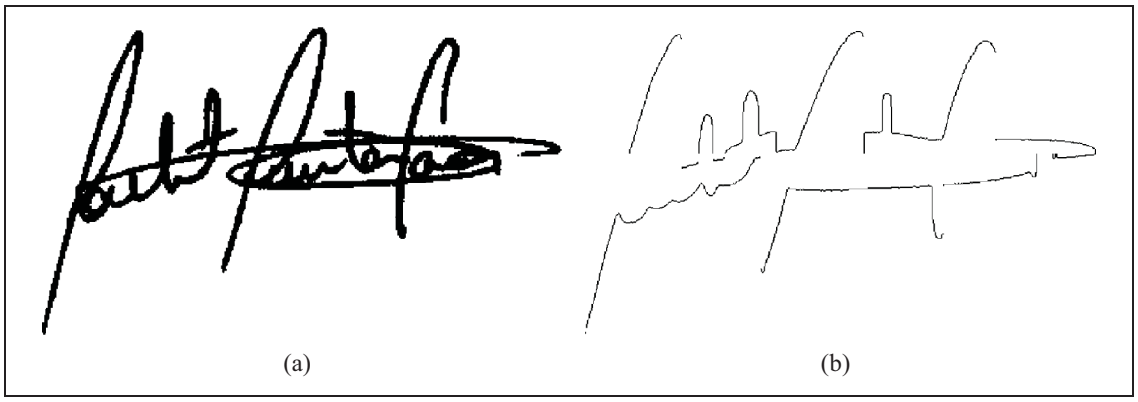

Figure 1.5 : (a) Example of a handwritten signature and (b) its upper and lower envelopes (Bertolini et al., 2010).

Mathematic transforms have been used to represent signature images. Nemcek and Lin (Nemcek and Lin, 1974) chose the fast Hadamard transform in their feature extraction process as a tradeoff between computational complexity and representation accuracy, when compared to other transforms. Discrete Radon transform is used to extract an observation sequence of the signature, which is used as a feature set (Coetzer et al., 2004).

Finally, signature images can also undergo a series of transformations before feature extraction. For example, Tang *et al.* (Tang et al., 2002) used a central projection to reduce the signature image to a 1-D signal that is in turn transformed by a wavelet before fractal features are extracted from its fractal dimension.

1.2.2 Geometrical Features

Global geometric features measure the shape of a signature. The height, the width (Armand et al., 2006a) and the area (or pixel density) (El-Yacoubi et al., 2000) (Abdelghani and Amara, 2006) of the signature are basic features pertaining to this category. The height and width can be combined to form the aspect ratio (or caliber) (Oliveira et al., 2005), as depicted in Figure 1.6 .

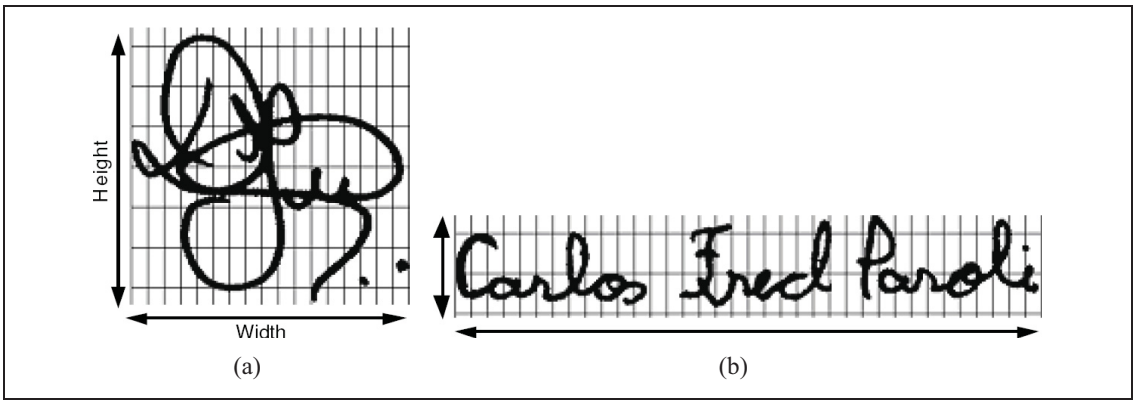

Figure 1.6 : Examples of handwritten signatures with two different calibers: (a) large, and (b) medium (Oliveira et al., 2005).

More elaborate geometric features consist of the proportion, the spacing and the alignment to baseline. Proportion, as depicted in Figure 1.7 , measures the height variations of the signature while spacing, depicted in Figure 1.8 , describes the gaps in the signature (Oliveira et al., 2005). Alignment to baseline extracts the general orientation of the signature according to a baseline reference (Abdelghani and Amara, 2006) (Armand et al., 2006a) (Frias-Martinez et al., 2006) (Oliveira et al., 2005) (Senol and Yildirim, 2005) and is illustrated in Figure 1.9 .

Connected components can also be extracted as global features, such as the number of 4-neighbors and 8-neighbors pixels in the signature image (Frias-Martinez et al., 2006).

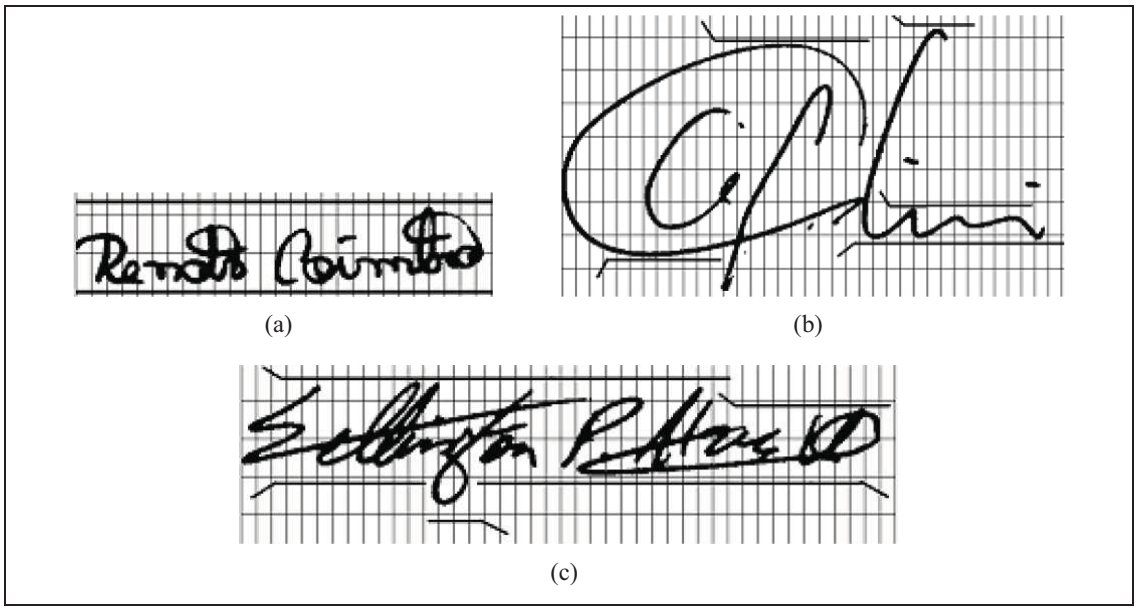

Figure 1.7 : Examples of handwritten signatures with three different proportions: (a) proportional, (b) disproportionate, and (c) mixed (Oliveira et al., 2005).

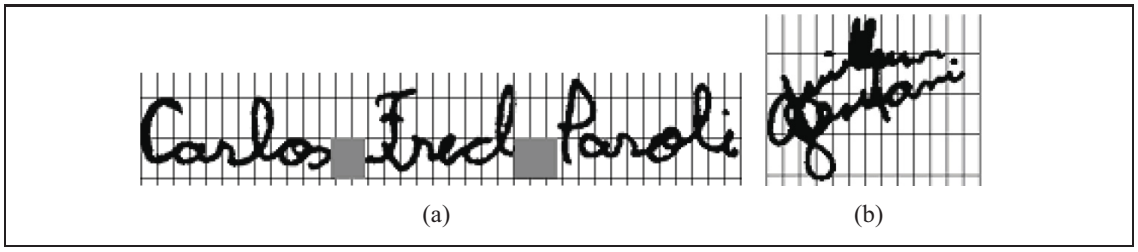

Figure 1.8 : Examples of handwritten signatures (a) with spaces and (b) no space (Oliveira et al., 2005).

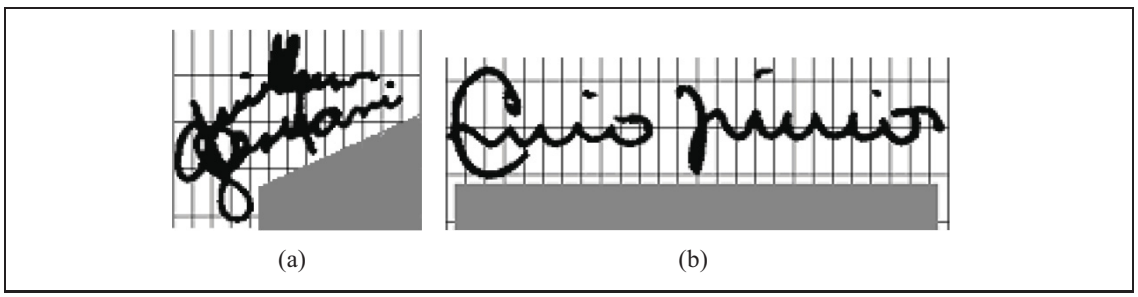

Figure 1.9 : Examples of handwritten signatures with an alignment to baseline of (a) $22°$**, and (b)** $0°$ **(Oliveira et al., 2005).**

1.2.3 Statistical Features

Many authors use projection representation. It consists in projecting every pixel on a given axis (usually horizontal or vertical), resulting in a pixel density distribution. Statistical features, such as the mean (or center of gravity), global and local maximums can be extracted from this distribution (Frias-Martinez et al., 2006) (Ozgunduz et al., 2005) (Senol and Yildirim, 2005). Moments - which can include central moments (i.e. skewness and kurtosis) (Frias-Martinez et al., 2006) (Bajaj and Chaudhury, 1997) and moment invariants (Al-Shoshan, 2006) (Lv et al., 2005) (Oz, 2005) - are also extracted from the pixel distributions.

Moreover, other types of distributions can be extracted from a signature. Drouhard *et al.* (Drouhard et al., 1996) extracted Directional PDF (Probability Density Function) from the gradient intensity representation of the silhouette of a signature, as depicted in Figure 1.10 . Stroke direction distributions have been extracted using structural elements and morphologic operators (Frias-Martinez et al., 2006) (Lv et al., 2005) (Ozgunduz et al., 2005) (Madasu, 2004). A similar technique is used to extract edge-hinge (strokes changing direction) distributions (Madasu, 2004). Based on an envelope representation of the signature, slope distributions are also extracted in this way (Fierrez-Aguilar et al., 2004) (Lee and Lizarraga, 1996). Whereas Madasu *et al.* (Madasu et al., 2003) extracted distributions of angles with respect to a reference point from a skeleton representation.

1.2.4 Similarity Features

Similarity features differ from other kinds of features in the sense that they are extracted from a set of signatures. Thus, in order to extract these features, one signature is the questioned signature while the others are used as references.

In literature, Dynamic Time Warping seems to be the matching algorithm of choice. However, since it works with 1D signals, the 2D signature image must be reduced to one dimension. To that effect, projection and envelope representations (Fang et al., 2003) (Kholmatov, 2003) have been used. A weakness of the Dynamic Time Warping is that it cumulates errors and for this

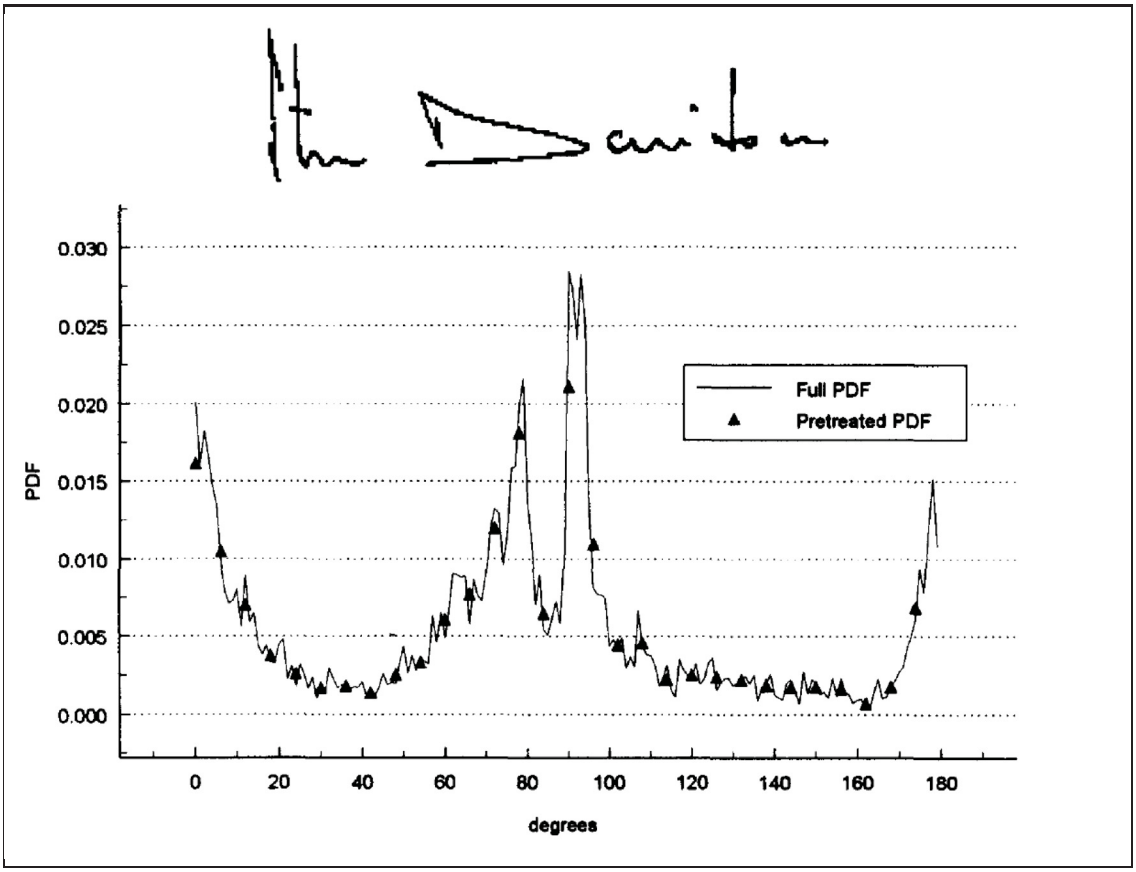

Figure 1.10 : Example of a directional PDF extracted from the handwritten signature shown in the upper part of the figure (Drouhard et al., 1996). The peaks around $0°$, $90°$ and $180°$ indicates the predominance of horizontal and vertical strokes.

reason the sequences to match must be the shortest possible. To solve this problem, a wavelet transform can be used to extract inflection points from the 1D signal. Then, Dynamic Time Warping matches this shorter sequence of points (Deng et al., 2003). The inflection points can also be used to segment the wavelet signal into shorter sequences to be matched by the Dynamic Time Warping algorithm (Ye et al., 2005).

Among other methods, a local elastic algorithm has been used to match the skeleton representations of two signatures (You et al., 2005) (Fang et al., 2003) and cross-correlation has been

used the extract correlation peak features from multiple signature representations obtained from identity filters and Gabor filters (Fasquel and Bruynooghe, 2004).

1.2.5 Fixed Zoning

Fixed zoning defines arbitrary regions and uses them for all signatures. To perform fixed zoning based on pixels, all the pixels of a signature are sent to the classifier after the signature image has been normalized to a given size (Frias-Martinez et al., 2006) (Martinez et al., 2004) (Mighell et al., 1989). Otherwise, numerous fixed zoning methods are described in the literature. Usually, the signature is divided into strips (vertical or horizontal) or using a layout like a grid or angular partitioning. Then, geometric features (Abdelghani and Amara, 2006) (Armand et al., 2006b) (Ferrer et al., 2005) (Justino et al., 2005) (Ozgunduz et al., 2005) (Senol and Yildirim, 2005) (Martinez et al., 2004) (Santos et al., 2004) (Huang and Yan, 1997) (Qi and Hunt, 1994), wavelet transform features (Abdelghani and Amara, 2006) and statistical features (Frias-Martinez et al., 2006) (Hanmandlu et al., 2005) (Justino et al., 2005) (Fierrez-Aguilar et al., 2004) (Madasu, 2004) can be extracted. Figure 1.11 illustrate an example of feature extraction from a grid cell of a handwritten signature.

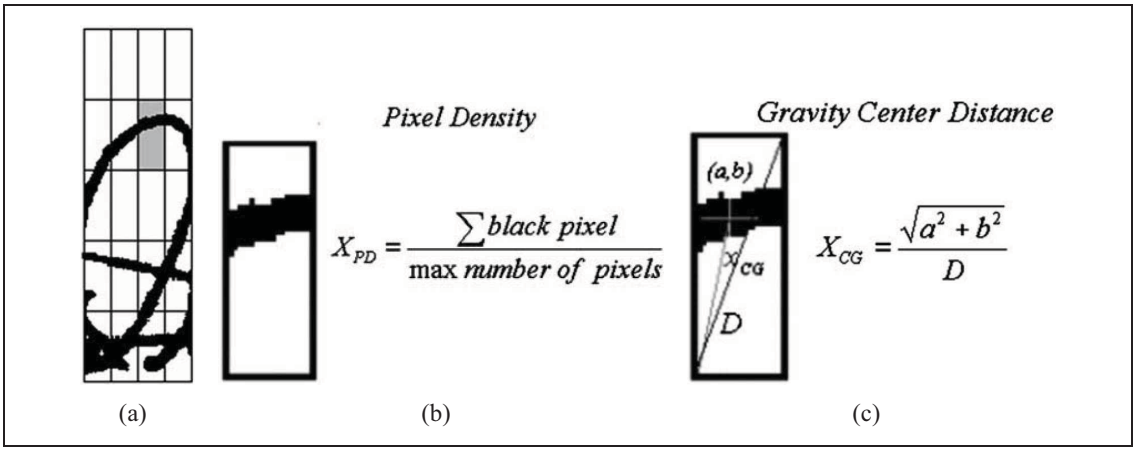

Figure 1.11 : (a) Example of a grid-like fixed zoning and of two feature extraction techniques applied to a given cell: (b) pixel density and (c) gravity center distance (Justino et al., 2005).

Other techniques are specially designed for extracting local features. Strips based methods include peripheral features extraction from horizontal and vertical strips of a signature edge representation. Peripheral features measure the distance between two edges and the area between the virtual frame of the strip and the first edge of the signature (Fang and Tang, 2005) (Fang et al., 2002).

Most fixed zoning techniques use a grid layout. For example, the Modified Direction Feature (MDF) technique (Armand et al., 2006b) extracts the location of the transitions from the background to the signature and their corresponding direction values for each cell of grid superposed on the signature image. The Gradient, Structural and Concavity (GSC) technique (Kalera et al., 2004a) (Srihari et al., 2004a) extracts gradient features from edge curvature, structural features from short strokes and concavity features from certain hole types independently for each cell a grid covering the signature image. The Extended Shadow Code technique, proposed by Sabourin and colleagues (Sabourin et al., 1993) (Sabourin and Genest, 1994) (Sabourin and Genest, 1995) centers the signature image on a grid layout where each rectangular cell of the grid is composed of six bars: one bar for each side of the cell plus two diagonal bars stretching from a corner of the cell to the other in an 'X' fashion. The pixels of the signature are projected perpendicularly on the nearest horizontal bar, the nearest vertical bar, and also on both diagonal bars. The features are extracted from the normalized area of each bar that is covered by the projected pixels. The envelope-based technique (Ramesh and Murty, 1999) (Bajaj and Chaudhury, 1997) describes, for each grid cell, the comportment of the upper and lower envelope of the signature. The pecstrum technique (Sabourin et al., 1997b) (Sabourin et al., 1996) centers the signature image on a grid of overlapping retinas and then uses successive morphological openings to extract local granulometric size distributions.

1.2.6 Signal Dependent Zoning

Signal dependent zoning generates different regions adapted to individual signature. When signal dependent zoning is performed using the pixels of the signature as local regions, position features are extracted from each pixel with respect to a coordinate system. Martinez *et*

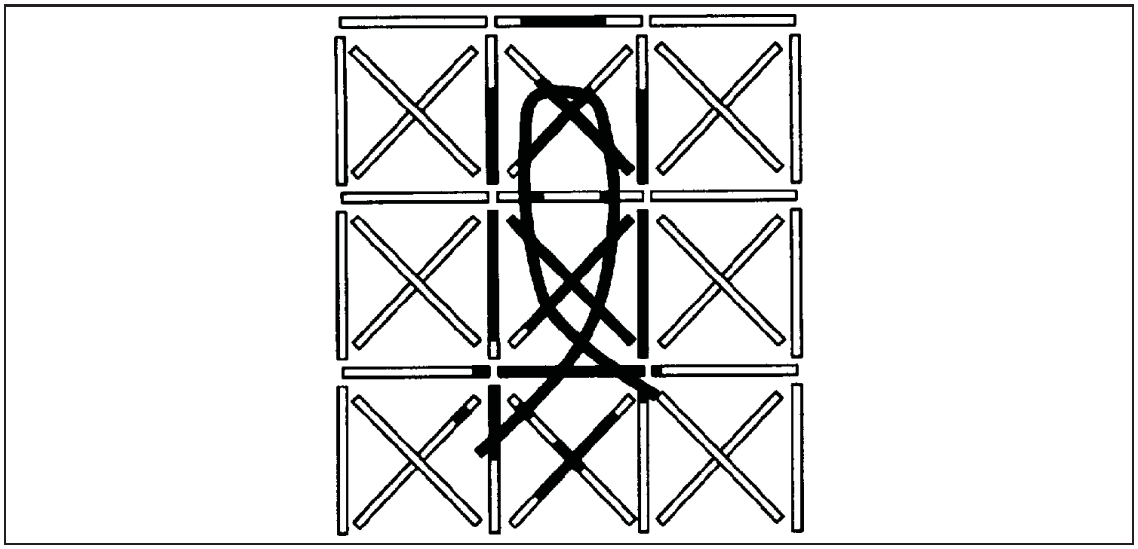

Figure 1.12 : Example of feature extraction on a looping stroke by the Extended Shadow Code technique (Sabourin et al., 1993). Pixel projections on the bars are shown in black.

al. (Martinez et al., 2004), followed by Ferrer *et al.* (Ferrer et al., 2005), extracted position features from a contour representation in polar coordinates. Still using the polar coordinate system, signal dependent angular-radial partitioning techniques have been developed. These techniques adjust themselves to the circumscribing circle of the signature to achieve scale invariance and they achieve rotation invariance by synchronizing the sampling with the baseline of the signature, as depicted in Figure 1.13 . Shape matrices have been defined this way to sample the silhouette of two signatures and extract similarity features (Sabourin et al., 1997a). A similar method is used by Chalechale *et al.* (Chalechale et al., 2004), though edge pixel area features are extracted from each sector and rotation invariance is obtained by applying a 1-D discrete Fourier transform to the extracted feature vector.

In Cartesian coordinate system, signal dependent retinas have been used to define local regions best capturing the intrapersonal similarities from the reference signatures of individual writers (Ando and Nakajima, 2003). A genetic algorithm is used to optimize the location and size

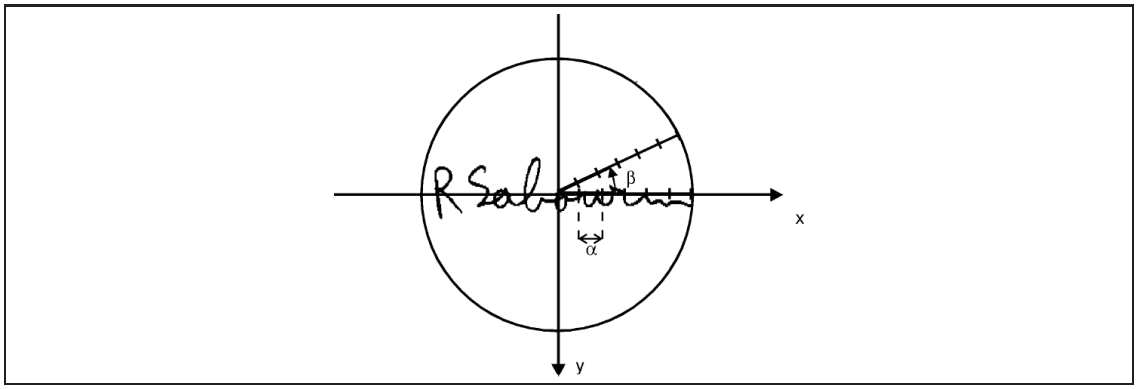

Figure 1.13 : Example of polar sampling on an handwritten signature. The coordinate system is centered on the centroid of the signature to achieve translation invariance and the signature is sampled using a sampling length α and an angular step β (Sabourin et al., 1997a).

of these retinas before similarity features are extracted from the questioned signature and its reference set.

Connectivity analysis has been performed on a signature image to generate local regions before extracting geometric and position features from each region (Igarza et al., 2005). Even more localized, signal dependent regions are achieved using stroke segmentation. Perez-Hernandez *et al.* (Perez-Hernandez et al., 2004) achieved stroke segmentation by first finding the direction of each pixel of the skeleton of the signature and then using a pixel tracking process. Then, the orientation and endpoints of the strokes are extracted as features. Another technique is to erode the stroke segments into bloated regions before extracting similarity features (Franke et al., 2002).

Instead of focusing on the strokes, the segmentation can be done in other signature representations. Chen and Srihari (Chen and Srihari, 2006) matched two signature contours using Dynamic Time Warping before segmenting and extracting Zernike moments from the segments. Xiao and Leedham (Xiao and Leedham, 2002) segmented upper and lower envelopes where their orientation changes sharply. After that, they extracted length, orientation, position and pointers to the left and right neighbors of each segment.

1.2.7 Pseudo-dynamic Features

The lack of dynamic information is a serious constrain for offline signature verification systems. The knowledge of the pen trajectory, along with speed and pressure, gives an edge to online systems. To overcome this difficulty, some approaches use dynamic signature references to develop individual stroke models that can be applied to offline questioned signatures. For instance, Guo *et al.* (Guo et al., 2000) used stroke-level models and heuristic methods to locally compare dynamic and static pen positions and stroke directions. Lau *et al.* (Lau et al., 2005) developed the Universal Writing Model (UWM), which consists of a set of distribution functions constructed using the attributes extracted from online signature samples. Whereas Nel *et al.* (Nel et al., 2005) used a probabilistic model of the static signatures based on Hidden Markov Models (HMM) where the HMMs restrict the choice of possible pen trajectories describing the morphology of the signature. Then, the optimal pen trajectory is calculated using a dynamic sample of the signature.

However, without resorting to online examples, it is possible to extract pseudo-dynamic features from static signature images. Pressure features can be extracted from pixel intensity (i.e. grey levels) (Lv et al., 2005) (Santos et al., 2004) (Wen-Ming et al., 2004) (Huang and Yan, 1997) and stroke width (Lv et al., 2005) (Oliveira et al., 2005). Whereas speed information can be extrapolated from stroke curvature (Santos et al., 2004) (Justino et al., 2005), stroke slant (Justino et al., 2005) (Oliveira et al., 2005) (Senol and Yildirim, 2005), progression (Oliveira et al., 2005) (Santos et al., 2004) and form (Oliveira et al., 2005). Figure 1.14 and 1.15 illustrates stroke progression and form, respectively.

1.3 Verification Strategies and Experimental Results

This section categorizes some research in offline signature verification according to the technique used to perform verification, that is, Distance Classifiers, Artificial Neural Networks, Hidden Markov Models, Dynamic Time Warping, Support Vector Machines, Structural Techniques and Bayesian Networks.

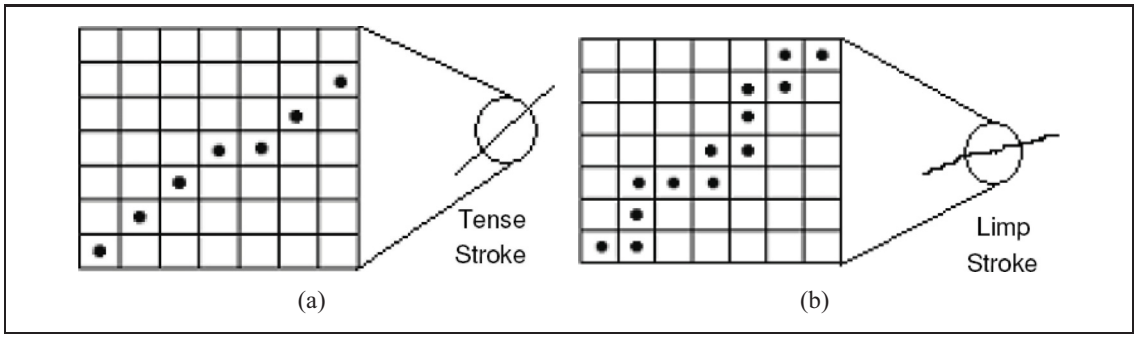

Figure 1.14 : Examples of stroke progression: (a) few changes in direction indicates a tense stroke, and (b) a limp stroke changes direction many times (Oliveira et al., 2005).

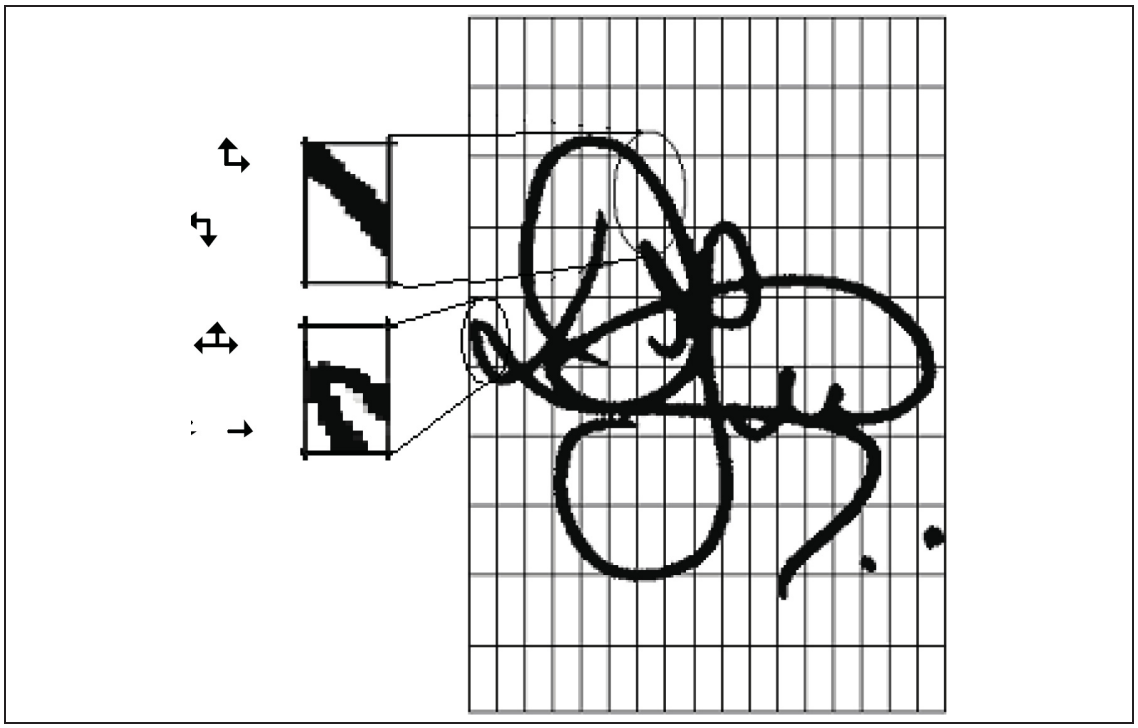

Figure 1.15 : Example of stroke form extracted from retinas using concavity analysis (Oliveira et al., 2005).

In signature verification, the verification strategy can either be categorized as writer-independent or writer-dependent (Srihari et al., 2004a). With writer-independent verification, a single

classifier deals with the whole population of writers. In contrast, the writer-dependent verification necessitates a different classifier for each writer. As the majority of the research presented in literature is designed to perform writer-dependent verification, this aspect is mentioned only when writer-independent verification is considered.

Before describing the verification strategies, a word on the measures used to evaluate the performance of signature verification systems.

1.3.1 Performance Evaluation Measures

The simplest way to report the performance of signature verification systems is in terms of error rates. The False Rejection Rate (FRR) is related to the number of genuine signatures erroneously classified by the system as forgeries. Whereas the False Acceptance Rate (FAR) is related to the number of forgeries misclassified as genuine signatures. FRR and FAR are also known as type 1 and type 2 errors, respectively. Finally, the Average Error Rate (AER) is related to the total error of the system, that is, the type 1 and type 2 errors together.

On the other hand, if the decision threshold of a system is set to have the FRR approximately equal to the FAR, the Equal Error Rate (EER) is being calculated.

1.3.2 Distance Classifiers

A simple Distance Classifier is a statistical technique which usually represents a pattern class with a Gaussian probability density function (PDF). Each PDF is uniquely defined by the mean vector and covariance matrix of the feature vectors belonging to a particular class. When the full covariance matrix is estimated for each class, the classification is based on Mahalanobis distance. On the other hand, when only the mean vector is estimated, classification is based on Euclidean distance (Coetzer, 2005).

Approaches based on Distance Classifiers are traditionally writer-dependent. The reference samples of a given author are used to compose the class of genuine signatures and a subset of samples from each other writer is chosen randomly to compose the class of (random) forgeries.

The questioned signature is classified according to the label of its nearest reference signature in the feature space. Further, if the classifier is designed to find a number of k nearest reference signatures, a voting scheme is used to take the final decision.

Distance Classifiers were one of the first classification techniques to be used in offline signature verification. One of the earliest reported research was by Nemcek and Lin (Nemcek and Lin, 1974). By using a fast Hadamard transform as feature extraction technique on genuine signatures and simple forgeries, and Maximum Likelihood Classifiers, they obtained an FRR of 11% and an FAR of 41%.

Then, Nagel and Rosenfeld (Nagel and Rosenfeld, 1977) proposed a system to discriminate between genuine signatures and simple forgeries using images obtained from real bank checks. A number of global and local features were extracted considering only the North American's signature style. Using Weighted Distance Classifiers, they obtained FRRs ranging from 8% to 12% and an FAR of 0%.

It is only years later that skilled forgeries began to be considered in offline signature verification. Besides proposing a method to separate the signatures from noisy backgrounds and to extract pseudo-dynamic features from static images, Ammar and colleagues were the first to try to detect skilled forgeries using an offline signature verification system. In their research (Ammar et al., 1985) (Ammar et al., 1988) (Ammar, 1991), distance classifiers were used combined with the leave-one-out cross validation method, since the number of signatures samples was small.

Qi and Hunt (Qi and Hunt, 1994) presented a signature verification system based on global geometric features and local grid-based features. Different types of similarity measures, such as Euclidean distance, were used to discriminate between genuine signatures and forgeries (including simple and skilled). They achieved an FRR ranging from 3% to 11.3% and an FAR ranging from 0% to 15%.

Sabourin and colleagues have done extensive research in offline signature verification since middle 80's (Sabourin and Plamondon, 1986). In one of their research (Sabourin et al., 1993), the Extended Shadow Code was used in order to extract local features from genuine signatures and random forgeries. The first experiment used a k-Nearest Neighbors classifier (k-NN) with a voting scheme, obtaining an AER of 0.01% when $k = 1$. The second experiment used a Minimum Distance Classifier, obtaining an AER of 0.77% when 10 training signatures were used for each writer. In another relevant research (Sabourin et al., 1997b), they used granulometric size distributions as local features, also in order to eliminate random forgeries. By using k-Nearest Neighbors and Threshold Classifiers, they obtained an AER around 0.02% and 1.0%, respectively.

Fang *et al.* (Fang et al., 2001) developed a system based on the assumption that the cursive segments of skilled forgeries are generally less smooth than those of genuine signatures. Besides the utilization of global shape features, a crossing and a fractal dimension methods were proposed to extract the smoothness features from the signature segments. Using a simple Distance Classifier and the leave-one-out cross-validation method, an FRR of 18.1% and an FAR of 16.4% were obtained. More recently (Fang et al., 2002), they extracted a set of peripheral features in order to describe internal and the external structures of the signatures. To discriminate between genuine signatures and skilled forgeries, they used a Mahalanobis distance classifier together with the leave-one-out cross-validation method. The obtained AERs were in the range of 15.6% (without artificially generated samples) and 11.4% (with artificially generated samples).

1.3.3 Artificial Neural Networks

An Artificial Neural Network (ANN) is a massively parallel distributed system composed of processing units capable of storing knowledge learned from experience (samples) and using it to solve complex problems (Haykin, 1998). Multilayer Perceptron (MLP) trained with the error Back Propagation algorithm (Rumelhart et al., 1986) has been so far the most frequently ANN architecture used in pattern recognition.

Mighell *et al.* (Mighell et al., 1989) were the first to apply ANNs to offline signature verification. In order to eliminate simple forgeries, they used the raw images as input to an MLP. In the experiments, by using a training set composed of genuine signatures and forgeries, they achieved an EER of 2%.

Sabourin and Drouhard (Sabourin and Drouhard, 1992) used directional PDFs as global feature vectors and MLP as classifier in order to eliminate random forgeries. Since their database was composed of few data, some signature samples were artificially generated by rotating the directional PDFs. In the experiments, they obtained an FRR of 1.75% and an FAR of 9%.

Cardot *et al.* (Cardot et al., 1994) used the outline of the signature images and geometric features to compose two types of feature vectors. The most important contribution of their research was the proposal of a multi-stage architecture to eliminate random forgeries. The first level is composed of two Kohonen maps (one for each set of features), in order to perform an initial classification and to choose the random forgeries to train the networks of the second level. As the number of writers was very large (over 300), they had to limit the number of classes to less than 50. In the second level, two MLPs for each writer are used to perform writer-dependent verification. Finally, in the last level, an MLP accepts or rejects the signature. By using a dataset of signatures extracted from real postal checks, they achieved an FRR of 4% and an FAR of 2%.

Murshed *et al.* (Murshed et al., 1995) proposed a verification strategy based on Fuzzy ARTMAPs in the context of random forgeries. Differently from other neural networks types, the Fuzzy ARTMAPs allows training by using examples of only one class. Therefore, in this approach, the genuine signatures are used for training and the random forgeries (as well as some unseen genuine signatures samples), for testing. In order to simulate different experts examining different regions of the signature, the image is divided in a number of overlapping squares, according to the writer signature shape. After that, each signature region is reduced, by applying a MLP network, and verified by a specialized Fuzzy ARTMAP. Finally, based on the results

given by each Fuzzy ARTMAP, the final decision is taken. In the experiments, they obtained an AER of 9.14%.

Bajaj and Chaudhary (Bajaj and Chaudhury, 1997) used an ensemble of MLPs to perform writer identification. In order to discriminate between genuine signatures and random forgeries, one MLP was trained per signature representation: moments, upper envelope and lower envelope. Moreover, each MLP was composed of 10 outputs (one for each writer). In the verification phase, the output of the three classifiers was combined to obtain a final decision. In the experiments, a substantial reduction of the error rate was obtained when using the three classifiers together (FRR=1%; FAR = 3%).

Fadhel and Bhattacharya (Fadhel and Bhattacharyya, 1999) proposed a signature verification system based on Steerable Wavelets as feature extraction technique and MLP as classifier. In the first experiment, by selecting only the first 2 of the 16 coefficients which represent each signature image, they obtained a classification rate of 85.4%. Whereas in a second experiment, by using all the 16 coefficients, the classification rate was improved to 93.8%.

Sansone and Vento (Sansone and Vento, 2000) proposed a three-stage multi-expert system in order to deal with all the types of forgeries. The first stage was designed to eliminate random and simple forgeries by using only the signature's outline as feature. The second stage receives the signatures accepted by the previous stage, which can be classified as genuine or as skilled forgery. The features used in this stage are the high pressure regions. Finally, a third stage takes the final decision. Using MLP as classifiers, they obtained an FRR of 2.04% and FARs of 0.01%, 4.29% and 19.80% on random, simple and skilled forgeries, respectively.

Baltzakis and Papamarkos (Baltzakis and Papamarkos, 2001) used global geometric features, grid features and texture features to represent the signatures. They proposed a two-stage system in order to eliminate random forgeries. In the first stage, three MLPs (one for each feature set) and the Euclidean distance metric perform a coarse classification. After that, a RBF (Radial Basis Function) neural network, trained with samples which were not used in the first stage, takes the final decision. An FRR of 3% and an FAR of 9.8% were obtained in the experiments.

Quek and Zhou (Quek and Zhou, 2002) proposed a system based on Fuzzy Neural Networks, in order to eliminate skilled forgeries. To represent the signatures, they used reference pattern-based features, global baseline features, pressure features and slant features. In the first set of experiments, using both genuine signatures and skilled forgeries to train the network, an average EER of 22.4% was obtained. Comparable results were obtained in the second set of experiments, in which only genuine signatures were used as training data.

Vélez *et al.* (Vélez et al., 2003) performed signature verification by comparing sub-images or positional cuttings of a test signature to the representations stored in Compression Neural Networks. In this approach, neither image preprocessing nor feature extraction is performed. By using one signature per writer, together with a set of artificially generated samples, they obtained a classification rate of 97.8%.

Armand *et al.* (Armand et al., 2006b) proposed the combination of the Modified Direction Feature (MDF) extracted from the signature's contour with a set of geometric features. In the experiments, they compared RBF and Resilient Backpropagation (RBP) neural network performances. Both networks performed writer identification and contained 40 classes: 39 corresponding to each writer and one corresponding to the forgeries. In this case, skilled forgeries were used in the training phase. The best classification rates obtained were 91.21% and 88.0%, using RBF and RBP, respectively.

1.3.4 Hidden Markov Models

Hidden Markov Models (Rabiner, 1989) are finite stochastic automata used to model sequences of observations. Although this technique is more suitable to model dynamic data (such as speech and online signatures) it has also been applied to offline signatures. Generally, HMMs are used to perform writer-dependent verification, by modeling only the genuine signatures of a writer. In this case, the forgeries are detected by thresholding.

Rigoll and Kosmala (Rigoll and Kosmala, 1998) presented a comparison between online and offline signature verification using discrete HMMs. To represent the signatures in the online

model, they used both static and pseudo-dynamic features. In the first set of experiments, in which each feature was investigated separately, surprising results were obtained. The bitmap feature was the most important one, achieving a classification rate of 92.2%. The Fourier feature also supplied a high classification rate. Finally, another surprise was the low importance of the acceleration. As expected, good results were obtained using the velocity feature. Other experiments, using several features together, were performed in order to obtain high classification rates. The best result (99%) was obtained when only 4 features (bitmap, velocity, pressure and Fourier feature) where combined.

To represent the signatures in the offline model, they subdivided the signature image into several squares of 10×10 pixels. After that, the grey value of each square was computed and used as feature. In the experiments, a classification rate of 98.1% was achieved. The small difference between the online and offline classification rates is an important practical result, since offline verification is simpler to implement.

El-Yacoubi *et al.* (El-Yacoubi et al., 2000) proposed an approach based on HMM and pixel density feature in order to eliminate random forgeries. To perform training while choosing the optimal HMM parameters, the Baum-Welch algorithm and the cross-validation method were used. In the experiments, each signature was analyzed under three resolutions (100×100, 40×40 and 16×16 pixels) by applying the Forward algorithm. Finally, a majority-vote rule took the final decision. An AER of 0.46% was obtained when both genuine and impostor spaces were modeled, and AER of 0.91% was obtained when only the genuine signatures were modeled.

Justino (Justino, 2001) used HMMs to detect random, simple and skilled forgeries. Also using a grid-segmentation scheme, three features were extracted from the signatures: pixel density feature, Extended Shadow Code and axial slant feature. They applied the cross-validation method in order to define the number of states for each HMM writer model. Using the Bakis model topology and the Forward algorithm, they obtained an FRR of 2.83% and FARs of 1.44%, 2.50% and 22.67%, for random, simple and skilled forgeries, respectively.

Coetzer *et al.* (Coetzer et al., 2004) used HMMs and Discrete Radon Transform to detect simple and skilled forgeries. In this research, some strategies were proposed in order to obtain noise, shift, rotation and scale invariances. By using a left-to-right ring model and the Viterbi algorithm, EERs of 4.5% and 18% were achieved for simple and skilled forgeries, respectively.

1.3.5 Dynamic Time Warping

Widely applied in Speech Recognition, Dynamic Time Warping is a Template Matching technique used for measuring similarity between two sequences of observations. The primary objective of Dynamic Time Warping is to nonlinearly align the sequences before they are compared (or matched) (Coetzer, 2005). Despite being more suitable to model data which may vary in time or speed, Dynamic Time Warping has been used in offline signature verification. As it usually occurs with similarity-based approaches, a test signature is compared to the genuine ones of a writer and a forgery is detected by thresholding.

Wilkinson and Goodman (Wilkinson and Goodman, 1990) used Dynamic Time Warping to discriminate between genuine signatures and simple forgeries. Assuming that curvature, total length and slant angle are constant among different signatures of a same writer, they used a slope histogram to represent each sample. In the experiments, they obtained an EER of 7%. Increases in the error rates were observed when the forgers had some *a priori* knowledge about the signatures.

Deng *et al.* (Deng et al., 1999) proposed a Wavelet-based approach to eliminate simple and skilled forgeries. After applying a Closed-Contour Tracing algorithm to the signatures, the curvature data obtained were decomposed into multi-resolution signals using Wavelets. Then, Dynamic Time Warping were used to match the corresponding zero-crossings. Experiments were performed using English and Chinese signature datasets. For the English dataset, an FRR of 5.6% and FARs of 21.2% on skilled forgeries and 0% on simple forgeries were obtained. Whereas using the Chinese dataset, an FRR of 6.0% and FARs of 13.5% and 0% were achieved on skilled and simple forgeries, respectively.

Fang *et al.* (Fang et al., 2003) proposed a method based on Dynamic Time Warping and one-dimensional projection profiles in order to deal with intra-personal signature variations. To achieve discrimination between genuine signatures and skilled forgeries, nonlinear Dynamic Time Warping was used in a different way. Instead of using the distance between a test signature and a reference sample to take a decision, the positional distortion at each point of the projection profile was incorporated into a distance measure. Using the leave-one-out cross-validation method and the Mahalanobis distance, they obtained AERs of 20.8% and 18.1%, when binary and grey level signatures were considered, respectively.

1.3.6 Support Vector Machines

Support Vector Machines (SVM) (Vapnik, 1999) use a kernel-based learning technique which has shown successful results in various domains such as pattern recognition, regression estimation, density estimation, novelty detection and others.

Signature verification systems that use SVM as classifier are designed in a similar way to those that use neural networks. That is, in a writer-dependent approach, there is one class for the genuine signatures and other class for the forgeries. In addition, by using one-class SVMs (Scholkopf et al., 2001), it is possible to perform training by using only genuine signatures. In the research of Srihari *et al.* (Srihari et al., 2004a) they tried to use it in the context of skilled forgeries. However, by using the traditional two-class approach, the AER decreased from 46.0% to 9.3%.

Martinez *et al.* (Martinez et al., 2004) used SVM with RBF kernel in order to detect skilled forgeries. In the experiments, different types of geometrical features, as well as raw signatures were tested. The best result, an FAR of 18.85%, was obtained when raw images with a scale of 0.4 were used.

Justino *et al.* (Justino et al., 2005) performed a comparison between SVM and HMM classifiers in the detection of random, simple and skilled forgeries. By using a grid-segmentation scheme, they extracted a set of static and pseudo-dynamic features. Under different experimental con-

ditions, that is, varying the size of the training set and the types of forgeries, the SVM with a linear kernel outperformed the HMM.

Ozgunduz *et al.* (Ozgunduz et al., 2005) used Support Vector Machines in order to detect random and skilled forgeries. To represent the signatures, they extracted global geometric features, direction features and grid features. In the experiments, a comparison between SVM and ANN was performed. Using a SVM with RBF kernel, an FRR of 0.02% and an FAR of 0.11% were obtained. Whereas the ANN, trained with the Backpropagation algorithm, provided an FRR of 0.22% and an FAR of %0.16. In both experiments, skilled forgeries were used to train the classifier.

1.3.7 Structural Techniques

In Structural Techniques, the patterns are organized hierarchically in a way that, at each level, they are viewed as being composed of simpler subpatterns. By using a small number of primitives (the most elementary subpatterns) and grammatical rules, it is possible to describe a large collection of complex patterns (Coetzer, 2005). Therefore, it is possible to interpret the scene both globally and locally.

Sabourin *et al.* (Sabourin et al., 1994) were the first ones to propose a structural representation of handwritten signatures images. In their approach, a segmentation process breaks up the signature into a set of primitives. From these shape primitives, both static and pseudo-dynamic features are extracted. The comparison process is composed of two stages: Local Interpretation of Primitives (LIP) and Global Interpretation of the Scene (GIS). In the LIP stage, a template match process is performed, in which each primitive of the test signature image is labeled taking into account the reference set. Finally, the GIS stage takes the final decision by computing a similarity measure between the test primitive set and the reference primitive set. The experiments were performed in order to eliminate random forgeries. By using a minimum distance classifier with two reference signatures, they obtained an AER of 1.43%.

Bastos *et al.* (Bastos et al., 1997) proposed a mathematical signature representation in terms of ellipses, parabolas and hyperbolas. The goal of this approach is to allow a simplification of the signature tracing when detecting random forgeries. After performing a thinning process, junction and end points are found in the signatures. Next, an algorithm is applied in each part of the signature tracing (between an end point and a junction point) in order to obtain all necessary points for modeling a mathematical equation. Finally, the Least Square Method of curve adjusting is applied to each set of tracing points, resulting in number of equations of ellipses, parabolas and hyperboles. Performing superpositions between the found equations and the respective signatures, they obtained similarity indices ranged from 86.3% and 97.3%, with respect to different writers.

Huang and Yan (Huang and Yan, 2002) proposed a two-stage signature verification system based on ANN and a structural approach. To represent the signatures, they used geometric and directional frontier features. In the first stage of the system, a neural network attributes to the signature three possible labels: pass (genuine signature), fail (random or less skilled forgery) and questionable (skilled forgery). For the questionable signatures, the second stage uses a Structural Feature Verification algorithm to compare the detailed structural correlation between the test signature and the reference samples. In the experiments, the first classifier rejected 2.2% of the genuine signatures, accepted 3.6% of the forgeries and was undecided on 32.7% of the signatures. The second classifier rejected 31.2% of the questionable genuine signatures and accepted 23.2% of the questionable forgeries. Therefore, for the combined classifier, an FRR of 6.3% and an FAR of 8.2% were obtained.

1.4 Dealing With A Limited Amount Of Data

Mainly for practical reasons, a limited number of signatures per writer is available to train a classifier for signature verification. For example, a bank client is asked to supply from 3 to 5 signature samples at the time of her subscription. On the other hand, a high number of features are generally extracted from handwritten signature images. This combination - few samples and a high dimensionality representation space - is likely to result into unsatisfactory

verification performance since class statistics estimation errors may be significant (Fang and Tang, 2005). However, this crucial issue has received little attention in literature. Possible solutions are:

1) *Selecting the most discriminating features.* In the research of Xuhua *et al.* (Xuhua et al., 1996), for example, Genetic Algorithms were used in order to select the optimal set of partial curves from an online signature and the best features of each partial curve;

2) *Using regularization techniques,* in order to obtain a stable estimation of the covariance matrix (Fang and Tang, 2005);

3) *Generating synthetic samples.* This can be done by adding noise or applying transformations to the real signatures (Huang and Yan, 1997) (Vélez et al., 2003) (Fang et al., 2002) (Fang and Tang, 2005);

4) *Using Dissimilarity Representation.* This technique, used to design writer-independent verification systems, allows to reduce the number of classes, as well as to increase the quantity of feature vectors (Santos et al., 2004) (Srihari et al., 2004a) (Kalera et al., 2004a).

The rest of this section describes approaches generating synthetic samples as a solution. Writer-independent approaches based on dissimilarity representation are covered in details in Chapter 2.

Huang and Yan (Huang and Yan, 1997) applied slight transformations to the genuine signatures, in order to generate additional training samples; and heavy transformations, also to the genuine signatures, in order to generate forgeries. In the two cases, the transformations were: slant distortions, scalings in horizontal and vertical directions, rotations and perspective view distortions.

Whereas Vélez *et al.* (Vélez et al., 2003) tried to reproduce intrapersonal variability while using only one signature per writer. To generate additional training samples, they applied rotations

(in the range of $\pm 15°$), scalings (in the range of $\pm 20\%$), horizontal and vertical displacements (in the range of $\pm 20\%$) and different types of noise for each original signature.

By using a different approach, Fang and Tang (Fang and Tang, 2005) proposed the generation of additional samples in the following way:

1) Two samples are selected from the set of genuine signatures;

2) An Elastic Matching Algorithm is applied to the pair of signatures in order to establish correspondences between individual strokes;

3) Corresponding stroke segments are linked up by displacement vectors;

4) These displacement vectors are used to perform an interpolation between the two signatures and, thus, to produce a new training sample.

1.5 Discussion

This chapter presented a survey of techniques developed in the field of offline signature verification over the last twenty years. Even if error rates are reported, it is very difficult to compare performances between verification strategies since each research uses different experimentation protocols, and signature databases (see Table 1.1).

Moreover, for security reasons, it is not easy to make a signature dataset available to the signature verification community, especially if the signatures come from a real application, as banking documents, for example. However, the availability of datasets could make possible to define a common experimentation protocol in order to perform comparative studies in this field.

As we could observe, despite the vast amount of research performed in order to solve this problem, there are still fundamental problems facing signature verification: the large number of users, the large number of features, the limited number of reference signatures for train-

Table 1.1: Signature verification databases (I = Individual; G = Genuine; F = Forgeries; S = Samples)

References	Images	Signatures	Forgery Types
(Nemcek and Lin, 1974)	128x256 pixels binary	600G / 15I 120F / 4I	Simple
(Nagel and Rosenfeld, 1977)	500 ppi 64 grey levels	11G / 2I 14F / 2I	Simple
(Ammar et al., 1985)	256x1024 pixels 256 grey levels	200G / 10I 200F / 10I	Simple
(Qi and Hunt, 1994)	300 dpi 256 grey levels	300G / 15I 150F / 10I	Simple Skilled
(Sabourin and Drouhard, 1992) (Sabourin et al., 1993) (Sabourin and Genest, 1994) (Sabourin et al., 1997b)	128x512 pixels 256 grey levels	800G / 20I	Random
(Fang et al., 2002) (Fang et al., 2003)	300 dpi 256 grey levels	1320G / 55I 1320F / 12I	Skilled
(Mighell et al., 1989)	128x64 pixels binary	80G / 1I 66F	Skilled
(Cardot et al., 1994)	1024x512 pixels 256 grey levels	6000G/ 300I	Random
(Murshed et al., 1995)	128x512 pixels 256 grey levels	200G / 5I	Random
(Bajaj and Chaudhury, 1997)	200 dpi binary	150G / 10I	Random
(Fadhel and Bhattacharyya, 1999)	340 dpi 256 grey levels	300S / 30I	Skilled

Continued on Next Page. . .

References	Images	Signatures	Forgery Types
(Sansone and Vento, 2000)	300 dpi 256 grey levels	980G / 49I 980F / 49I	Simple Skilled
(Baltzakis and Papamarkos, 2001)	binary	2000G / 115I	Random
(Quek and Zhou, 2002)	516x184 pixels 256 grey levels	535G / 24I 15-20F / 5I	Skilled
(Vélez et al., 2003)	300 dpi 256 grey levels	112S / 28I	not specified
(Armand et al., 2006b)	not specified	936G / 39I 1170F / 39I	Skilled
(Rigoll and Kosmala, 1998)	not specified	280G / 14I 60F	Simple Skilled
(El-Yacoubi et al., 2000)	300 dpi binary	4000G / 100I	Random
(Justino, 2001) (Justino et al., 2005)	300 dpi 256 grey levels	4000G / 100I 1200F / 10I	Simple Skilled
(Coetzer, 2005)	300 dpi binary	660G / 22I 264F / 6I	Simple Skilled
(Deng et al., 1999)	600 ppi 256 grey levels	1000G / 50I 2500G / 50I	Simple Skilled
(Srihari et al., 2004a)	300 dpi 256 grey levels	1320G/ 55I 1320F / 55I	Skilled
(Martinez et al., 2004)	not specified	3840G / 160I 4800F / 160I	Skilled
(Ozgunduz et al., 2005)	256 grey levels	1320S / 70I	Skilled
(Bastos et al., 1997)	not specified	120G / 6I	Random
(Huang and Yan, 2002)	100 dpi 256 grey levels	1272G / 53I 7632F / 53I	Skilled

ing, the high intra-personal variability of the signatures and the unavailability of forgeries as counterexamples.

Some important feature extraction techniques used to extract global and local information from signatures were presented. The choice of using global or local features depends, mainly, on the types of forgeries to be detected by the system. The global features are extracted at a low computational cost and they have good noise resilience. However, they have less capacity to discriminate between genuine signatures and skilled forgeries. On the other hand, local features are more suitable to identify skilled forgeries, despite their dependence on a zoning process. Thus, a verification system designed to eliminate random, simple and skilled forgery could benefit from using both global and local features. In this respect, Extended Shadow Code (Sabourin and Genest, 1994) appears to be a good trade-off between global and local features; since it permits the projection of the handwritten at several resolutions. On the other hand, such an approach is likely to generate a very high number of potential features. Consequently, a feature selection process could improve the system performances by disregarding irrelevant or redundant features.

Despite the great recognition rates obtained by using classifiers learning from examples (as ANNs, HMMs, and SVMs), there are some difficulties to be faced. The first one, which occurs mainly with ANNs and SVMs, is the necessity of using forgery counterexamples in the training set in order to allow class separation by the classifier. However, some authors have already been dealing with this problem by using one-class classifiers (Murshed et al., 1995) (Srihari et al., 2004a), computer generated forgeries (Mighell et al., 1989) and a subset of genuine signatures from other writers as random forgeries.

Another difficulty is the large number of examples required to ensure that the classifier will be able to generalize on unseen data (Leclerc and Plamondon, 1994). On the other hand, classifiers without explicit training phase, such as Distance Classifiers, while not requiring many reference samples tend to have a low generalization capability. In that respect, writer-independent approaches, described in the next chapter, are very interesting since they cope

with the problem of having a reduced training set and they also tackle the problem of having to design a single classifier for each user of the signature verification system.

CHAPTER 2

WRITER-INDEPENDENT SIGNATURE VERIFICATION

As with most biometric applications, the performance of offline signature verification systems degrades due to the large numbers of users and limited number of available references per person. Writer-independent signature verification systems based on a dissimilarity representation approach alleviates both these problems (Santos et al., 2004) (Srihari et al., 2004a) (Kalera et al., 2004a). This chapter reviews writer-independent systems for offline signature verification. First, dichotomy transformation (Cha and Srihari, 2000) is described, followed by its application to signature verification (Santos et al., 2004). Finally, an ensemble of dichotomizers approach to writer-independent signature verification (Bertolini et al., 2010) is presented. As with the standard writer-dependent case, writer-independent systems input handwritten signatures and output verification results. However, as depicted by Figure 2.1 , when enrolling

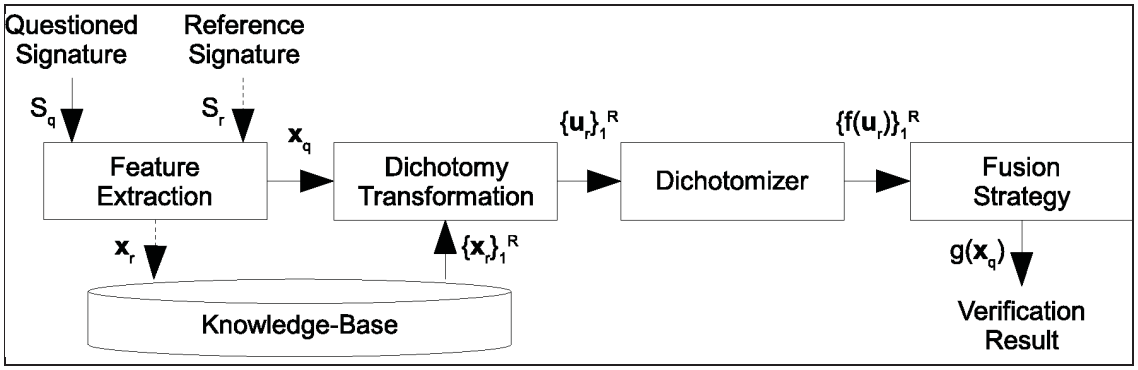

Figure 2.1 : Generic writer-independent signature verification system. Enrollment process is indicated by dotted arrows while solid arrows illustrate the authentication process.

(dotted arrows in the Figure) a new reference signature S_r, the feature vector $\mathbf{x}_r$ is extracted from the image of the signature and is stored for later use as a user template in the knowledge-base of the system. In verification mode (solid arrows in the Figure), the image of the ques-

tioned signature S_q is presented to the system and its feature vector $\mathbf{x}_q$ is extracted from the image. Along with the user's reference set $\{\mathbf{x}_r\}_1^R$ previously stored in the knowledge-base, the questioned feature vector is sent to the dichotomy transformation module, described in Section 2.1. Then, as described in Section 2.2, the set of distance vectors $\{\mathbf{u}_r\}_1^R$ produced by the dichotomy transformation module is sent to a 2-class classifier, called a dichotomizer, to reproduce the document expert approach by making a set of partial decision $\{f(\mathbf{u}_r)\}_1^R$, before a fusion strategy is applied to provide a final decision $g(\mathbf{x}_q)$ about the nature of the questioned signature.

2.1 Dichotomy Transformation

The objective of the dichotomy transformation is to transform a seemingly insurmountable pattern recognition problem where the number of classes is very large or unspecified into a 2-class problem (Cha and Srihari, 2000). Automatic signature verification on bank checks is an example of such a problem; the number of bank customers (i.e. classes or more accurately, writers) can easily reach the tens of thousands. Another difficulty encountered by such a real application is a limited number of signatures per writer. In most cases, sampling a sufficiently large sample from each writer is intractable.

2.1.1 Illustrative Example

Figure 2.2 illustrates a dichotomy transformation. Suppose there are three writers, $\{\omega_1, \omega_2, \omega_3\}$ and each writer provides three signatures. The feature extraction process extracts a vector of two features $(x_1\, x_2)^{\mathrm{T}}$ from each signatures. The left panel of Fig. 2.2 plots the vectors of the signatures into the feature space. The dichotomy transformation calculates the distance between the features of each pair of signatures to form vectors $(u_1\, u_2)^{\mathrm{T}}$ in the distance space, as depicted in the right panel. When both signatures come from the same writer, the distance vector is associated to the *within* class denoted $\omega_{\oplus}$ and when the signatures are from different writers, the distance vector is associated to the *between* class denoted $\omega_{\ominus}$.

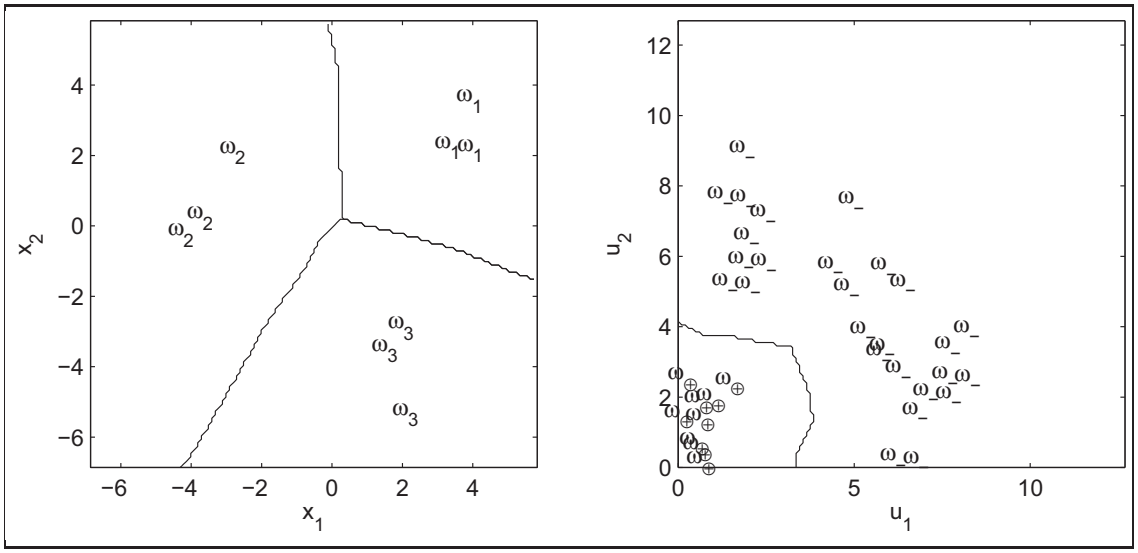

Figure 2.2 : Vectors from three different writers $\{\omega_1, \omega_2, \omega_3\}$ in feature space (left) projected into distance space (right) by the dichotomy transformation to form two classes $\{\omega_\oplus, \omega_\ominus\}$. Decision boundaries in both spaces are inferred by the nearest-neighbor algorithm.

The dichotomy transformation affects the geometry of the distributions. In this example, multiple boundaries are needed to separate the three writers in the feature space as opposed to only one in the distance space. Also, the vectors in the distance space are always non-negative since they are made up of distances. Finally, the dichotomy transformation augments the number of samples in the distance space because they are made up of every pairs of signatures.

2.1.2 Mathematical Formulation

Let $\mathbf{x}_q$, $\mathbf{x}_r$ be two *feature vectors* from the feature domain labeled y_q, y_r, respectively and $\mathbf{u}_r$ be the *distance vector* in the distance domain resulting from the dichotomy transformation:

$$\mathbf{u}_r = |\mathbf{x}_q - \mathbf{x}_r| \tag{2.1}$$

where $|\cdot|$ is the absolute value. It is important to emphasize that each element of vector $\mathbf{u}_r$ equals the distance between the corresponding elements of vectors $\mathbf{x}_q$ and $\mathbf{x}_r$, thus distance

vector and feature vectors have the same dimensionality. In the distance domain, indifferently of the number of writers, there are only two classes: the *within* class $\omega_{\oplus}$ and the *between* class $\omega_{\ominus}$. The distance vector $\mathbf{u}_r$ is assigned the label v_r according to:

$$v_r = \begin{cases} \omega_{\oplus} & \text{if } y_q = y_r \\ \omega_{\ominus} & \text{otherwise.} \end{cases} \tag{2.2}$$

Intuitively, signatures from the same writer should be near one to each other in the feature space, thus clustering near the origin in distance space whereas signatures from different writers should be distant from each other in the feature space and thus be scattered away from the origin in the distance space. This is illustrated in the example of Fig. 2.2 .

As for the number of distance vectors generated by the dichotomy transformation, if K writers provide a set of R references each, (2.1) generates up to $\binom{KR}{2}$ different distance vectors. Of these, $K\binom{R}{2}$ are of the *within* class and $\binom{K}{2}R^2$ are of the *between* class. Thus, using a small sample of references from each writer, the dichotomy transformation generates an appreciable quantity of samples in the distance domain.

2.2 Verification and Writer-Independence

Based in the context of the dichotomy transformation, the handwritten signature verification problem is formulated as follow; given a signature of reference and a questioned signature, the handwritten signature verification problem is to determine wether the two signatures were written by the same writer. Figure 2.3 presents the process of the signature verification using the dichotomy transformation. Let S_q and S_r be the questioned signature and the signature of reference, respectively. First, features are extracted from both handwritten signatures, giving feature vectors $\mathbf{x}_q$ and $\mathbf{x}_r$. Then the dichotomy transformation (2.1) computes the distance vector $\mathbf{u}_r$ which is in turn presented to the dichotomizer. Finally, the dichotomizer outputs the confidence rate $f(\mathbf{u}_r)$ of the distance vector $\mathbf{u}_r$ being part of the *within* class. In other words,

the dichotomizer outputs the confidence rate of the questioned signature S_q and the signature of reference S_r being written by the same writer.

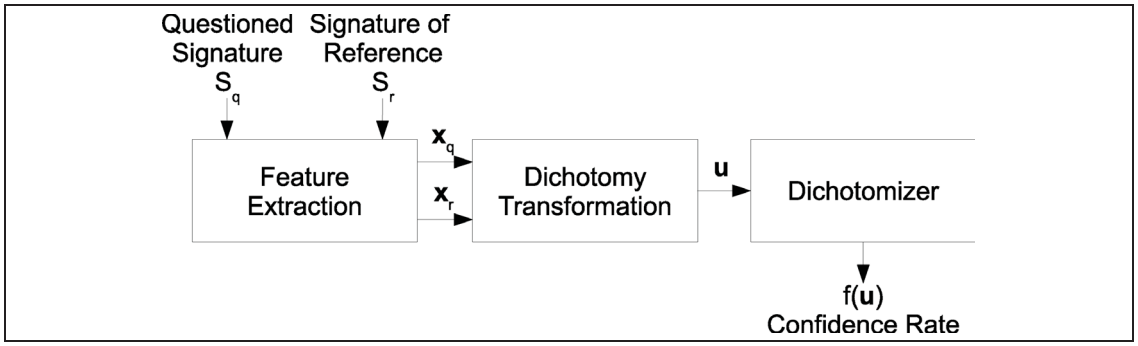

Figure 2.3 : Writer-independent signature verification process using the dichotomy transformation.

To illustrate how the verification process is independent from the writer being verified, suppose writers $\{\omega_1, \omega_2, \omega_3\}$ form the training set from which the dichotomizer is inferred (see section 2.1.1) and let $\mathbf{x}_q$, $\mathbf{x}_r$ be a questioned and reference feature vectors, respectively, both from new writer ω_4. The dichotomy transformation (2.1) computes the distance vector $\mathbf{u}$ from $\mathbf{x}_q$ and $\mathbf{x}_r$. Figure 2.4 illustrates both feature vectors and the distance vector in the context of the previous example. As it can be seen in the distance space (right panel), the distance vector $\mathbf{u}$ is located in the *within* region defined by the dichotomizer, which means that it authenticates both questioned and reference signatures as from the same writer. On the other hand, the feature space boundaries (left panel) fail utterly by classifying one signature ($\mathbf{x}_q$) to writer ω_2 and the other ($\mathbf{x}_r$) to writer ω_3. In fact, it is impossible for the feature domain model to adequately classify the signatures as from writer ω_4 since this writer did not participate to the training set. Hence the writer-independence is provided by the distance domain model.

2.2.1 Writer-Independence versus Accuracy Trade-off

The dichotomy transformation brings to handwritten signature verification tractability and writer-independence. Since the number of writers is very large or unspecified and that acquir-

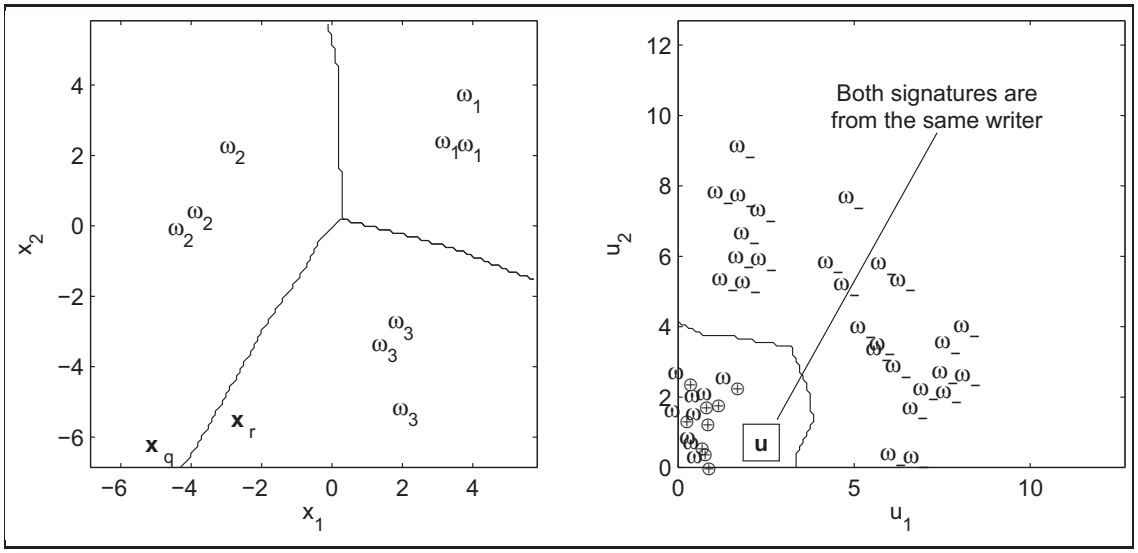

Figure 2.4 : The dichotomizer from the previous example is asked to authenticate the questioned signature x_q with respect to the reference signature x_r. The distance vector u resulting from their comparison is assigned to the *within* class, meaning both signatures come from the same writer.

ing a sufficiently large sample from each of them is intractable, the dichotomy transformation makes the problem tractable by reducing it to a 2-class problem and by increasing the quantity of samples available to build the dichotomizer.

However, there is a drawback to the dichotomy transformation; perfectly clustered writers in feature domain may not be perfectly dichotomized in distance domain (Cha and Srihari, 2000). To illustrate this, suppose the distributions of each writer $\{\omega_1, \omega_2, \omega_3\}$ are known, so that the Bayesian error can be evaluated both in feature and distance domains. Table 2.1 presents the gaussian distribution parameters of the three writers.

The center of each distribution is located at 6.92 units from the others, that is more than six standard deviations, which imply negligible overlap between the distributions. As such, the Bayesian error in the feature domain is evaluated numerically to 0.05%. Once projected into distance domain, the Bayesian error between the *within* and *between* classes is evaluated numerically to 1.76%. Figure 2.5 depicts the probability function for each distribution both in

Table 2.1: Gaussian distribution parameters $N(\boldsymbol{\mu}, \boldsymbol{\Sigma})$ for writers $\{\omega_1, \omega_2, \omega_3\}$

Writers	Mean $\boldsymbol{\mu}$	Variance $\boldsymbol{\Sigma}$
ω_1	$\begin{pmatrix} 2.83 \\ 2.83 \end{pmatrix}$	$\begin{pmatrix} 1 & 0 \\ 0 & 1 \end{pmatrix}$
ω_2	$\begin{pmatrix} -3.86 \\ 1.04 \end{pmatrix}$	$\begin{pmatrix} 1 & 0 \\ 0 & 1 \end{pmatrix}$
ω_3	$\begin{pmatrix} 1.04 \\ -3.86 \end{pmatrix}$	$\begin{pmatrix} 1 & 0 \\ 0 & 1 \end{pmatrix}$

the feature space and the distance space. In the distance space, it can be observed that the *within* class is clustered near the origin whereas the *between* class is distributed into three modes away from the origin. These three modes are the result of the comparison between writers ω_1 and ω_2, writers ω_1 and ω_3 and writers ω_2 and ω_3.

By increasing the variance of the distributions, as depicted by Figure 2.6 where the gaussian distribution parameter $\boldsymbol{\Sigma} = \left(\begin{smallmatrix} 5 & 0 \\ 0 & 5 \end{smallmatrix}\right)$, the Bayesian error is increased in both domains but the effect is more apparent in the distance domain. Table 2.2 presents the Bayesian error in both spaces in function of the gaussian distribution parameter $\boldsymbol{\Sigma}$ while the parameter $\boldsymbol{\mu}$ of each writer is fixed.

When comparing the Bayesian error in both spaces it is obvious that a model in the distance domain is less robust to the overlap between the writers. In other words, the broader the spread of the feature distributions among the writers, the less the dichotomizer is able to detect real differences between signatures who do not differ greatly (Cha and Srihari, 2000). Thus, the performance of the dichotomizer is crucially affected by the choice of the feature set extracted from the handwritten signatures. Moreover, because the dichotomy transformation affects the spatial geometry of the distributions, the best feature set may not be the same in feature domain and in distance domain. The solution proposed in this research to tackle this drawback is to

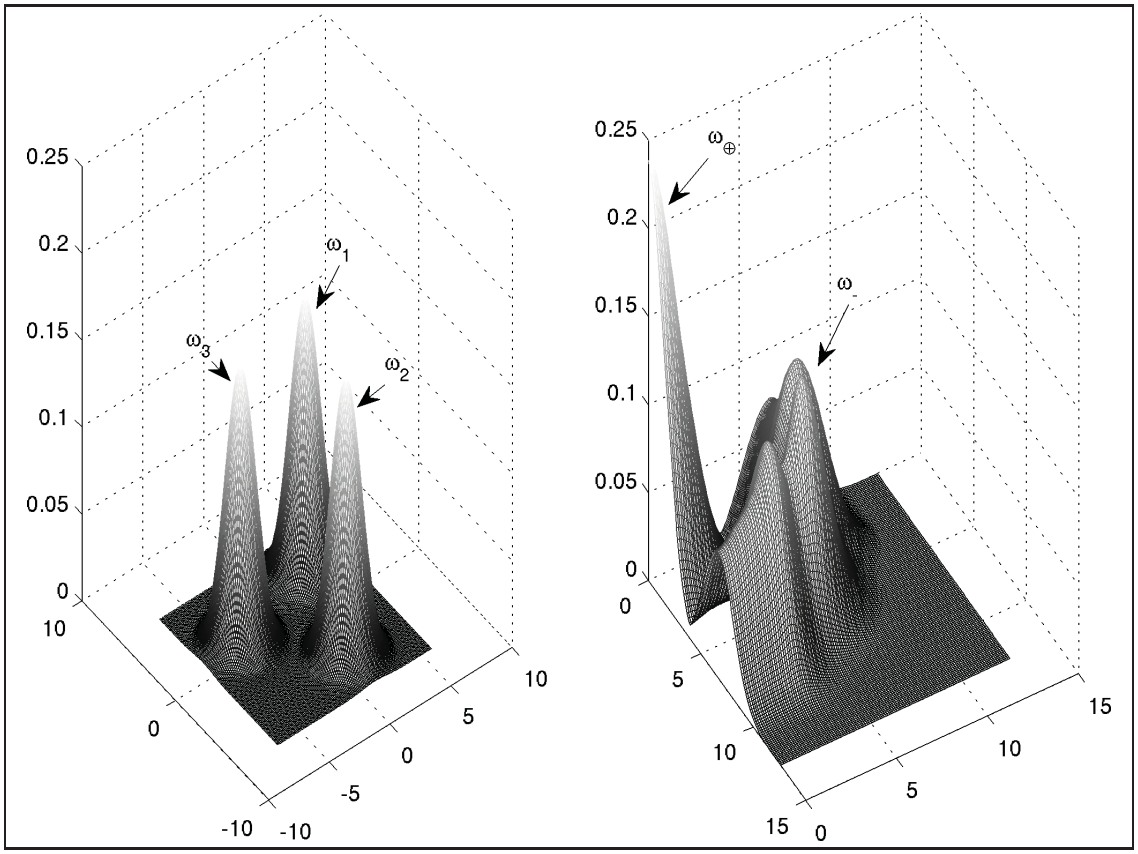

Figure 2.5 : Distributions in feature space (left) projected into distance space by the dichotomy transformation (right).

extract a very large set of potential features to efficiently select a small set of discriminant features in the distance domain.

2.2.2 Questioned Document Expert Approach

The Questioned Document Expert's approach (Santos et al., 2004) is an extension to the dichotomy transformation that applies when users have more than one template stored in the knowledge-base. The idea is to emulate the expert's approach, which consists of comparing the input questioned signature to a set of genuine signatures. Each comparison leads to a partial decision from the expert, his/her final decision being based on all partial decisions. Intuitively,

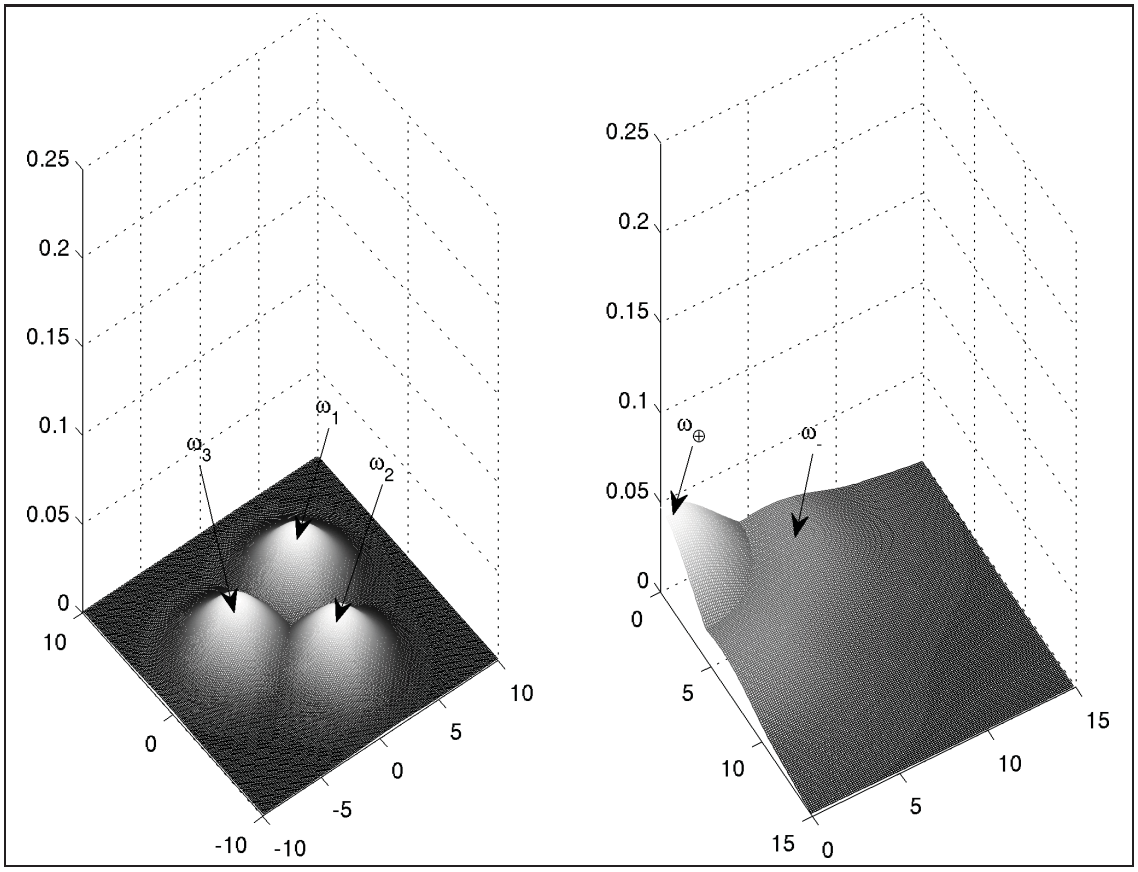

Figure 2.6 : Distributions in feature space (left) projected into distance space by the dichotomy transformation (right) with a larger gaussian distribution parameter Σ.

the more reference signatures available for comparison with the questioned signature, the more accurate the final decision will be.

Formally, the dichotomy transformation is applied between the questioned signature's feature vector $\mathbf{x}_q$ and the user's reference set $\{\mathbf{x}_r\}_1^R$ from the knowledge-base, giving the set of distance vectors $\{\mathbf{u}_r\}_1^R$. The dichotomizer evaluates individually each distance vector and outputs a set of confidence values $\{f(\mathbf{u}_r)\}_1^R$ representing the partial decisions from the expert. The final decision of the system about the questioned signature is based on the fusion of all confidence values by a function $g(\cdot)$. The choice of fusion function is dependent on the nature of the

Table 2.2: Bayesian error (%) in both feature and distance spaces in function of parameter Σ.

Variance Σ	**Feature space (%)**	**Distance space (%)**
$\begin{pmatrix} 1 & 0 \\ 0 & 1 \end{pmatrix}$	0.05	1.76
$\begin{pmatrix} 2 & 0 \\ 0 & 2 \end{pmatrix}$	1.35	10.51
$\begin{pmatrix} 3 & 0 \\ 0 & 3 \end{pmatrix}$	4.15	19.16
$\begin{pmatrix} 4 & 0 \\ 0 & 4 \end{pmatrix}$	7.39	25.92
$\begin{pmatrix} 5 & 0 \\ 0 & 5 \end{pmatrix}$	10.54	31.48

dichotomizer's output. For instance, if the output of the dichotomizer is a label, then the majority vote is an appropriate fusion strategy. On the other hand, if the output of the dichotomizer is a probability, then a wider range of fusion strategies are available such as the sum, mean, median, max and min functions, to name a few.

Specifically in (Santos et al., 2004), four grid-based feature extraction techniques, namely, pixel distribution, pixel density, stroke curvature and stroke slant are used to extract a feature set of 640 features at a single grid scale. Then a multilayer perceptron as a dichotomizer on distance vectors generated from a learning set of 180 writers, using a subset of 40 writers for hold-out validation. Finally, the system is tested on an independent test set of 60 writers. The results demonstrate the validity of the writer-independent approach. However, the recognition rate could benefit from extracting features at different scales.

2.2.3 Ensemble of writer-independent Dichotomizers

In (Bertolini et al., 2010), the original writer-independent offline signature verification framework is improved on by replacing the single dichotomizer by an ensemble of dichotomizers. To achieve ensemble diversity, Support Vector Machines are trained on a learning set of 40

writers using 16 different scales of segmentation grid during feature extraction. The same four grid-based feature extraction techniques of (Santos et al., 2004) are used except for stroke curvature information which is extracted based on cubic Bezier curves. Thus, a pool of 64 Support Vector Machines is overproduced, from which a genetic algorithm chooses a subset to form the final ensemble of dichotomizers. These dichotomizers are combined with the Sum rule fusion strategy.

Different objective functions were tried on the genetic algorithm and the authors conclude that maximization of the Area Under the Receiver Operating Characteristic Curve (AUC) is the more suitable. In all simulations, the fitness of the objective function is evaluated on an independent validation set of 20 writers. The influence of the number of reference signatures in the validation set is evaluated by increasing their numbers from 3 to 15, repeating the ensemble optimization every time. The authors conclude that the authentication rate depends on a tradeoff between the number of references and the intra-class variability of the reference set.

Overall, authentication by ensembles of dichotomizers show an improvement over classification by a single dichotomizer. However, this approach complicates the verification system, specifically in (Bertolini et al., 2010), ensembles count an average of 13 SVMs, using a total of 2300 features and thus increasing the use of resources while reducing recognition speed. Moreover, the ensemble optimization process being stochastic in nature, each run may lead to a different ensemble, as demonstrated by their results.

The gain in authentication is, first and foremost, a result of extracting different features at different scales. However, the features are integrated at the confidence score level and it is generally believed that it is more effective to integrate combined information as early as possible in the verification system (Jain et al., 2004). Integrating combined information at feature level should result in better improvement since at this level information about the signatures is richer.

2.3 Discussion

This chapter reviewed writer-independent signature verification systems based on the dissimilarity representation. To achieve writer-independence, a dissimilarity representation technique known as the dichotomy transformation is used. This technique allows the reduction of a K-class problem into a 2-class problem that is used to train the system's classifier. Then, given a reference signature and a questioned signature, the classifier determines if both signatures were written by the same person. The main advantage of the writer-independent approach is that it tackles two fundamental problems of signature verification:

1) *Large number of users.* By applying the dichotomy transform to a given questioned signature and the reference signatures of the user stored in the knowledge-base, writer-independent distance vectors are obtained. These distance vectors are presented to a writer-independent classifier that have associated small distances to genuine signatures and large distances to forgeries. As such, the references of *any* writer can be used, even from writers that are not part of the training set. Hence, writer-independence implies independence from the number of writers using the verification system, provided at least one reference signature is available for each of these writers.

2) *Limited number of reference signatures for training.* Since dichotomy transform reduces any K-class problem into a 2-class problem learned by the system's classifier, the training set may be composed of signatures collected beforehand from K writers that do not need to be the system users since the classifier is writer-independent. However, the underlying hypothesis is that their signatures are representative of those of the legitimate users of the signature verification system.

However, there is a drawback to the dichotomy transformation; perfectly clustered writers in feature domain may not be perfectly dichotomized in distance domain. This occurs when feature distributions are broadly spread among the writers, with the negative effect that the classifier is able to detect forgeries from genuine signatures (Cha and Srihari, 2000). Thus, the

performance of the classifier is crucially affected by the choice of the feature set extracted from the handwritten signatures. Moreover, because the dichotomy transformation affects the spatial geometry of the distributions, the best feature set may not be the same in feature domain and in distance domain. The solution proposed in this research and presented in the next chapter is to extract a very large set of potential features to efficiently select a small set of discriminant features in the distance domain.

CHAPTER 3

WRITER-INDEPENDENT OFFLINE SIGNATURE VERIFICATION FRAMEWORK

This chapter presents an efficient writer-independent offline signature verification system based on multiple feature extraction techniques. As described in this section, this novel system uses an ensemble of dichotomizers to combine features from across several scales and feature extraction techniques, leading to lighter and more accurate verification systems. As depicted by Figure 3.1 , the proposed system respects the architecture of generic writer-independent signature verification systems. However, as described in the following sections, it uses (i) the Extended Shadow Code and Directional Probability Density Functions techniques at the multiscale feature extraction level, and (ii) the Boosting Feature Selection technique at the classifier level.

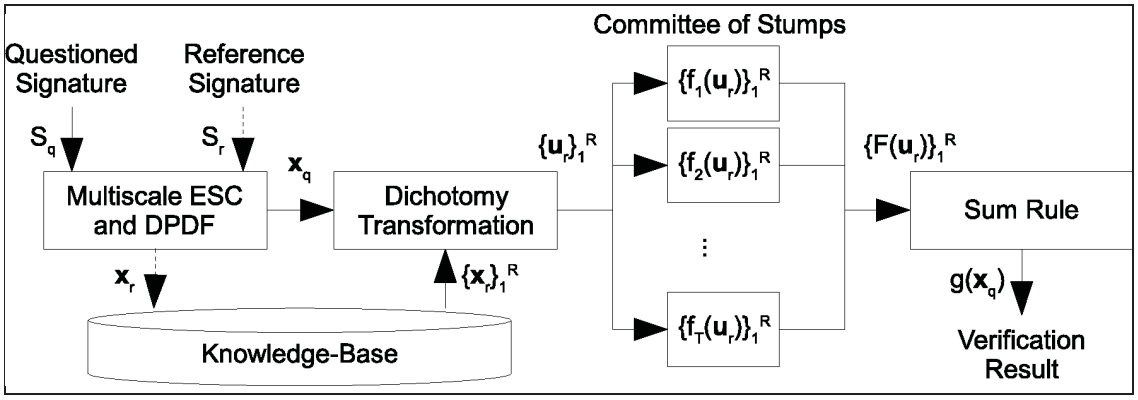

Figure 3.1 : Overview of the proposed writer-independent offline signature verification system with multiscale Extended Shadow Code and Directional Probability Density Functions at the feature extraction and a committee of stumps built by Boosting Feature Selection at the classifier level.

3.1 Multiscale Feature Extraction

Regarding handwritten signatures, it is important for the feature extraction process to be text insensitive. In other words, the measurements taken on signature must not rely on the segmen-

tation of specific letters, a very difficult task especially if the signature is highly personalized (Sabourin and Genest, 1994). A practical alternative is to partition the signatures using a virtual grid and to take local measurements in each of the grid cells. By varying the scale of the virtual grid, nearly global to very local features are extracted. In the literature, grid based approaches generally tend to find a grid scale suitable to their signature database. Here the proposed approach is to extract features at multiple scales and let the classifier select the features most adapted to its needs.

When a new signature is enrolled or questioned, it is presented to the system as a gray-level image. From there, two preprocessing steps are necessary in order to prepare the signature for feature extraction. First, the signature is automatically segmented from its background using Otsu's threshold selection method from gray-level histograms (Otsu, 1979). According to questioned document experts, the proportion and orientation of handwritten signatures are intrinsic characteristics of the writer when guided by a form (Harrison, 1981). Consequently, the second preprocessing step corrects the binary signature images in translation by aligning their centroid with the center of the feature extraction grid.

3.1.1 Fast Extended Shadow Code

The Extended Shadow Code (Sabourin and Genest, 1994), (Sabourin and Genest, 1995) consists in the superposition of bar mask array over the binary image of a handwritten signature as depicted by Figure 3.2 . Each bar is assumed to be a light detector related to a spatially constrained area of the 2D signal. A shadow projection is defined as the simultaneous projection of each black pixel into its closest horizontal, vertical and diagonal bars. Figure 3.3 illustrates each projection in details for a given grid cell. A projected shadow turns on a set of bits distributed uniformly along the bar. After all the pixels on a signature are projected, the number of *on* bits in each bar is counted and normalized to the range of $[0, 1]$.

This section presents the a formal description of the Extended Shadow Code and shows how the technique can be improved with look-up tables to achieve real-time speed. Formally, a binary signature of height M and width N is defined as $\{S(m,n)\}_{1\leq n\leq N}^{1\leq m\leq M}$ where $S(m,n) = 0$ if the

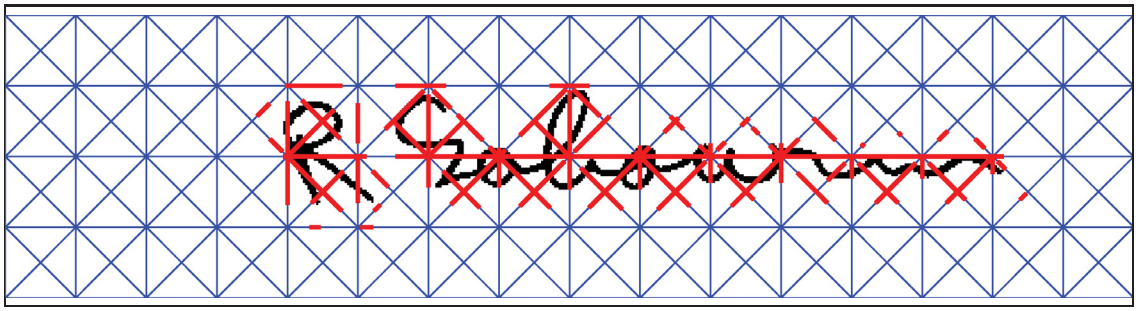

Figure 3.2 : Example of the Extended Shadow Code technique applied to the extraction of features from a binary signature image.

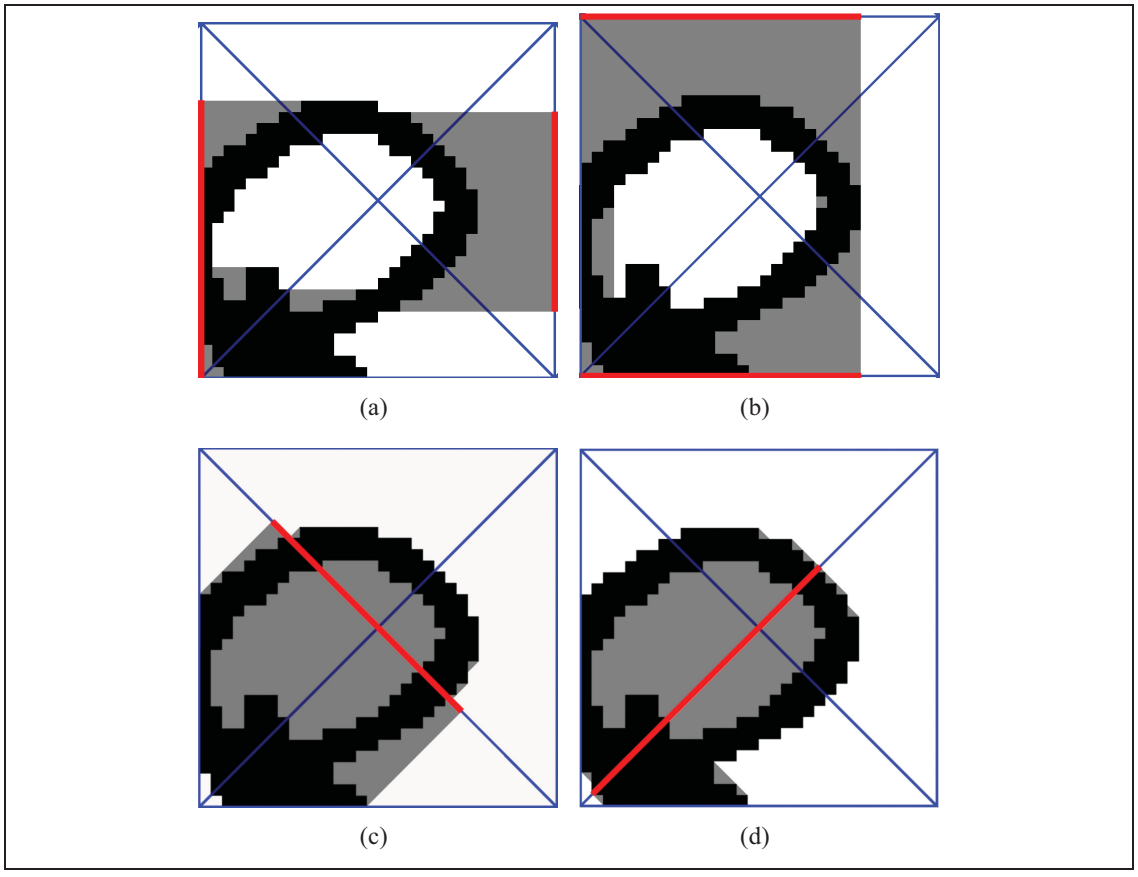

Figure 3.3 : Details of each shadow projection for a given grid cell: (a) horizontal, (b) vertical, (c) main diagonal and (d) secondary diagonal.

pixel at location (m, n) is part of the signature and $S(m, n) = 1$ if it is part of the background. The virtual grid consists of I rows and J columns of cells individually identified $C_{i,j}$. Each cell segments a surface of $M' \times N'$ pixels of the image defined as $\{C(m, n)\}_{1 \le n \le N'}^{1 \le m \le M'}$ where $M' = \frac{M}{I}$ and $N' = \frac{N}{J}$. If necessary, the image is padded with background pixels to make sure M' and N' are integers. The relation between the pixels covered by the grid cell $C_{i,j}$ and those of S is given by

$$C_{i,j}(m, n) = S\big((i-1) \cdot M' + m, (j-1) \cdot N' + n\big). \tag{3.1}$$

Each grid cell is bounded by a bar on its left, right, top and bottom sides plus two extra bars following its main and secondary diagonals, for a total of six bars. The left and right bars make the set of vertical bits $\{B^{\text{vert}}(b)\}_{1 \le b \le 2M'}$ on which dark pixels are projected horizontally and their location (m, n) is defined by

$$\mathbf{B}^{\text{vert}}(b) = \begin{bmatrix} B_m^{\text{vert}}(b) \\ B_n^{\text{vert}}(b) \end{bmatrix}, \tag{3.2a}$$

$$B_m^{\text{vert}}(b) = \begin{cases} b & \text{if } b \le M' \\ b - M' & \text{otherwise} \end{cases}, \tag{3.2b}$$

$$B_n^{\text{vert}}(b) = \begin{cases} \frac{1}{2} & \text{if } b \le M' \\ N' + \frac{1}{2} & \text{otherwise} \end{cases}. \tag{3.2c}$$

Similarly, the top and bottom bars make the set of horizontal bits $\big\{B^{\text{horz}}(b)\big\}_{1 \le b \le 2N'}$ on which dark pixels are projected vertically and their location (m, n) is defined by

$$\mathbf{B}^{\text{horz}}(b) = \begin{bmatrix} B_m^{\text{horz}}(b) \\ B_n^{\text{horz}}(b) \end{bmatrix}, \tag{3.3a}$$

$$B_m^{\text{horz}}(b) = \begin{cases} \frac{1}{2} & \text{if } b \leq N' \\ M' + \frac{1}{2} & \text{otherwise} \end{cases}, \tag{3.3b}$$

$$B_n^{\text{horz}}(b) = \begin{cases} b & \text{if } b \leq N' \\ b - N' & \text{otherwise} \end{cases}. \tag{3.3c}$$

In contrast, shadow projection occurs simultaneously on both diagonal bars. The set of bits of the main diagonal (from upper left to lower right) is defined by $\left\{B^{\text{main}}(b)\right\}_{1 \leq b \leq O}$ where the number of bits $O = \left\lfloor \sqrt{(M')^2 + (N')^2} \right\rceil$, the symbol $\lfloor \cdot \rceil$ being the nearest integer function, and their location (m, n) is defined by

$$\mathbf{B}^{\text{main}}(b) = \begin{bmatrix} B_m^{\text{main}}(b) \\ B_n^{\text{main}}(b) \end{bmatrix}, \tag{3.4a}$$

$$B_m^{\text{main}}(b) = \frac{M'}{O} b - \frac{M'}{2O}, \tag{3.4b}$$

$$B_n^{\text{main}}(b) = \frac{N'}{O} b - \frac{N'}{2O}. \tag{3.4c}$$

Similarly, the set of bits of the secondary diagonal (from lower left to upper right) is defined by $\{B^{\text{seco}}(b)\}_{1 \leq b \leq O}$ and their location (m, n) is defined by

$$\mathbf{B}^{\text{seco}}(b) = \begin{bmatrix} B_m^{\text{seco}}(b) \\ B_n^{\text{seco}}(b) \end{bmatrix}, \tag{3.5a}$$

$$B_m^{\text{seco}}(b) = \frac{M'}{O}(O - b + 1) - \frac{M'}{2O}, \tag{3.5b}$$

$$B_n^{\text{seco}}(b) = \frac{N'}{O}(O - b + 1) - \frac{N'}{2O}. \tag{3.5c}$$

Figure 3.4 illustrates the disposition of the light detectors inside a grid cell along with the indices of their bits.

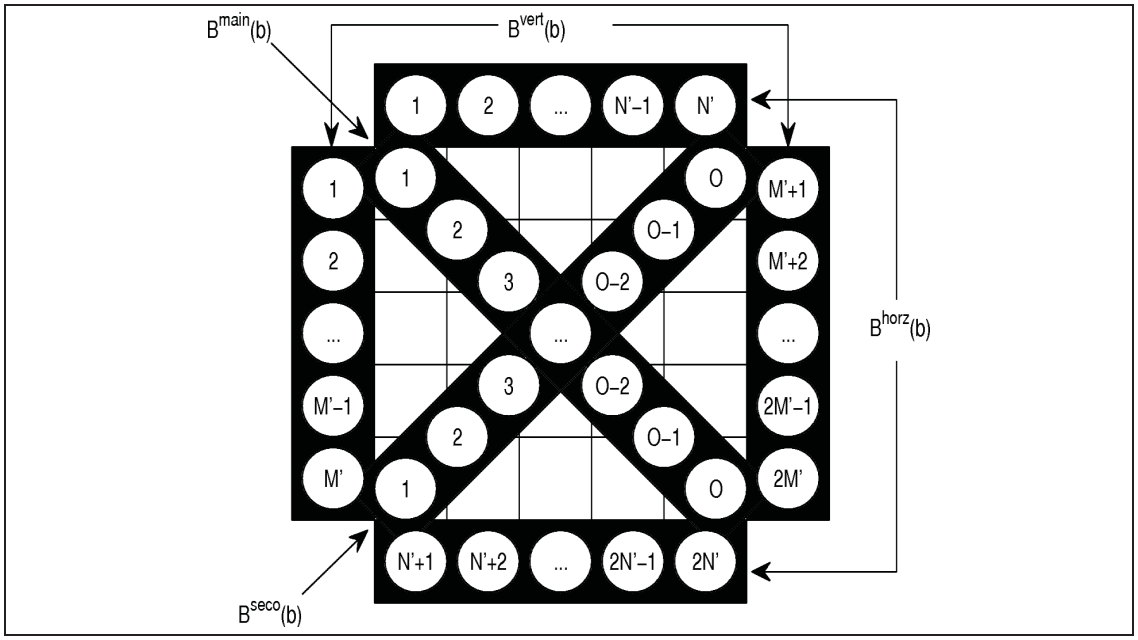

Figure 3.4 : Disposition of the light detectors $\mathbf{B}^{\text{vert}}$, $\mathbf{B}^{\text{horz}}$, $\mathbf{B}^{\text{main}}$ and $\mathbf{B}^{\text{seco}}$ inside a grid cell along with the indices of their bits.

The shadow projection occurs simultaneously into the four sets of bits previously defined. In their normal state, the bits are turned off $B(b) = 0$ and a dark pixel $C(m, n) = 0$ at location (m, n) defined as the vector $\mathbf{C}$ turns on the closest bit b^* of each set such as

$$b^* = \arg\min_b \|\mathbf{C} - \mathbf{B}(b)\|, \tag{3.6a}$$

$$B(b^*) = 1, \tag{3.6b}$$

where the operator $\|\cdot\|$ is the Euclidean distance. Figure 3.5 shows, for the four simultaneous shadow projections, the value of b^* at every position (m, n) according to the cell previously illustrated in Figure 3.4 .

Traditional Extended Shadow Code is computationaly expensive since the distances from each dark pixel to all bits of the bar mask have to be computed to determine which is the nearest bit. By noting that for any given pixel the nearest bits of the bar mask are always the same, Figure 3.5 can be used as look-up tables of the nearest bits whenever a dark pixel is encountered, thus greatly reducing the computational burden of the feature extraction technique.

Since light detectors on the boundary of two grid cells detect dark pixels in both cells, juxtaposed cells must share turned on bits such as

$$B^{\text{vert}}_{i,j}(b) \leftarrow B^{\text{vert}}_{i,j}(b) \vee B^{\text{vert}}_{i,j-1}(b + M'), 1 \leq b \leq M', 1 \leq i \leq I, 2 \leq j \leq J, \tag{3.7a}$$

$$B^{\text{horz}}_{i,j}(b) \leftarrow B^{\text{horz}}_{i,j}(b) \vee B^{\text{horz}}_{i-1,j}(b + N'), 1 \leq b \leq N', 2 \leq i \leq I, 1 \leq j \leq J, \tag{3.7b}$$

where the operator $\vee$ is a logical disjunction. For a given cell (i, j) and its eight neighbors, Figure 3.6 (a) illustrates with continuous lines the two boundaries where the information exchange takes place.

Once shadow projection is completed, features are extracted from the light detectors. Each grid cell yields four features such as

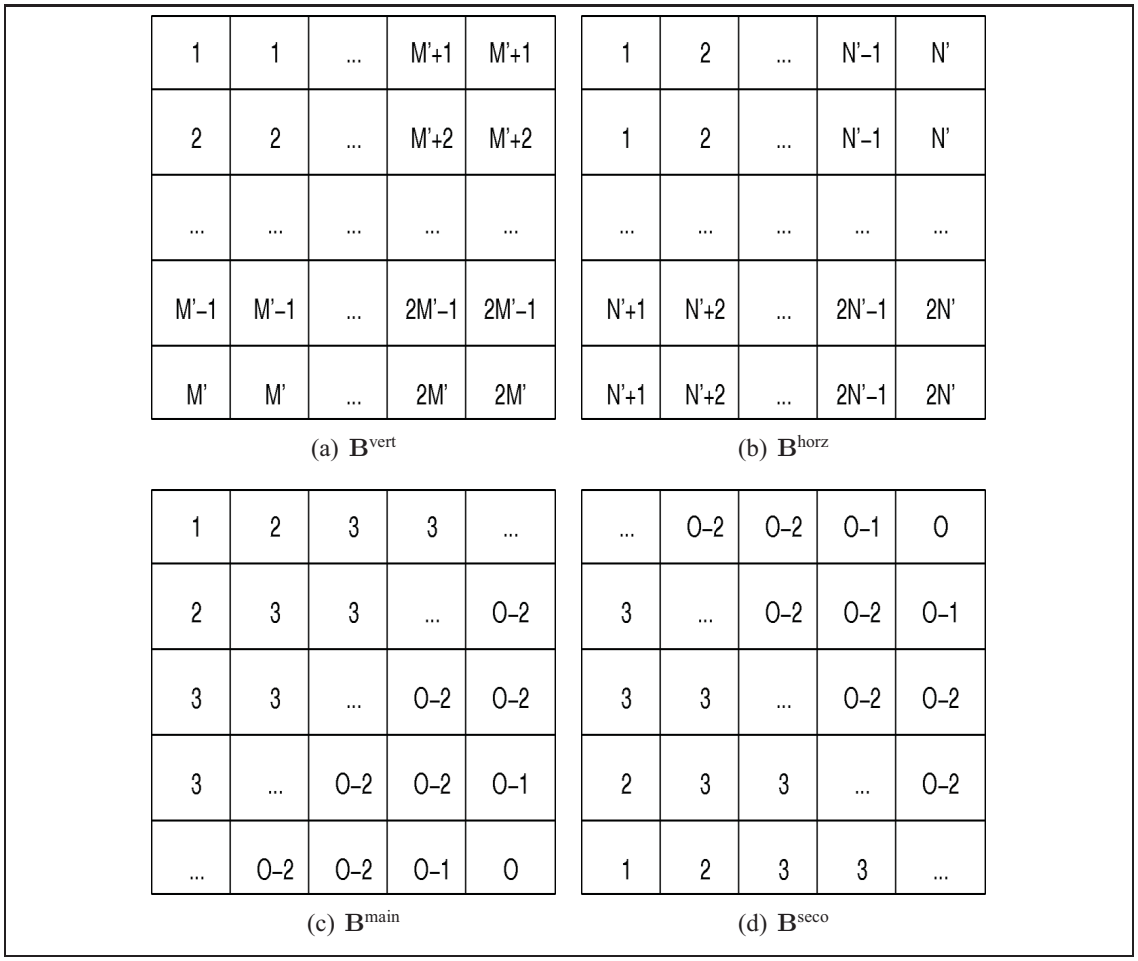

1	1	...	M'+1	M'+1
2	2	...	M'+2	M'+2
...	...	...	...	...
M'–1	M'–1	...	2M'–1	2M'–1
M'	M'	...	2M'	2M'

(a) $\mathbf{B}^{\text{vert}}$

1	2	...	N'–1	N'
1	2	...	N'–1	N'
...	...	...	...	...
N'+1	N'+2	...	2N'–1	2N'
N'+1	N'+2	...	2N'–1	2N'

(b) $\mathbf{B}^{\text{horz}}$

1	2	3	3	...
2	3	3	...	O–2
3	3	...	O–2	O–2
3	...	O–2	O–2	O–1
...	O–2	O–2	O–1	O

(c) $\mathbf{B}^{\text{main}}$

...	O–2	O–2	O–1	O
3	...	O–2	O–2	O–1
3	3	...	O–2	O–2
2	3	3	...	O–2
1	2	3	3	...

(d) $\mathbf{B}^{\text{seco}}$

Figure 3.5 : Values of b^* at every position (m, n) obtained for the four simultaneous shadow projections, according to the cell illustrated in Figure 3.4 .

$$x^{\text{vert}} = \frac{1}{M'} \sum_{b=1}^{M'} B^{\text{vert}}(b), \tag{3.8a}$$

$$x^{\text{horz}} = \frac{1}{N'} \sum_{b=1}^{N'} B^{\text{horz}}(b), \tag{3.8b}$$

$$x^{\text{main}} = \frac{1}{O} \sum_{b=1}^{O} B^{\text{main}}(b), \tag{3.8c}$$

$$x^{\text{seco}} = \frac{1}{O} \sum_{b=1}^{O} B^{\text{seco}}(b) \tag{3.8d}$$

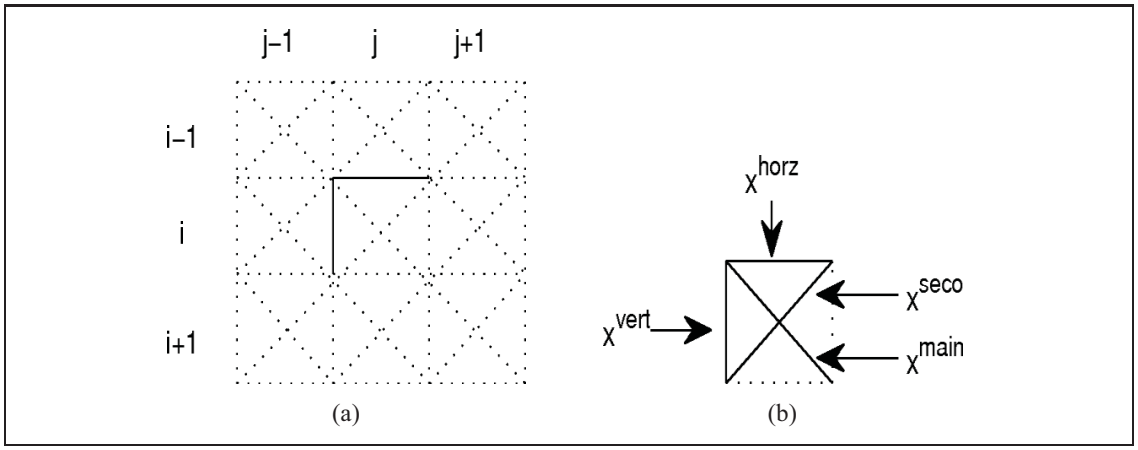

Figure 3.6 : (a) For a given cell (i, j) and its eight neighbors, the information exchange takes place at the two boundaries represented by continuous lines. (b) Location of the four features extracted from each grid cell.

and illustrated by Figure 3.6 (b). The feature vector extracted from the whole signature image consists of the concatenation of the feature extracted from each cell (i, j) such as

$$\mathbf{x}^{\text{ESC}} = \bigcup_{i=1}^{I}\bigcup_{j=1}^{J}\left\{x_{i,j}^{\text{vert}}, x_{i,j}^{\text{horz}}, x_{i,j}^{\text{main}}, x_{i,j}^{\text{seco}}\right\}\bigcup_{i=1}^{I}\left\{x_{i,J+1}^{\text{vert}}\right\}\bigcup_{j=1}^{J}\left\{x_{I+1,j}^{\text{horz}}\right\} \tag{3.9}$$

Notice that in the case of x^{vert}, the extraction process goes up to column $J + 1$ to account for the last vertical bar at the extreme right of the grid. Similarly, the extraction process goes up to row $I + 1$ to account for the last x^{horz} at the bottom of the grid. Thus, the cardinality of the Extended Shadow Code feature vector is equal to

$$\left|\mathbf{x}^{\text{ESC}}\right| = 4IJ + I + J. \tag{3.10}$$

3.1.2 Local Directional Probability Density Functions

Directional Probability Density Functions (Drouhard et al., 1996) have been used as a global shape factor for automatic offline handwritten signature verification. The rationale of this ap-

proach is that the stroke orientation of handwritten signatures is stable enough to properly discriminate writers. Thus this technique extracts features based on the frequency distribution of the orientation of the gradient at the edge of the signature. Gradient features are used by other signature verification systems, for instance (Kalera et al., 2004b).

The approach described therein innovates by extracting local Directional Probability Density Functions from within each cell of a virtual grid placed over the handwritten signature image. This way, local information is extracted from different parts of the signature, consequently increasing its discriminating power. Moreover, the information extracted from the signature is complementary to that extracted using the Extended Shadow Code technique. While the Extended Shadow Code extracts information about the spatial distribution of the signature, Directional Probability Density Functions extracts information about the orientation of the strokes. Since the same grid scale is used for both techniques, this leads to a powerful spatio-directional representation of handwritten signatures.

The gradient is computed from the binarized version of the signature image after it has been smoothed using a 3×3 normalized, rotationally symmetric, Gaussian lowpass filter with standard deviation $\sigma = 0.5$ defined by

$$G_{\text{LPF}}(m, n) = e^{-\delta^2(m,n)/2\sigma^2} \tag{3.11}$$

where $\delta(m, n)$ is the Euclidean distance from the center of the filter. The Gaussian lowpass filter reduces the impact that residual noise can have on the two key derivatives used for gradient computation. It may seems counter-intuitive to compute the gradient on a smoothed binary image when its gray-level version is available but this approach has the definitive advantage that the intensity of the image is already normalized, consequently there is no need of a threshold to detect the edges of the image. In fact, the binary segmentation process has already managed to detect the edges of the signature and the remaining task is to determine their orientation.

The gradient measures the first derivatives of an image within a small neighborhood of each pixel. This research uses Sobel operators, illustrated in Figure 3.7 , to compute the gradient vertical and horizontal components.

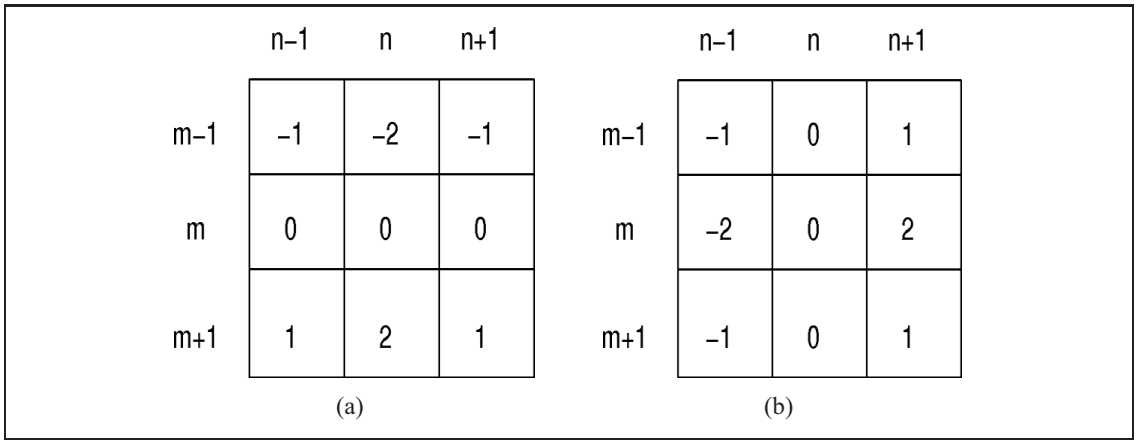

Figure 3.7 : Sobel operator masks used for convolution: (a) vertical component, and (b) horizontal component.

Formally, for an image $S(m,n)$ of size $M \times N$, each pixel neighborhood is convolved with both masks to determine vertical and horizontal components G_m and G_n, respectively

$$G_m(m,n) = S(m+1,n+1) + 2S(m+1,n) + S(m+1,n-1) - S(m-1,n+1) - 2S(m-1,n) - S(m-1,n-1), \quad (3.12a)$$

$$G_n(m,n) = S(m+1,n+1) + 2S(m+1,n) + S(m+1,n-1) - S(m-1,n+1) - 2S(m-1,n) - S(m-1,n-1). \quad (3.12b)$$

Then the magnitude of the gradient vector is equal to

$$\mathrm{mag}\,(m,n) = \sqrt{G_m^2\,(m,n) + G_n^2\,(m,n)} \tag{3.13}$$

and its direction is calculated as

$$\mathrm{ang}\,(m,n) = \tan^{-1}\frac{G_m\,(m,n)}{G_n\,(m,n)}. \tag{3.14}$$

Figure 3.8 illustrates the gradient of a handwritten signature image using arrows to indicate its direction and magnitude at each pixel location. Since the signature consists of a binary image, gradient is null in the background of the image and within the strokes of the signature where intensity is constant. Gradient is non-null along the edges of the signature and its direction varies perpendicularly to the contour of the signature.

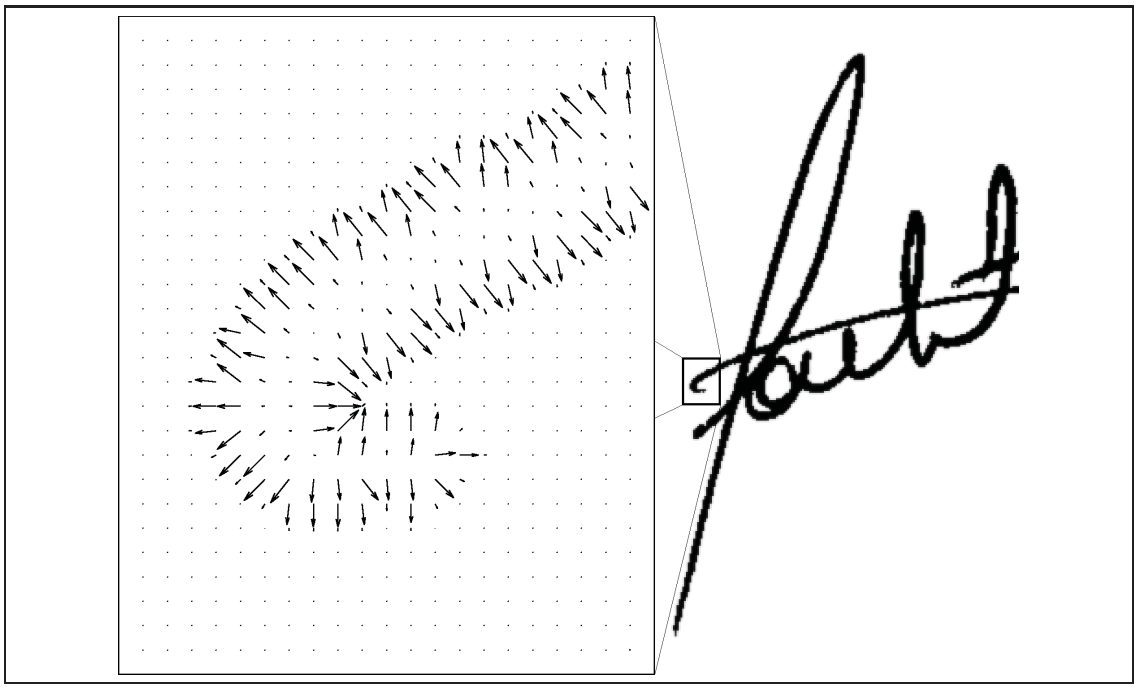

Figure 3.8 : Example of a gradient representation. Arrows indicates direction and magnitude of the gradient at each pixel location.

In order to obtain a fixed number of features, gradient directions are quantized into an even Φ number of ranges by the quantization function:

$$\mathrm{qnt}\,(m,n) = \left\lfloor \frac{\mathrm{ang}\,(m,n) + \pi/\Phi}{\Phi} \right\rfloor + 1 \tag{3.15}$$

where $\lfloor \cdot \rfloor$ is the floor function. A greater Φ results into a more exact representation of the gradient of the signature, thus increasing between-writers discrimination. However, the more exact the representation, the more sensitive it is to intra-personal variance, thus lowering generalization capabilities. As a tradeoff, this research uses $\Phi = 8$ as depicted by Figure 3.9 .

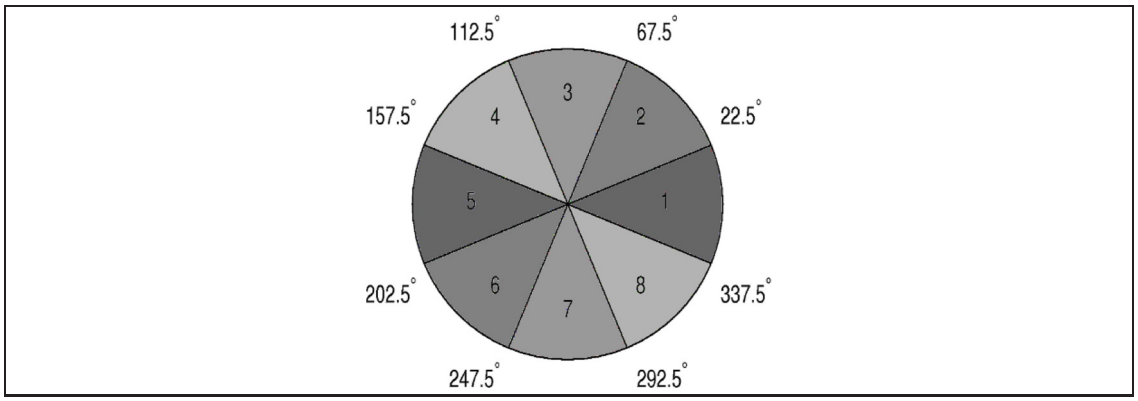

Figure 3.9 : Example of quantized values over a full circle for a quantization process with $\Phi = 8$.

Since the objective of this feature extraction technique is to extract the orientation of the strokes composing the signature, it is important to realize that for any stroke orientation there are two admissible quantized values. For example, in Figure 3.9 both values 1 and 5 refer to an horizontal gradient, thus a vertical stroke; the whole quantization process is depicted in Figure 3.10 for a given signature.

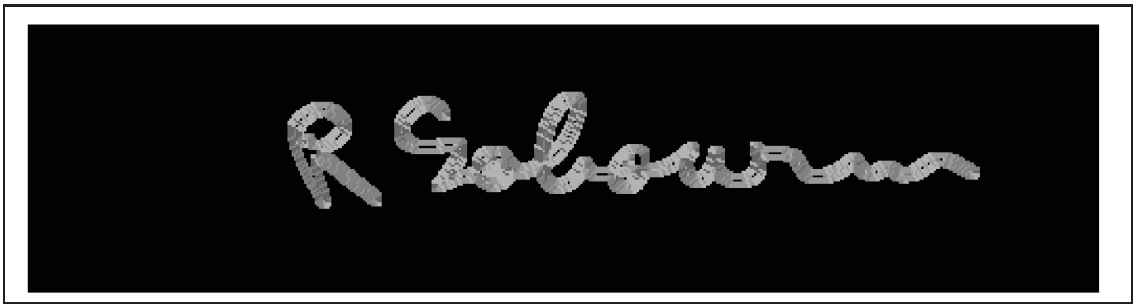

Figure 3.10 : Example of signature where the gradiant angle has been quantized according to the process depicted in Figure 3.9 .

Generally speaking, given an even Φ number of ranges and a quantized value ϕ comprised between $\left[1, \frac{\Phi}{2}\right]$, both ϕ and $\phi + \frac{\Phi}{2}$ indicate the same stroke orientation. Consequently, each cell (i, j) of the virtual grid partitioning the signature image yields a $\frac{\Phi}{2}$ elements feature vector $\mathbf{x}_{i,j}^{\text{DPDF}}$ where element $x_{i,j}^{\text{DPDF}}(\phi)$ is the sum of the gradient magnitude at all location (m, n) where the quantized gradient direction is either ϕ or $\phi + \frac{\Phi}{2}$. Formally,

$$x_{i,j}^{\text{DPDF}}(\phi) = \sum_{\text{qnt}(m,n) \in \left\{\phi, \phi + \frac{\Phi}{2}\right\}} \text{mag}(m, n) \tag{3.16}$$

where $1 \leq \phi \leq \frac{\Phi}{2}$. The feature vector extracted from the whole image is given by

$$\mathbf{x}^{\text{DPDF}} = \bigcup_{i=1}^{I} \bigcup_{j=1}^{J} \bigcup_{\phi=1}^{\Phi/2} \left\{x_{i,j}^{\text{DPDF}}(\phi)\right\} \tag{3.17}$$

and has a cardinality of

$$\left|\mathbf{x}^{\text{DPDF}}\right| = \frac{1}{2} I J \Phi. \tag{3.18}$$

3.2 Boosting Feature Selection

Boosting is a machine-learning procedure which combines the performance of many weak classifiers into a powerful committee. The rationale behind boosting is that finding many moderately inaccurate rules of thumb using many simple classifiers can be easier than finding a single highly accurate prediction rule using a more elaborate learning algorithm. Boosting methods have proved to be very competitive in terms of generalization in a variety of applications (Schapire, 2003). The general idea of boosting is to form a committee of weak classifiers iteratively by adding one weak classifier at a time. At the beginning of the training procedure, a uniform weighting is assigned to the patterns of the training data set. Each time a new classifier is added to the committee, the samples in the training data are reweighted to reflect the performance of this weak classifier, assigning more importance to misclassified samples. Thus, the next weak classifier focuses on more difficult samples and the procedure ends after a predefined number of weak classifiers have been trained.

The problem of feature selection is defined as follows: given a set of potential features, the objective is to select the best subset under some classification objectives. This procedure has three goals: (i) to reduce the cost of extracting features, (ii) to improve the classification accuracy, and (iii) to improve the reliability of the estimate of performance (Kudo, 2000). The Boosting Feature Selection algorithm (Tieu and Viola, 2004) (and further studied in (Redpath and Lebart, 2005)) explicitly incorporates feature selection into AdaBoost (Freund and Schapire, 1996), the most commonly used variant of boosting. Boosting Feature Selection is performed by designing a weak classifier that selects the single most discriminant feature of a set of potential features and finds a threshold to separate the two classes to learn, effectively a decision stump. Consequently, features are selected in a greedy fashion according to the weighting *while* learning is conducted by the boosting algorithm. Given a very large set of features, the result is a committee built on the best subset of features representing the training data.

The next sections describe the boosting algorithm and the weak classifier used in this research and are followed by a complexity study of the resulting committee.

3.2.1 Gentle AdaBoost

The problem of handwritten signature verification can have a significant class overlap, especially between genuine signatures and simulated forgeries, and as mentioned previously the dichotomy transformation can exacerbate this phenomenon. Also, it has been observed by several authors that AdaBoost is not an optimal method on very noisy problems (Dietterich, 2000), (Rätsch et al., 2001), (Servedio, 2003). By design, Adaboost focuses on misclassified samples and this may result in fitting the noise.

Several boosting methods address the overfitting problem, mostly by adjusting the weighting scheme. For instances, MadaBoost (Domingo and Watanabe, 1999) bounds the weight assigned to each sample by its initial probability, Gentle AdaBoost (Friedman et al., 2000) takes adaptive Newton steps to update the weights more slowly, BrownBoost (Freund, 2001) uses a non-monotone weighting function decreasing the weight of samples far from the margin, AdaBoost$_\tau$ (Rätsch et al., 2001) and AdaBoost$^*_\nu$ (Rätsch and Warmuth, 2005) both uses the concept of soft margin to regularize by allowing for misclassification, SmoothBoost (Servedio, 2003) constructs smooth distributions which do not put too much weight on any single sample and NadaBoost (Nakamura et al., 2004) prevents too high weight values by thresholding.

Moreover, validation sets have long been used in machine learning to limit overfitting, and, as noted by the authors of AdaBoost (Freund and Schapire, 1997), a validation set could be used for early stopping. This research makes use of Gentle AdaBoost and early stopping to address the significant class overlap problem. Early stopping is implemented using a hold-out validation set. The early stopping criterion is based on the maximization of area under the receiver operating characteristics curve (AUC, see Section 3.2.4) on the hold-out validation set.

Algorithm 3.1 describes Gentle AdaBoost with early stopping. Let $\mathcal{L} = \{\mathbf{u}_l, v_l, w_l\}_1^L$ be a learning set of L feature vectors $\mathbf{u}_l \in \mathbb{R}^D$ labelled to $v_l \in \{-1, 1\}$ and weighted by the distribution $w_l \in [0, 1], \sum_{l=1}^{L} w_l = 1$. Similarly, let $\mathcal{H} = \{\mathbf{u}_h, v_h\}_1^H$ be a hold-out validation set of H non-weighted samples. Let also $T_\mathcal{L}, T_\mathcal{H} \in \mathbb{N}$ be the maximum iteration stopping criterion

and the early stopping criterion, respectively. The first half of the algorithm implements the four steps of the Gentle AdaBoost algorithm: (i) train a new decision stump $f_t(\mathbf{u})$ based on $\mathcal{L}$, (ii) add $f_t(\mathbf{u})$ to the committee $F(\mathbf{u})$, (iii) update the weights w_l according to the response of $f_t(\mathbf{u}_l)$, and (iv) renormalize the weights to ensure a distribution. The second half implements a hold-out validation scheme using the AUC for criterion. The AUC is computed using Algorithm 2 described in (Fawcett, 2006). If the algorithm reaches $T_{\mathcal{H}}$ iterations without increase of the AUC, it early stops. The Gentle AdaBoost with early stopping procedure outputs the committee $F(\mathbf{u})$ composed of T decision stumps.

Inputs: Learning set $\mathcal{L} = \{\mathbf{u}_l, v_l\}_1^L$, hold-out validation set $\mathcal{H} = \{\mathbf{u}_h, v_h\}_1^H$, early stopping criterion $T_{\mathcal{H}}$, maximum iteration stopping criterion $T_{\mathcal{L}}$.
Output: Classifier $\operatorname{sign}[F(\mathbf{u})] = \operatorname{sign}\left[\sum_{t=1}^{T} f_t(\mathbf{u})\right]$.
Initialize: $w_l = 1/L$, $F = 0$, $A_{\text{max}} = -\infty$.
for $t = 1$ to $T_{\mathcal{L}}$ **do**
    /* Gentle AdaBoost algorithm */
    Train $f_t(\mathcal{L}, w)$.
    Update $F \leftarrow F + f_t$.
    Update $w_l \leftarrow w_l \exp(-v_l f_t(\mathbf{u}_l))$.
    Renormalize $w_l \leftarrow w_l / w_{\text{tot}}$, where $w_{\text{tot}} = \sum_l w_l$.
    /* Early stopping check */
    if $\operatorname{AUC}(\mathcal{H}, F) > A_{\text{max}}$ **then**
        Update $A_{\text{max}} = \operatorname{AUC}(\mathcal{H}, F)$.
        Update $T = t$.
        Reset $counter = 0$.
    else
        Increment $counter \leftarrow counter + 1$.
        if $counter = T_{\mathcal{H}}$ **then**
            Exit by early stopping.
        end if
    end if
end for

Algorithm 3.1: **Gentle AdaBoost algorithm with early stopping.**

3.2.2 Decision Stumps

Decision trees classify a pattern through a sequence of questions (Duda et al., 2001). Each question tests a single feature of the data and is represented by a tree node, the first question being the root of the tree and each possible decision spanning a branch to new node (i.e. the next question) and so on until a terminal node, called a leaf, is reached and the pattern is classified. Each decision outcome is called a split since it effectively splits the data into subsets, binary decisions being referred to as single-splits and higher number of decisions as multi-splits. Decision stumps are one-level, single-split trees (Iba and Langley, 1992).

Formally, a decision stump $f_t(\mathbf{u})$ is composed of four parameters: d_t the dimension to split, τ_t the splitting threshold in that dimension, and ρ_t^{left}, ρ_t^{right} the weighted means of the response for the left and right leaves, respectively. Figure 3.11 illustrates these parameters and algorithm 3.2 describes the decision stump learning algorithm. The first step in the algorithm is to compute $W_{\oplus}$, $W_{\ominus}$ the positive and negative weight totals, respectively. Then the algorithm independently searches each problem dimension to find the best split-point (d_t, τ_t). For a given dimension, the samples are first sorted by increasing feature values, then the algorithm computes $w_{\oplus}$, $w_{\ominus}$ the positive and negative weight cumulative distribution functions, respectively. Based on the CDFs and the weight totals, the splitting threshold is selected to minimize the probability that a training sample would be misclassified. Once the split-point is optimized, the algorithm computes the weighted means of the response for both leaves.

When presented a sample $\mathbf{u}$ to classify, the decision stump $f_t(\mathbf{u})$ thresholds the feature d_t of $\mathbf{u}$ at τ_t and assigns the sample to the corresponding leave. Formally:

$$f_t(\mathbf{u}) = \begin{cases} \rho_t^{left} & \text{if } u_{d_t} < \tau_t \\ \rho_t^{right} & \text{otherwise.} \end{cases} \tag{3.19}$$

Decision stumps typically have high bias and low variance. However, boosting algorithms are capable of both bias and variance reduction, hence the increase in performance from committee

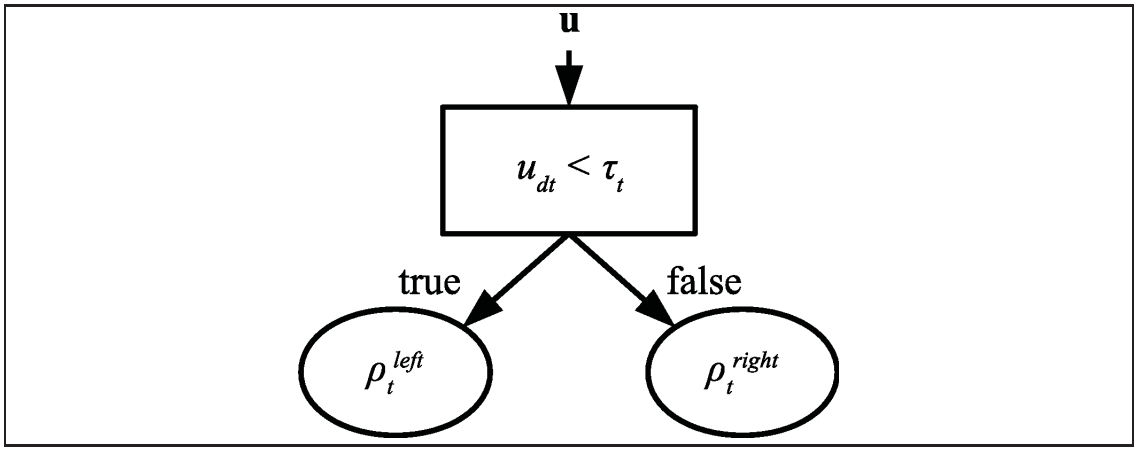

Figure 3.11 : Illustration of a decision stump.

of stumps (Friedman et al., 2000). Moreover, when boosting implements a reweighting strategy (as opposed to resampling), like it is the case for Gentle AdaBoost, decision stumps cause boosting to become deterministic in the sense that multiple runs on the same learning set will result in identical committees. Also, the order of presentation of the samples and of the features of the learning set does not affect the resulting committees. Finally, following (3.19), a decision stump classifies a pattern using a single feature. This means that boosting decision stumps will greedily select informative features *while* building the committee, ignoring redundant and irrelevant features. It is worth noting that the committee may learn several stumps based on the same feature, each with a different decision threshold and response. Appendix I contains an illustrative example of the boosting decision stumps process.

3.2.3 Complexity analysis

Suppose a committee composed of T decision stumps built from a two-class D-dimensional problem with training and validation datasets of $L = |\mathcal{L}|$ and $H = |\mathcal{H}|$ patterns, respectively. Let t_1 be the time taken to perform an addition, substraction or comparison, and t_2 the time for a multiplication, division or exponentiation. For the purpose of this analysis, suppose that later operations are an order of magnitude greater than the former such as $t_2 = 10t_1$.

Inputs: Pre-sorted weighted learning set $\mathcal{L} = \{\mathbf{u}_l, v_l, w_l\}_1^L$.
Output: Decision stump $f_t(\mathbf{u})$ with parameters d_t, τ_t, ρ_t^{left} and ρ_t^{right}.
Initialize: ρ_t^{left}, $\rho_t^{right} \leftarrow 0$, and local variables $\varepsilon_{tot} \leftarrow \infty$, $W_\oplus$, $W_\ominus$, W_{left}, $W_{right} \leftarrow 0$.
/* Compute total positive and negative weights */
$W_\oplus = \sum_l w_l$ where $v_l = 1$
$W_\ominus = 1 - W_\oplus$
/* Find the best split point for this learning set */
for $d = 1$ to D **do**
  Sort $\mathcal{L}$ by increasing u_d values
  $w_\oplus \leftarrow 0$, $w_\ominus \leftarrow 0$
  for $l = 1$ to $L - 1$ **do**
    if v_l is a positive sample **then**
      $w_\oplus \leftarrow w_\oplus + w_l$
    else
      $w_\ominus \leftarrow w_\ominus + w_l$
    end if
    if $u_{l,d} \neq u_{l+1,d}$ **then**
      $\varepsilon_{left} \leftarrow 1 - \max\{w_\oplus, w_\ominus\}$
      $\varepsilon_{right} \leftarrow 1 - \max\{W_\oplus - w_\oplus, W_\ominus - w_\ominus\}$
      if $\varepsilon_{left} + \varepsilon_{right} < \varepsilon_{tot}$ **then**
        $\varepsilon_{tot} \leftarrow \varepsilon_{left} + \varepsilon_{right}$
        $d_t \leftarrow d$
        $\tau_t \leftarrow \frac{u_{l,d} + u_{l+1,d}}{2}$.
      end if
    end if
  end for
end for
/* Compute weighted means of the response in the left and right leaves of the stump */
$\rho_t^{left} = \sum_l w_l \cdot v_l / \sum_l w_l$ where $u_{l,d_t} < \tau_t$
$\rho_t^{right} = \sum_l w_l \cdot v_l / \sum_l w_l$ where $u_{l,d_t} \geq \tau_t$
end

Algorithm 3.2: **Decision stump learning algorithm.**

During testing, a decision stump classifies (3.19) an input distance vector regardless of the number of features, and thus has a constant time complexity of t_1. A committee of stumps repeats this operation T times and then sums the $T - 1$ responses from the stumps. Thus, the total worst-case time required to classify an input vector using the committee in a normalized format is $\frac{t_{test}^{wc}}{t_1} = (2T - 1)$. The corresponding growing rate, valid when $T \gg 1$, is $\mathcal{O}(T)$,

making for very fast classification during the operation phase. By comparison, Radial Basis Function kernel Support Vector Machine (RBF-SVM) classification time complexity scales to $\mathcal{O}(DN_s)$ (Burges, 1998), where N_s is the number of support vectors. For noisy problems such as writer-independent signature verification, the set N_s increases dramatically and causes a major slowdown for SVM during operation. On the other hand, the boosting approach does not suffer from this inconvenience. Moreover, when working with high-dimensional databases such as in this research, $D \gg T$, which makes the boosting approach an attractive alternative to SVMs.

During training, the total worst case time required to learn with Gentle AdaBoost and early stopping includes the time for quicksort, training decision stumps, and computing the AUC. Using quicksort algorithm (Hoare, 1989), the worst case time to sort the values of one feature is

$$t_{sort}^{wc} = \left(\frac{L^2}{2} + \frac{L}{2}\right) t_1 \tag{3.20}$$

Once values are sorted, training a decision stump (see Algorithm 3.2) has a worst case time of

$$\begin{aligned} t_{stump}^{wc} &= (13D(L-1) + 5L)\, t_1 + (D(L-1) + L + 2)\, t_2 \\ &= (23DL - 23D + 15L + 20)\, t_1 \end{aligned} \tag{3.21}$$

The algorithm to compute the area under an ROC curve (Fawcett, 2006) has a worst case time of

$$\begin{aligned} t_{AUC}^{wc} &= t_{sort}^{wc} + (5H+3)t_1 + (2H+4)t_2 \\ &= \left(\frac{H^2}{2} + \frac{51H}{2} + 43\right) t_1 \end{aligned} \tag{3.22}$$

Thus the total worse case time required to perform the Gentle AdaBoost with early stopping in a normalized format (see Algorithm 3.1) is expressed by:

$$\begin{aligned} t_{GAB}^{wc} &= Dt_{sort} + Tt_{stump} + Tt_{AUC} + (TL + 2L + T)t_1 + 4Lt_2 \\ \frac{t_{GAB}^{wc}}{t_1} &= \frac{DL^2}{2} + \frac{H^2T}{2} + \frac{DL}{2} + \frac{51HT}{2} + 23DLT - 23DT + 16LT + 42L + 64T \end{aligned} \tag{3.23}$$

and the corresponding growth rate, when $D, L, T \gg 1$, is:

$$\mathcal{O}(DL^2 + TH^2 + DTL). \tag{3.24}$$

By comparison, the time complexity of computing a RBF kernel matrix for a SVM scales to $\mathcal{O}(DL^2)$ (Burges, 1998), not including the time spent on parameters selection.

It is worth noting that quicksort does much better in the average case with $t_{sort}^{ave} \approx L \log L$. Thus, the growth rate of the average case time complexity of the Gentle AdaBoost with early stopping is $\mathcal{O}(DLT)$. In computer simulations, the authors have observed the average case analysis to be more representative of the reality than the worst case analysis. Considering this, when working with large databases such as in this research, $L \gg T$, which makes the boosting approach a method of choice since $\mathcal{O}(DLT)$ grows significantly slower than $\mathcal{O}(DL^2)$ making the Gentle AdaBoost with early stopping a fast learning algorithm that scales linearly. Our simulations with SVMs were executed on the same machine as for Boosting Feature Selection, a dual-core Opteron 875 running at 2.2GHz with 32GB of memory, using the small and

medium single scale resolution datasets presented in this research at Chapter 4. By comparing execution durations, the SVM approach increased the time complexity by two and three orders of magnitude for learning and testing, respectively, thus confirming the theoretical complexity analysis presented herein. Given that the Boosting Feature Selection approach took 2 days to learn the largest of the multiscale datasets used in this research, the learning time of the SMV approach can be estimated to require up to 6 months, a prohibitive duration for most applications. Finally, the committee resulting from the Boosting Feature Selection approach classifies up to 4800 samples per second while the SVM classifier would classify only 5 samples per second. These numbers clearly point out the value of the Boosting Feature Selection approach when working with large databases such as in this research.

3.2.4 Receiver Operating Characteristics

Receiver operating characteristics (ROC) curves are graphs plotting the true positive rate of a classifier in function of its false positive rate. The points composing the curve are obtained by varying the decision threshold of the classifier (see Algorithm 1 of (Fawcett, 2006) for an efficient method for generation of ROC points). In the case of Gentle AdaBoost, this treshold needs to be added to the classifier equation such as

$$\operatorname{sign}\left[F\left(\mathbf{u}\right)+\Delta\right]=\operatorname{sign}\left[\sum_{t=1}^{T}f_t\left(\mathbf{u}\right)+\Delta\right] \tag{3.25}$$

where Δ is a real number representing the desired threshold. To fall back to the original classifier formulation, simply set $\Delta = 0$. Figure 3.12 gives an example of an ROC curve. Each point of the curve represents an operating point, the default operating point of Gentle AdaBoost (i.e. $\Delta = 0$) is indicated by an asterisk and all other points are obtained by varying Δ from $-\infty$ to ∞.

ROC curves have an attractive property: they are insensitive to change in class distribution (Fawcett, 2006). If the proportion of genuine signatures and forgeries changes between the design of a system and its exploitation, the ROC curves will not change. It is the case with

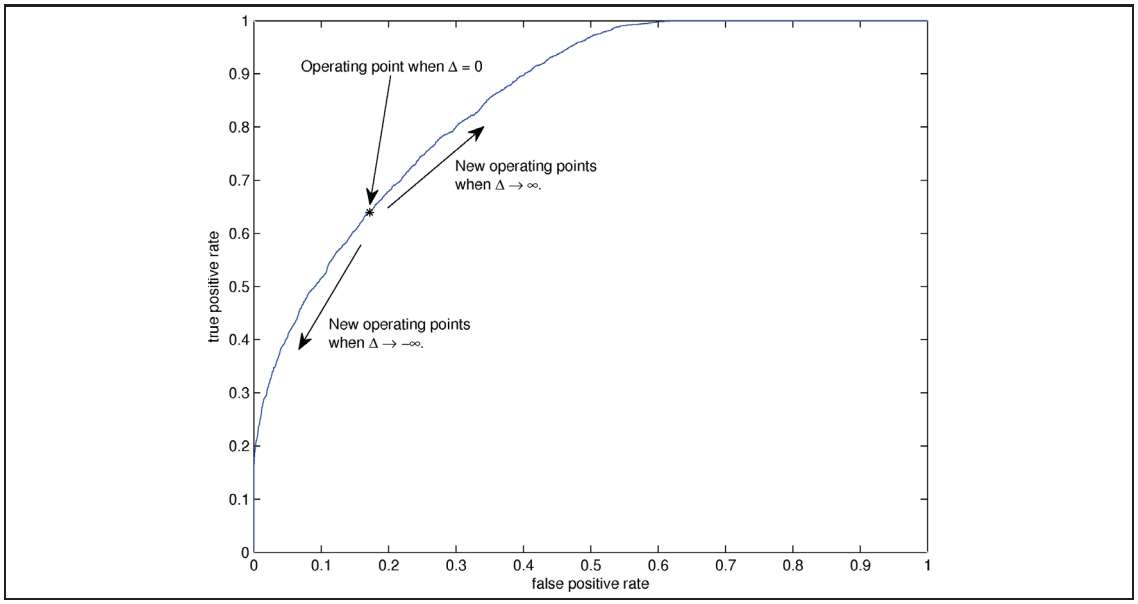

Figure 3.12 : Example of an ROC curve.

signature verification applications, as the proportions of fraud for real applications are likely to vary in time and from place to place.

The area under an ROC curve (AUC) can be computed using Algorithm 2 of (Fawcett, 2006). The AUC has an important statistical property: it is equivalent to the probability that the classifier will rank a randomly chosen positive instance higher than a randomly chosen negative instance (Fawcett, 2006). As such, the AUC is invariant to the decision threshold optimized by Gentle AdaBoost (i.e. $\Delta = 0$), which is a significant advantage in the context of this research since the decision threshold is learned using random forgeries as counterexamples when in fact the committee is tested against random, simple and simulated forgeries. Moreover, the decision threshold is function of the priors and the classification cost, both of which are likely to vary in a signature verification application.

CHAPTER 4

EXPERIMENTAL METHODOLOGY

The objective of this chapter is to describe the experimental protocols meant to assess the performance of offline signature verification systems based on multiple type of features and multiscale representations of handwritten signatures. Writer-independent verification implies that there is only one verification system for all writers. Therefore, the protocol makes use of two disjoint set of writers for system design (during development phase) and system testing (during exploitation phase), as depicted by Figure 4.1 . The underlying hypothesis is that the set of writers used for training is representative of the set of writers encountered during exploitation.

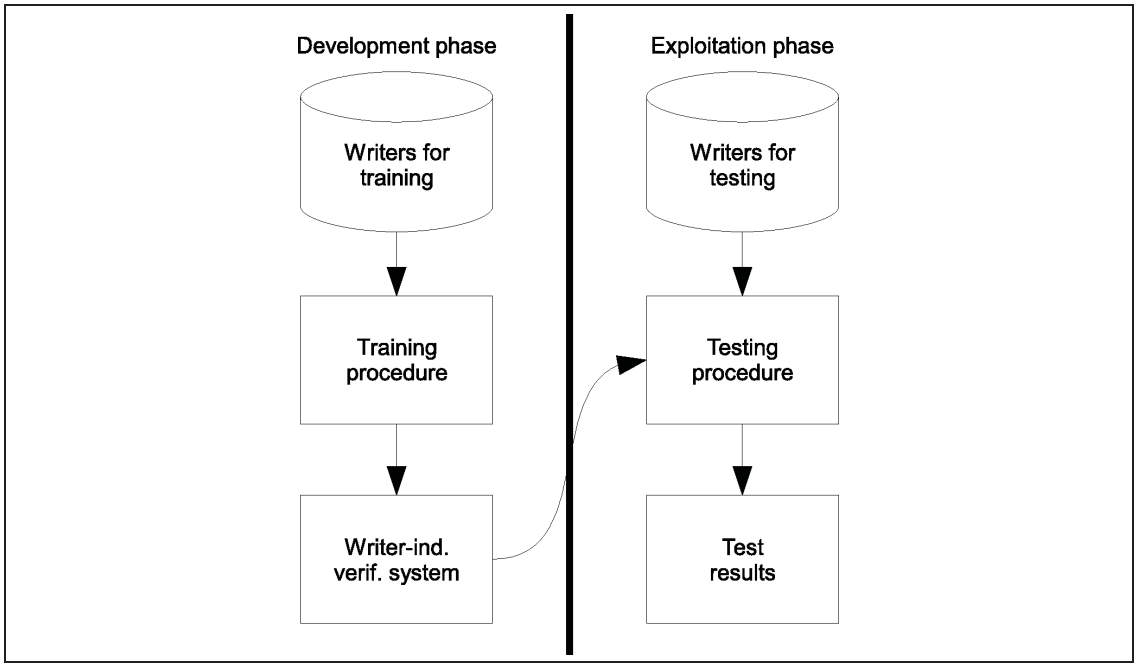

Figure 4.1 : Independence between the training or development phase and the testing or exploitation phase.

In most real-world applications, very few genuine signatures, and no forgeries, are available per writer. Consequently, random forgeries are usually the only kind of counterexamples available for designing a system. For this reason, only random forgeries were included in the training database, yet the system is tested against random, simple and simulated forgeries.

The following sections describe both signature databases, the feature sets extracted from the signatures, and the experimental protocols.

4.1 Signature Database

The signature database used in this research is composed of 168 writers divided into a 108 writers development database $\mathcal{D}$ and a 60 writers exploitation database $\mathcal{E}$ as presented in Table 4.1. As described in (Bertolini et al., 2010), the signatures were provided by 168 under-graduated students in four different sessions, ten samples at a time, once a week during one month, for a total of 40 genuine signatures per writer. The signatures were collected on an A4 white sheet of paper with no overlap and then scanned in gray level at 300 dpi. Regarding the forgeries, ten people with no experience in making forgeries were selected as forgers to produce one simple and one simulated forgery for the 60 first writers. Simple forgeries were produced by supplying only the name of the writer to the forger. Simulated forgeries were produced by showing the forger four genuine signatures of the writer.

Table 4.1: Signature Databases

	Development database $\mathcal{D}$	Exploitation database $\mathcal{E}$
Writers	108	60
Genuine Signatures	40	40
Simple Forgeries	-	10
Simulated Forgeries	-	10

To build a writer-independent classifier, distance vectors must be computed from the feature vectors using the dichotomy transformation as explained in Section 2.1. The learning set $\mathcal{L}$

and hold-out validation set $\mathcal{H}$ are both generated from the development database $\mathcal{D}$. To do so, the 40 genuine signatures of each writers of $\mathcal{D}$ are partitionned into a 30 and a 10 signatures subsets denoted $\mathcal{D}_1$ and $\mathcal{D}_2$, respectively.

The learning set $\mathcal{L}$ is generated using exclusively the genuine signatures of subset $\mathcal{D}_1$. The *within* class samples are computed using all genuine signatures from every writers, giving $108 \cdot \frac{30 \cdot 29}{2} = 46980$ distance vectors. To generate an equivalent number of counterexamples, the dichotomy transformation is applied, for each writer, to 29 genuine signatures used as signatures of references against 15 random forgeries selected from the genuine signatures of 15 other writers. The result is $108 \cdot 29 \cdot 15 = 46980$ *between* class distance vectors. Thus, the learning set is defined as $\mathcal{L} = \{\mathbf{u}_l, v_l\}_{l=1}^{93960}$.

The hold-out validation set $\mathcal{H}$ is generated using the genuine signatures of subset $\mathcal{D}_1$ as reference signatures against the genuine signatures of subset $\mathcal{D}_2$. Since each writer has 30 references signatures in $\mathcal{D}_1$ and 10 genuine signatures in $\mathcal{D}_2$, the number of *within* class samples is equal to $108 \cdot 30 \cdot 10 = 32400$. To generate an equivalent number of counterexamples, for each writer, 10 random forgeries are selected from 10 different writers in $\mathcal{D}_2$. The random forgeries are compared to the 30 references from $\mathcal{D}_1$, giving $108 \cdot 30 \cdot 10 = 32400$ *between* class distance vectors. Thus, the hold-out validation set is defined as $\mathcal{H} = \{\mathbf{u}_h, v_h\}_{h=1}^{64800}$.

To perform a writer-independent evaluation of the system, both reference $\mathcal{R}$ and questioned $\mathcal{Q}$ sets are generated from the exploitation database $\mathcal{E}$ whose writers are unknown to the verification system. The reference set $\mathcal{R}$ is composed of 30 randomly selected genuine signatures from each writer of the exploitation database $\mathcal{E}$. Thus, the reference set is defined as $\mathcal{R} = \{\mathbf{x}_r, y_r\}_{r=1}^{1800}$. The questioned set $\mathcal{Q}$ is composed of the 10 remaining genuine signatures and simple and simulated forgeries from each writer plus 10 random forgeries selected from the genuine signatures of 10 different writers. Thus, the questioned set is defined as $\mathcal{Q} = \{\mathbf{x}_q, y_q\}_{q=1}^{2400}$.

4.2 Feature Sets

Extended Shadow Code and Directional PDF feature vectors are extracted from both signature databases $\mathcal{D}$ and $\mathcal{E}$. Feature resolution depends on the size of the extraction grid; the smaller the grid cells, the higher the resolution. The highest resolution used in this research is a cell of 20×20 pixels. Since the width of a stroke measures an average of 10 pixels, higher resolutions would results mostly in saturated cells and empty cells. On the other hand, the lowest resolution is limited by the size of the image. Since the signature images are 400 pixels high by 1000 pixels wide, the lowest resolution consists of a single cell of that size. Let $\mathcal{I} = \{1, 2, 5, 10, 20\}$ be a set of 5 horizontal scales defined by their number of grid rows and $\mathcal{J} = \{1, 3, 6, 12, 25, 50\}$ be a set of 6 vertical scales defined by their number of grid columns. The Cartesian product $\mathcal{I} \times \mathcal{J}$ results in the 30 single scales used in this research. Finally, multiscale is achieved by combining feature sets from every scales, for a total of 15457 and 14744 features for Extended Shadow Code and Directional PDF, respectively, and a grand total of 30201 features when both techniques are combined, as detailled in Table 4.2.

4.3 Protocols

This section describes the experimental protocols used in this research. Firstly, individual evaluations of each single scale representation extracted from both Extended Shadow Code and Directional PDF is performed. This evaluation is followed by a comparison between information fusion applied at feature level and information fusion applied at score level.

4.3.1 Single Scale Representations

In order to independently characterize both Extended Shadow Code and Directional PDF feature extraction techniques, single scale committees are built using the following protocol. For each available feature set, the Gentle Adaboost algorithm with early stopping (see Algorithm 3.1) builds a committee of decision stumps on the learning set $\mathcal{L}$ using the hold-out validation set $\mathcal{H}$ to prevent overfitting. The early stopping criterion is set to $T_{\mathcal{H}} = 100$ and the maximum iteration stopping criterion to $T_{\mathcal{L}} = 100000$.

Table 4.2: Details of the Resolutions

	Pixels		Features	
Rows × Columns	Height	Width	Extended Shadow Code	Directional PDF
20×50	20	20	4070	4000
20×25	20	40	2045	2000
20×12	20	84	992	960
20×6	20	167	506	480
20×3	20	334	263	240
20×1	20	1000	101	80
10×50	40	20	2060	2000
10×25	40	40	1035	1000
10×12	40	84	502	480
10×6	40	167	256	240
10×3	40	334	133	120
10×1	40	1000	51	40
5×50	80	20	1055	1000
5×25	80	40	530	500
5×12	80	84	257	240
5×6	80	167	131	120
5×3	80	334	68	60
5×1	80	1000	26	20
2×50	200	20	452	400
2×25	200	40	227	200
2×12	200	84	110	96
2×6	200	167	56	48
2×3	200	334	29	24
2×1	200	1000	11	8
1×50	400	20	251	200
1×25	400	40	126	100
1×12	400	84	61	48
1×6	400	167	31	24
1×3	400	334	16	12
1×1	400	1000	6	4
		Total:	15457	14744
			Grand Total:	30201

The performance of each writer-independent committee is evaluated using reference signatures from new writers in the set $\mathcal{R}$ to authenticate the questioned signatures of set $\mathcal{Q}$. To measure the impact of the cardinality of the reference set, reference subsets containing 1, 3, 5, 7, 9, 11,

13 and 15 randomly selected signatures are used for authentication. To simulate the effect of enrolling new signatures over time, previously selected signatures are kept and new signatures are added to increase the size of the reference subsets. This procedure is repeated 100 times for variance estimation. Algorithm 4.1 presents the evaluation protocol in an algorithmic format.

for all committees **do**
  for replication 1 to 100 **do**
    $\mathcal{R} = \{\mathbf{x}_1, \mathbf{x}_2, \ldots, \mathbf{x}_R\}$
    $\overline{\mathcal{R}} = \{\emptyset\}$
    repeat
      /* randomly select signatures i and j from $\mathcal{R}$ */
      $\mathcal{R}' = \{\mathbf{x}_i, \mathbf{x}_j \mid \mathbf{x}_i, \mathbf{x}_j \in \mathcal{R}\}$
      $\mathcal{R} = \{\mathcal{R} \setminus \mathcal{R}'\}$
      $\overline{\mathcal{R}} = \{\overline{\mathcal{R}} \cup \mathcal{R}'\}$
      evaluate the committee on $\mathcal{Q}$ using $\overline{\mathcal{R}}$
    until $\left|\overline{\mathcal{R}}\right| = 15$
  end for
end for

Algorithm 4.1: **Committee Evaluation Protocol**

ROC analysis is used to select the optimal threshold for each committee while testing the questioned set; this must be done to ensure that the results presented herein can be compared with those published in the litterature (i.e. references (Bertolini et al., 2010) and (Santos et al., 2004)). Additionally, the committees are evaluated using their error rates on the questioned set. To do so, the decision threshold minimizing the zero-one loss is used to characterize the questioned set and also to allow for a straightforward comparison with previous systems.

4.3.2 Information Fusion at the Feature Level

Contrary to previous writer-independent system (Bertolini et al., 2010) which implements information fusion at the confidence score level, the proposed system implements information fusion at the feature extraction level. Three multiscale committees are compared:

1) Using a multiscale feature set only from the Extended Shadow Code technique;

2) Using a multiscale feature set only from the Directional PDF technique;

3) Using a multiscale feature set from both Extended Shadow Code and Directional PDF techniques.

Multiscale feature sets are achieved by concatenating appropriate single scale feature sets. To permit result comparison, training and evaluation protocols are the same as for single scale feature set, as described previously.

To complete this aspect of the study, the experimental protocol presented at Algorithm 4.2 is designed to evaluate the impact of the quantity of signature representations on the Boosting Feature Selection algorithm with early stopping. Let $\mathcal{L}$, $\mathcal{H}$, $\mathcal{Q}$, $\mathcal{R}$ be the learning, hold-out, questioned and references sets, respectively. They are all initialized as empty sets. Then, the 60 signature representations are randomly selected one at a time and added to the sets. When the sets contain 1, 5, 10, 15, 20, 25, 30, 40, 50 and 60 representations, the committee of stumps F_p is built from sets $\mathcal{L}$ and $\mathcal{H}$ using the Boosting Feature Selection algorithm with early stopping and then tested on set $\mathcal{Q}$ using 1, 3, 5, 7, 9, 11, 13, 15 references from set $\mathcal{R}$. This protocol is repeated 10 times to show replicability.

4.3.3 Information Fusion at the Confidence Score Level

In this section two protocols based on information fusion at the confidence score level are presented. The first reproduces the overproduce and choose approach used in (Bertolini et al., 2010) and the second evaluates the modularity of the proposed system.

4.3.3.1 Overproduce and Choose

The overproduce and choose approach used in (Bertolini et al., 2010) is reproduced here using our feature extraction techniques and database partitions in order to compare the two approaches. To perform information fusion at the confidence score level, committees built on

1: **for** replication 1 to 10 **do**
2: Initialize $\mathcal{L} = \mathcal{H} = \mathcal{Q} = \mathcal{R} = \{\emptyset\}$
3: **for** $p = 1$ to 60 **do**
4: Acquire new handwritten signature representation datasets $\mathcal{H}_p, \mathcal{L}_p, \mathcal{Q}_p, \mathcal{R}_p$ from feature extraction expert
5: Add $\mathcal{L} \leftarrow \mathcal{L} \cup \mathcal{L}_p$
6: Add $\mathcal{H} \leftarrow \mathcal{H} \cup \mathcal{H}_p$
7: Add $\mathcal{Q} \leftarrow \mathcal{Q} \cup \mathcal{Q}_p$
8: Add $\mathcal{R} \leftarrow \mathcal{R} \cup \mathcal{R}_p$
9: **if** $p \in \{1, 5, 10, 15, 20, 25, 30, 40, 50, 60\}$ **then**
10: Build committee of stumps $F_p \leftarrow GentleAdaBoost(\mathcal{L}, \mathcal{H})$
11: Evaluate F_p on $\mathcal{Q}$ using $1, 3, \ldots, 15$ references from $\mathcal{R}$
12: **end if**
13: **end for**
14: **end for**

Algorithm 4.2: **Protocol to evaluate the impact of the quantity of representations.**

single scale feature sets are combined together into an ensemble of committees by summating their individual confidence level output. Ensembles of committees are optimized with a genetic algorithm based on bit representation, one-point crossover, bit-flip mutation and roulette wheel selection with elitism. The parameter setting is the same as in (Bertolini et al., 2010): population = 100, number of generations = 300, probability of crossover = 0.7, and probability of mutation = 0.03. The chromosomes are composed of 60 bits, that is, one bit per single scale committee and for a given chromosome, turned on bits identify the selected committees. The fitness function is the maximization of the AUC on the hold-out validation set $\mathcal{H}$. Once an ensemble of committees is optimized, it is evaluated on the questioned set using the evaluation protocol described in Section 4.3.1. This procedure is also repeated 100 times for variance estimation to allow for direct comparison with the other approaches explored in this research.

4.3.4 Incremental Selection of Representations

In order to demonstrate the modularity of the proposed system, an experimental protocol is designed to implement an incremental selection of the handwritten signature representations. For instance, suppose that domain experts extract new representations from the design database.

As new signature representations become available, they are added incrementally to the verification system in order to increase its recognition rate.

A greedy incremental selection scheme is implemented to demonstrate the modularity of the proposed system. Single scale signature representations are presented to the system one at a time. For each representation, a committee of stumps is built and combined with previous committees to form an ensemble of committees. Then the AUC of the ensemble of committees is evaluated on the hold-out validation set $\mathcal{H}$ and the newly added committee is kept if it improves the AUC of the ensemble or dismissed otherwise. The 60 single scale representations are presented in random order and this procedure is replicated 100 times to evaluate the replicability.

1: **for** replication 1 to 100 **do**
2: Initialize $\mathcal{H} = \{\emptyset\}$
3: Initialize $F_{\text{eoc}} = 0$
4: Initialize $A_{\text{max}} = -\infty$
5: **for** $p = 1$ to 60 **do**
6: Acquire new handwritten signature representation datasets $\mathcal{H}_p, \mathcal{L}_p, \mathcal{Q}_p, \mathcal{R}_p$ from feature extraction expert
7: Build committee of stumps $F_p \leftarrow GentleAdaBoost(\mathcal{L}_p, \mathcal{H}_p)$
8: Add $F_{\text{eoc}} \leftarrow F_{\text{eoc}} + F_p$
9: Add $\mathcal{H} \leftarrow \mathcal{H} \cup \mathcal{H}_p$
10: **if** $AUC(\mathcal{H}, F_{\text{eoc}}) > A_{\text{max}}$ **then**
11: Update $A_{\text{max}} \leftarrow AUC(\mathcal{H}, F_{\text{eoc}})$
12: Add $\mathcal{Q} \leftarrow \mathcal{Q} \cup \mathcal{Q}_p$
13: Add $\mathcal{R} \leftarrow \mathcal{R} \cup \mathcal{R}_p$
14: Evaluate F_{eoc} on $\mathcal{Q}$ using $1, 3, \ldots, 15$ references from $\mathcal{R}$
15: **else**
16: Dismiss $\mathcal{H} \leftarrow \mathcal{H} \setminus \mathcal{H}_p$
17: Dismiss $F_{\text{eoc}} \leftarrow F_{\text{eoc}} - F_p$
18: **end if**
19: **end for**
20: **end for**

Algorithm 4.3: **Forward selection of represention protocol.**

Algorithm 4.3 details this experimental protocol. Given a signature representation p, the learning set $\mathcal{L}_p$ and hold-out validation set $\mathcal{H}_p$ are both generated from the design database $\mathcal{D}$ and the reference set $\mathcal{R}_p$ and questioned set $\mathcal{Q}_p$ are generated from the exploitation database $\mathcal{E}$ whose writers are unknown to the verification system. Committees of stumps are the result of the Gentle Adaboost algorithm with early stopping, described at Algorithm 3.1, and they are evaluated according to the evaluation protocol described in Section 4.3.1.

CHAPTER 5

RESULTS AND DISCUSSION

This chapter presents the results obtained from previously discussed protocols and their analysis.

5.1 Single Scale Representations

First, the results from committees built on single scale feature sets are presented. Table 5.1 and 5.2 present, respectively, the committee size and ratio of selected features for single scale with the Extended Shadow Code representations. Appendix II contains figures illustrating which features were selected. Since no committee has reached $T_{\mathcal{L}}$ iterations (as indicated by the number of stumps composing them), early stopping has occurred for every scales. The lower selection rate obtained at higher resolutions indicates the presence of redundant and irrelevant features. Best overall error rates from Extended Shadow Code representations are obtained at scale 2×3 and is presented in Table 5.3.

Table 5.1: Committee size (number of stumps) for single scale Extended Shadow Code representation committees

Rows \ Columns	50	25	12	6	3	1
20	1028	802	303	717	468	234
10	623	784	607	471	259	186
5	425	956	536	561	161	118
2	784	810	539	300	232	287
1	484	493	344	271	110	232

Table 5.4 and 5.5 present, respectively, the committee size and selected feature ratio from single scale Directional PDF representations. Appendix III contains figures illustrating which features were selected. Again, no committee has reached $T_{\mathcal{L}}$ iterations; early stopping has

Table 5.2: Selected feature ratio for single scale Extended Shadow Code representation committees

Rows \ Columns	50	25	12	6	3	1
20	0.16	0.22	0.21	0.44	0.54	0.64
10	0.20	0.34	0.43	0.54	0.62	0.86
5	0.26	0.53	0.57	0.74	0.74	1.00
2	0.69	0.82	0.87	0.96	1.00	1.00
1	0.78	0.96	0.98	1.00	1.00	1.00

Table 5.3: Error Rate (%) for the committee of Extended Shadow Code representation at scale 2×3

Types	Cardinality of the Reference Set							
	1	3	5	7	9	11	13	15
Genuine Signatures	21.99	16.75	15.40	14.39	14.29	14.07	13.59	13.26
Random Forgeries	0.77	0.45	0.39	0.37	0.34	0.33	0.32	0.35
Simple Forgeries	1.45	0.81	0.61	0.56	0.48	0.43	0.42	0.41
Simulated Forgeries	20.42	18.75	17.92	18.01	17.54	17.25	17.31	17.29
Overall	11.16	9.19	8.58	8.33	8.16	8.02	7.91	7.83

occurred for every scales. When compared to Extended Shadow Code representation committees, the Directional PDF representation committees are usually larger and have a higher ratio of selected features which indicate that Directional PDF representations generally contain less redundant and irrelevant information. Best overall error rates from Directional PDF representations are obtained at scale 20×6 and are presented in Table 5.6. Compared to the best Extended Shadow Code representation committee, the Directional PDF representation committee provides a lower error rate.

Table 5.4: Committee size (number of stumps) for single scale Directional PDF representation committees

Rows \ Columns	50	25	12	6	3	1
20	909	930	796	638	778	589
10	1358	761	836	598	628	361
5	1018	500	963	730	258	326
2	1288	939	983	1056	632	334
1	681	557	705	746	285	360

Table 5.5: Selected feature ratio for single scale Directional PDF representation committees

Rows \ Columns	50	25	12	6	3	1
20	0.15	0.25	0.33	0.45	0.64	0.96
10	0.28	0.32	0.45	0.56	0.76	1.00
5	0.38	0.41	0.62	0.77	0.78	1.00
2	0.86	0.94	1.00	1.00	1.00	1.00
1	0.94	1.00	1.00	1.00	1.00	1.00

5.2 Information Fusion at Feature Level

This section presents results from committees built on multiscale Extended Shadow Code representation, multiscale Directional PDF representation, and on the concatenation of both multiscale representations.

Table 5.6: Error Rate (%) for the committee of Directional PDF representation at scale 20×6

Types	Cardinality of the Reference Set							
	1	3	5	7	9	11	13	15
Genuine Signatures	20.69	16.47	14.65	14.96	15.12	14.93	15.07	15.33
Random Forgeries	0.87	0.69	0.60	0.53	0.49	0.48	0.44	0.43
Simple Forgeries	1.48	0.97	1.00	0.90	0.88	0.88	0.87	0.84
Simulated Forgeries	16.72	14.83	15.33	14.44	13.90	13.94	13.74	13.52
Overall	9.94	8.24	7.90	7.71	7.60	7.56	7.53	7.53

The committee built on multiscale Extended Shadow Code representation is composed of 1095 stumps. Table 5.7 details the individual ratio of selected features at each scale. Features from every scales have been selected for a total of 818 features out of 15457 resulting in an overall selected feature ratio of approximately 5%. Appendix IV contains figures illustrating which features were selected at each scale. Table 5.8 presents the mean error rates over 100 replications for the multiscale Extended Shadow Code respresentation committee. The multiscale approach leads to lower overall error rates compared to single scale Extended Shadow Code representation and this is explained by the greater quantity of potential features available to build the committee.

Table 5.7: Selected feature ratios for the Extended Shadow Code multiscale representation committee

Rows \ Columns	50	25	12	6	3	1
20	0.03	0.03	0.06	0.06	0.11	0.25
10	0.03	0.03	0.06	0.07	0.08	0.25
5	0.06	0.05	0.09	0.12	0.16	0.27
2	0.05	0.11	0.20	0.25	0.34	0.45
1	0.12	0.13	0.20	0.32	0.12	0.50
Overall selected feature rate: 0.05						

Table 5.8: Error Rate (%) for the committee of Extended Shadow Code multiscale representation

Type	Cardinality of the Reference Set							
	1	3	5	7	9	11	13	15
Genuine Signatures	19.37	14.41	13.67	13.34	12.81	12.46	12.29	12.19
Random Forgeries	0.14	0.07	0.05	0.05	0.03	0.02	0.01	0.02
Simple Forgeries	0.39	0.24	0.18	0.18	0.18	0.17	0.17	0.17
Simulated Forgeries	16.17	15.41	14.82	14.53	14.82	14.91	14.97	14.93
Overall	9.02	7.53	7.18	7.02	6.96	6.89	6.86	6.83

The committee built on Directional PDF multiscale representation is composed of 1288 stumps. Table 5.9 details the individual selected feature ratio for each scale. Features from every scales have been selected for a total of 888 features out of 14744 resulting in an overall selected feature ratio of approximately 6%; a result similar to the one obtained with multiscale Extended Shadow Code respresentation. Appendix V contains figures illustrating which features were selected at each scale.

Table 5.9: Selected feature ratios for the Directional PDF multiscale representation committee

Rows \ Columns	50	25	12	6	3	1
20	0.04	0.04	0.06	0.08	0.11	0.41
10	0.03	0.04	0.04	0.06	0.12	0.30
5	0.06	0.07	0.09	0.11	0.22	0.35
2	0.14	0.11	0.19	0.25	0.21	0.38
1	0.18	0.18	0.31	0.54	0.25	0.75
Overall selected feature ratio: 0.06						

Table 5.10 presents the mean error rates (in %) of the 100 replications for the multiscale Directional PDF respresentation committee. Similarly to the Extended Shadow Code multiscale respresentation, the multiscale approach leads to lower error rates compared to the single scale Directional PDF representation. However, the multiscale Directional PDF respresentation committee provides lower error rates than the multiscale Extended Shadow Code respresentation committee.

The committee built on both Extended Shadow Code and Directional PDF multiscale representations is composed of 679 terms. Table 5.11 details the selected feature ratio for both feature extraction techniques at each scale. Features from every scales have been selected for a total of 555 features out of 30201 resulting in an overall selected feature ratio of less than 2%. Thus, providing a more diversified information to the Boosting Feature Selection method results in a

Table 5.10: Error Rate for the committee of Directional PDF multiscale representation (%)

Type	Cardinality of the Reference Set							
	1	3	5	7	9	11	13	15
Genuine Signatures	15.68	11.44	10.61	10.23	10.23	10.21	9.94	9.88
Random Forgeries	0.21	0.15	0.15	0.14	0.12	0.11	0.11	0.12
Simple Forgeries	0.87	0.67	0.67	0.69	0.68	0.69	0.70	0.70
Simulated Forgeries	15.40	14.03	13.68	13.45	13.14	13.00	13.05	13.05
Overall	8.04	6.57	6.28	6.13	6.05	6.00	5.95	5.94

lighter committee using less features. Appendix VI contains figures illustrating which features were selected at each scale.

Table 5.11: Selected feature ratios for the Extended Shadow Code/Directional PDF multiscale representation committee

Rows \ Columns	50	25	12	6	3	1
20	0.01/0.01	0.01/0.01	0.02/0.02	0.02/0.03	0.03/0.05	0.11/0.23
10	0.01/0.01	0.01/0.01	0.02/0.02	0.04/0.03	0.02/0.06	0.10/0.17
5	0.01/0.01	0.02/0.03	0.04/0.02	0.06/0.05	0.10/0.12	0.23/0.25
2	0.02/0.03	0.04/0.04	0.05/0.07	0.09/0.12	0.07/0.12	0.27/0.25
1	0.02/0.03	0.06/0.05	0.13/0.08	0.13/0.12	0.12/0.08	0.50/0.25
Overall selected features rate: 0.02/0.02						

Table 5.12 presents the mean error rates (in %) of the 100 replications for the committee built on both Extended Shadow Code and Directional PDF multiscale representations. The error rates are better than those obtained from the committees based only on one of the two multiscale representations. This confirms that both multiscale representations are complementary and that together, they provide a more diversified information to the Boosting Feature Selection method.

Table 5.12: Error Rate for the Extended Shadow Code/Directional PDF multiscale representation committee (%)

Type	Cardinality of the Reference Set							
	1	3	5	7	9	11	13	15
Genuine Signatures	13.53	10.66	9.83	9.75	9.36	9.69	9.80	9.77
Random Forgeries	0.12	0.06	0.04	0.03	0.03	0.02	0.03	0.02
Simple Forgeries	0.43	0.33	0.32	0.33	0.32	0.33	0.32	0.32
Simulated Forgeries	14.95	12.52	11.87	11.36	11.55	11.11	10.77	10.65
Overall	7.26	5.89	5.52	5.37	5.32	5.29	5.23	5.19

Figure 5.1 presents the mean error rate in function of both the number of references per writer and the number of representations used by the verification system. The mean error rate decreases monotonically for both the number of representations and the number of references. In both cases, their seems to be a limit to the improvement provided by adding new references and new representations since the improvement lessens as more references or representation are added. However, the figure clearly shows that adding new representations (the "$*$") has a greater impact on accuracy than by adding new references (the "$\circ$").

5.3 Information Fusion at the Confidence Score Level

This section presents the results obtained from the protocols dealing with information fusion at the confidence score level.

5.3.1 Overproduce and Choose

The overproduce and choose approach selected a mean of 19.81 committees per replication. Each committee uses a mean of 1736.93 Extended Shadow Code features and 2004.12 Directional PDF features for a total of 3741.05 features. Table 5.13 details the individual selection ratio of each representation. Of the 30 resolutions, 4 are systematically selected for both types of representation and 11 are systematically discarded. Interestingly, the remaining fifteen (that is, half of the resolutions available) are equally shared between both types of representation which is an indication of the complementarity of the two feature extraction techniques.

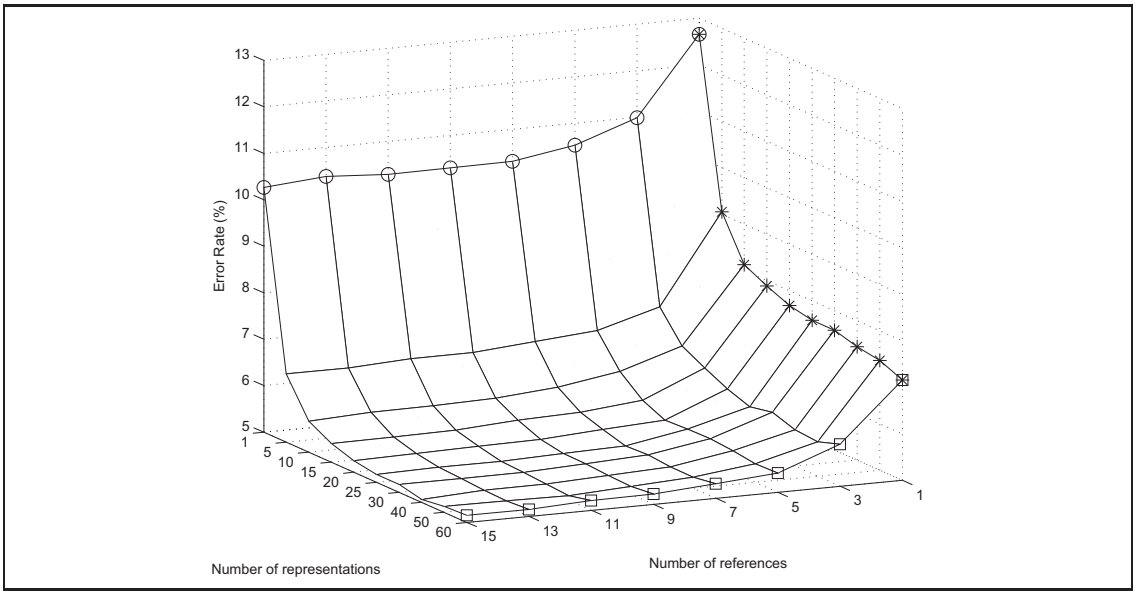

Figure 5.1 : Mean error rate in function of both the number of references per writer and the number of representations *presented* to the system.

Table 5.13: Selection ratio of each single Extended Shadow Code/Directional PDF representation from the overproduce and choose approach

Rows \ Columns	50	25	12	6	3	1
20	0.00/0.00	0.00/0.00	0.00/1.00	0.94/1.00	0.82/0.97	1.00/1.00
10	0.00/0.46	1.00/0.00	0.48/0.01	0.16/0.01	0.00/0.53	0.99/0.98
5	0.29/0.99	1.00/0.03	1.00/0.01	0.84/0.00	0.09/0.00	0.00/0.85
2	0.01/0.60	0.00/0.00	0.00/0.96	0.00/0.01	0.00/0.00	0.00/0.00
1	0.98/0.00	0.70/0.00	0.10/0.00	0.00/0.00	0.00/0.00	0.00/0.00
Overall Extended Shadow Code/Directional PDF representation selection rate: 0.35/0.31						

Table 5.14 presents the mean error rates over 100 replications for the ensemble of committees. The overall error rates are better than those obtained from the committees based only on one of the two multiscale representations but not as good as those obtained from the committee based on both multiscale representations.

Table 5.14: Error rate (%) from the overproduce and choose approach

Type	Cardinality of the Reference Set							
	1	3	5	7	9	11	13	15
Genuine Signatures	14.36	12.29	11.32	11.42	11.49	11.39	11.38	11.00
Random Forgeries	0.02	0.00	0.00	0.00	0.00	0.00	0.00	0.00
Simple Forgeries	0.35	0.23	0.21	0.20	0.18	0.17	0.17	0.19
Simulated Forgeries	14.24	12.11	11.98	11.49	11.16	11.03	10.90	11.15
Overall	7.24	6.16	5.88	5.78	5.71	5.65	5.61	5.59

5.3.2 Incremental Selection of Representations

This section presents results from the incremental selection of representations scheme. Figure 5.2 presents the mean error rate in function of both the number of references per writer and the number of representations *presented* to the system. The actual number of *selected* representations is indicated on Figure 5.3 using the mean number of *used* features in function of the number of representations that has been presented to the system.

The mean error rate decreases monotonically for both the number of representations and the number of references. In both cases, their seems to be a limit to the improvement provided by adding new references and new representations since the improvement lessens as more references or representation are added. However, the graphic clearly shows that adding new representations has a greater impact on accuracy than by adding new references.

5.4 Discussion

Tables 5.15 sums up the results presented so far. Regarding both best single scale representations, Directional PDF are significantly more discriminant than Extended Shadow Code representations. However, an interesting fact is that Extended Shadow Code performs better at low resolution while Directional PDF provides better performance at higher resolution; in this respect, the two feature extraction techniques are complementary.

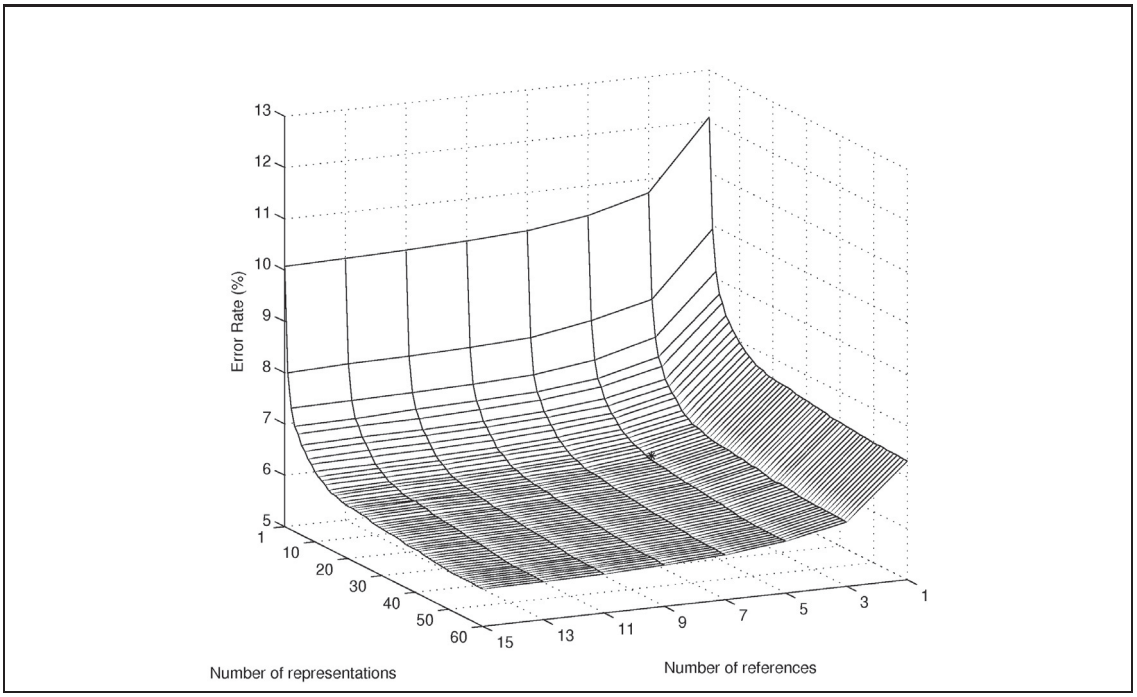

Figure 5.2 : Mean error rate in function of both the number of references per writer and the number of representations *presented* to the system.

Table 5.15: Error rates (%) comparison with other systems

Approach	Features	Cardinality of the Reference Set							
		1	3	5	7	9	11	13	15
ESC scale 2×3	29	11.16	9.19	8.58	8.33	8.16	8.02	7.91	7.83
DPDF scale 20×6	216	9.94	8.24	7.90	7.71	7.60	7.56	7.53	7.53
Multiscale ESC	818	9.02	7.53	7.18	7.02	6.96	6.89	6.86	6.83
Multiscale DPDF	888	8.04	6.57	6.28	6.13	6.05	6.00	5.95	5.94
Multiscale ESC/DPDF	555	7.26	**5.89**	**5.52**	**5.37**	**5.32**	**5.29**	**5.23**	**5.19**
Using All Representations	10137	7.54	6.59	6.34	6.27	6.24	6.20	6.20	6.17
Incremental Selection of Represent.	5178	7.31	6.25	6.01	5.87	5.81	5.76	5.74	5.73
Overproduce & Choose (herein)	3741	**7.24**	6.16	5.88	5.78	5.71	5.65	5.61	5.59
Over. & Choo. (Bertolini et al., 2010)	-	-	7.86	7.32	6.32	7.04	7.19	6.73	6.48
MLP (Santos et al., 2004)	-	-	-	8.02	-	-	-	-	-

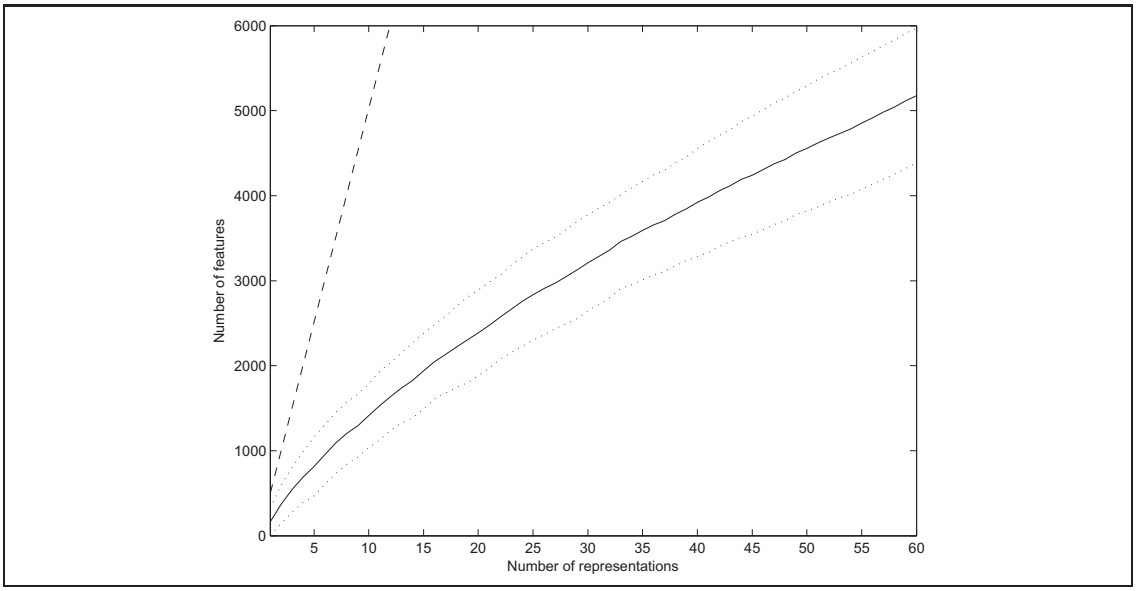

Figure 5.3 : Mean (solid line) and standard deviation (dotted lines) of the number of features *used* by the system in function of the number of representations that has been presented. The dashed line represents the number of feature that would be used by the system, should it select all representations presented to it. The dashed line continues outside the graphic to reach 30201 features when the 60 representations have been presented.

Figure 5.4 presents a notched box and whisker plot of the error rates of the different approaches explored in this research. The notches represent a robust estimate of the uncertainty about the medians for box-to-box comparison. Boxes whose notches do not overlap indicate that the medians of the two groups differ at the 5% significance level. All error rates significantly differ except for the multiscale Directional PDF and the approach combining all 60 independent committees, whose notches overlap.

The proposed solution is highly modular in the sense that each new representation can generate an independent classifier which in turn can be added to the classification module to increase performance. For instance, if all independent committees built from every representations extracted in this research are combined to form ensemble of 60 committees, this system "Using All Representations" (see Table 5.15) provides better performance than any system built on a single scale representation.

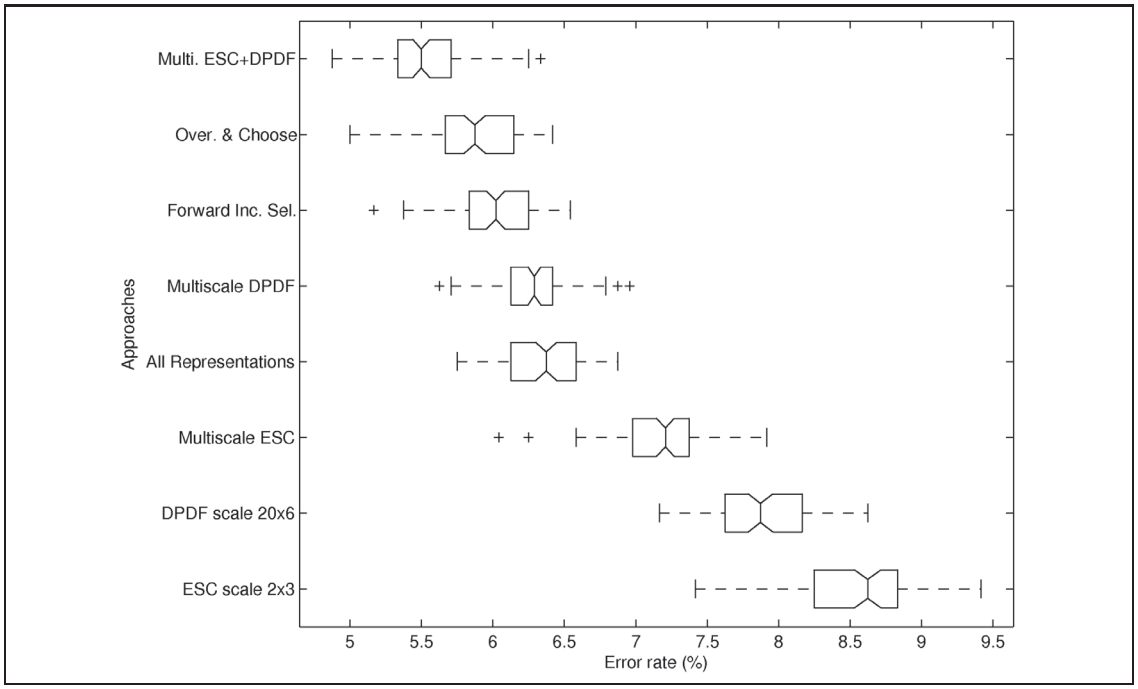

Figure 5.4 : Comparison of the error rates of the different approaches presented in this research using boxes and whiskers. Error rates are obtained with reference sets of 5 signatures.

Moreover, the ensemble of committees can be optimized using genetic algorithm to further improve performance by filtering out redundant and irrelevant representations. The drawback of this approach is that the optimization process needs to be repeated each time a new representation is available. In this case, an incremental selection of representations strategy is more appropriate. Results show that even greedy incremental selection, arguably the simplest incremental selection scheme, provides a viable mean to filter representations and increase performance. An interesting fact shown by Figure 5.2 , is that there is more to be gained from extracting new representations than by sampling new references. Consequently, such a verification system can run with a few signatures of reference if it is composed of adequate representations.

The combination of independent committees into ensemble of committees result in the fusion of information at the confidence score level. When committees are built across multiple rep-

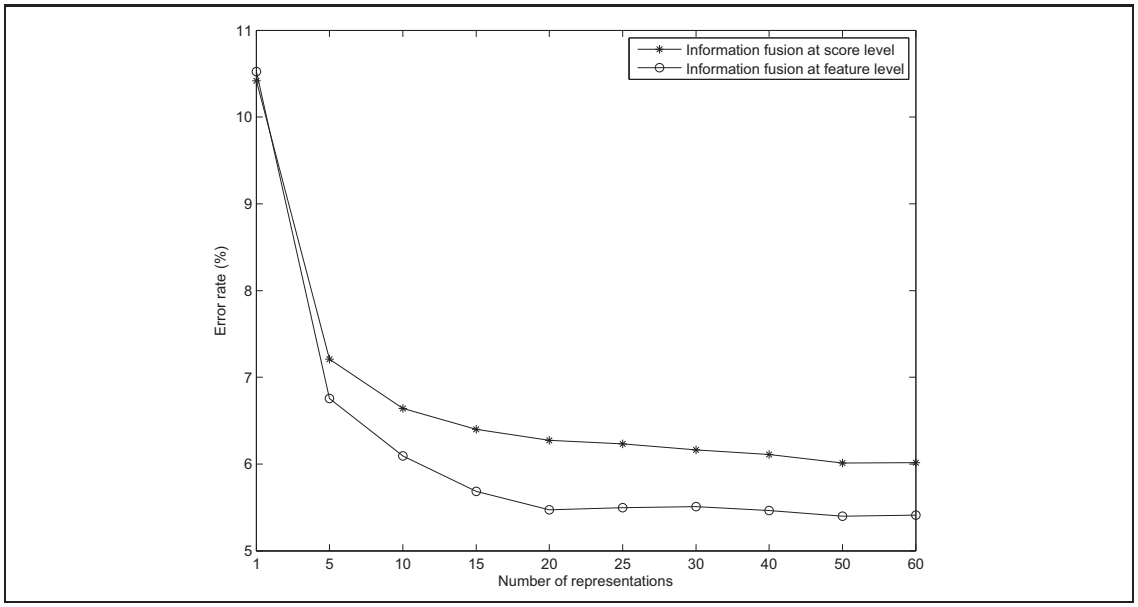

Figure 5.5 : Mean error rate in function of number of signature representations using 5 references.

resentations the information fusion occurs at the feature level and result in smaller committees with better generalization performances. Both multiscale Extended Shadow Code and multiscale Directional PDF committees outrank their single representation counterparts and use only 5% and 6% of all available features, respectively. This result is even more convincing for a multiscale committee built across all 60 representations; the committee uses even less features (2%) and provides a lower error rate. Figure 5.5 compares the mean error rates when applying information fusion at the feature level compared to the confidence score level for an growing number of representations, using 5 reference signatures. Error rates are similar when a single representation is available; an expected result since the learning context, at this point, is identical for both fusion strategy, that is one representation and one classifier. However, as more representation are made available to the verification system, information fusion at the feature level clearly performs better then information fusion at the score level. An expected result which is explained by the richer information conveyed by features rather then scores (Jain et al., 2004).

CONCLUSION

This research presented a practical solution to the fundamental problems encountered with signature verification: a large number of users, a large number of features, a limited number of reference signatures, a high intra-personal variability of the signatures and the unavailability of forgeries as counterexamples. The solution consists of a writer-independent framework, based on the dichotomy transformation, that palliates the large number of users and reduced number of reference signatures. Experimental methodology and results clearly demonstrated the writer-independence by training and testing the system on two disjoint sets of writers and even indicate the possibility of signature *verification using a single reference* signature for each writer. Further, results demonstrate the viability of using random forgeries to train a classifier in the distance space of the dichotomy transformation, thus tackling the unavailability of forgeries.

The high intra-personal variability of handwritten signatures is dealt with by extracting multi-scale features using Extended Shadow Code and Directional PDF, two complementary feature extraction techniques, resulting in a powerful multiscale spatio-directional representation of the signatures. The large number of extracted features is dealt with using Boosting Feature Selection, a feature selection *while* learning technique originally proposed for traditional feature vectors, which proves also effective with distance vectors resulting from the dichotomy transformation. Further, this approach result in light-weight, efficient classifiers viable for real-time applications.

Another significant advantage of the proposed framework resides in the modularity of its classification module. Using the properties inherited from the writer-independent approach, new samples as well as new signature representations can be added to the system during the exploitation phase. From there, a single classifier may be built over all available signature representations, thus implementing a fusion of the information at the feature level. Or one classifier may be built per representation and then grouped into an ensemble of classifiers, thus implementing in a fusion of the information at the confidence score level. The former approach

results into more efficient classifiers, however it requires all representations to be available during the design phase. On the other hand, the latter allows the system to be designed using a single representation and then incrementally updated when a new representation is available. Interestingly, results show that starting with a single representation and a single reference signature, the accuracy of the system is better improved by adding more representations than references, making the proposed framework ideally suited to applications where few samples are available.

Further research will focus on dynamically adapting the classification module to the writer, or even to the signature to authenticate, thus combining the advantages of both writer-independent and writer-dependent approaches. Other feature extraction techniques are also to be considered to increase information diversity and thus the system accuracy. Finally, significant improvement in learning time are expected from a distributed implementation of the Boosting Feature Selection algorithm.

APPENDIX I

BOOSTING DECISION STUMPS

This section presents the process of boosting decision stumps based on a toy problem composed of 20 examples from two classes ("X" and "O") as illustrated in the left panel of Figure I.1. The horizontal and vertical lines represent the two split points considered by the first decision stump built by the Gentle AdaBoost algorithm (see Algorithm 3.1).

The center panel of Figure I.1 represents the search made by the decision stump algorithm (see Algorithm 3.2) for the best split point in the x_1 dimension. This search imply to test all split points admissible by the data; since there are 20 examples, 19 split points are tested. Doing so, the errors on both distributions (represented by the curves marked by "X" and "O") are computed as well as the total error from both distributions (represented by the top curve). The best split point in x_1 is the point minimizing the total error (represented by an asterisk) which in this case equals 1.3 and is obtained by splitting the data between the fourth and fifth examples.

The right panel of Figure I.1 represents the same search process but in the x_2 dimension. It gives a minimal total error of 1.2 when splitting the data between the 14th and 15th examples. Since $1.2 < 1.3$, this is the split point selected by the decision stump.

The left panel of Figure I.2a illustrates the current classification result from the decision stump; the top region is labelled "O" and contains no misclassifications while the bottom region is labelled "X" and contains four misclassified examples. The right panel shows the weight update by the Gentle AdaBoost algorithm in function of the result of the first decision stump ($t = 1$); the font size of each example being proportional to its new weight. The four "Os" below the decision stump threshold are misclassified, hence their weight is increased accordingly. The next decision stump will have to take these new weights into account when optimizing its split point.

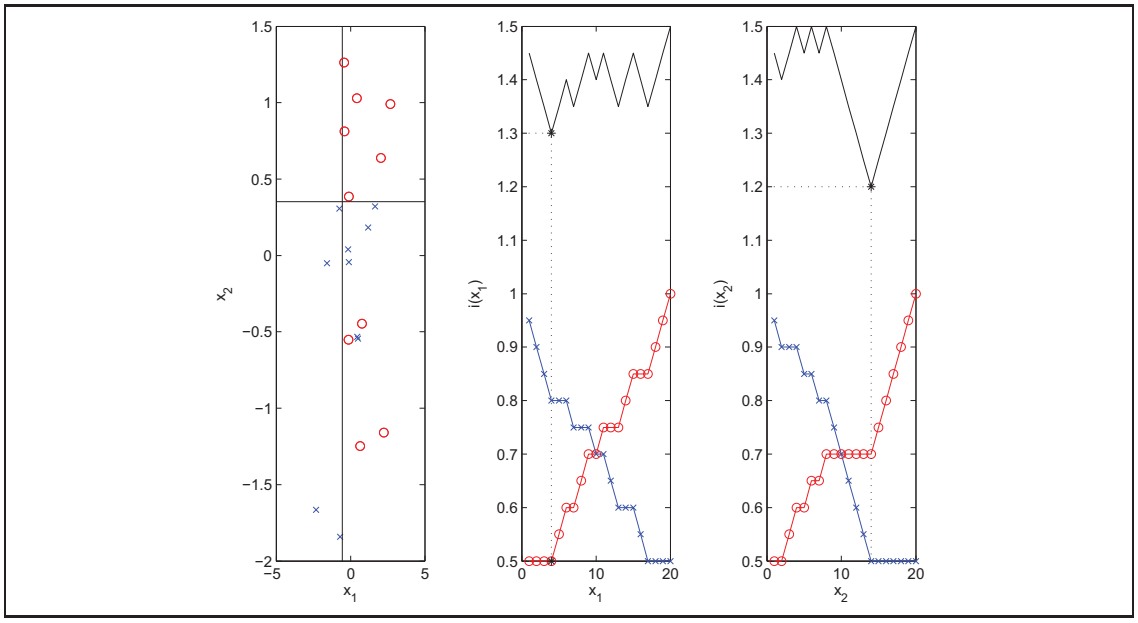

Figure I.1: Building of a decision stump based on a toy problem. Left panel illustrates the two dimensional problem. Center and right panels describe how the parameters of the stump are determined.

The right panel of Figure I.2b shows the split point of the second decision stump ($t = 2$) and the subsequent weight update. The left panel illustrates the frontier drawn by the committee of stumps (EoC). The top-right region is closely fitting the six "Os" in that region but still there are four "Os" misclassified.

The right panel of Figure I.2c shows the result of the third decision stump ($t = 3$) and the subsequent weight update. The left panel illustrates the new frontier drawn by the committee of stumps. A second region, at the bottom-right of the feature space is now labelled "O", leaving a single "O" example misclassified. This last example is more difficult to classify and its weight is increased accordingly. In fact, Gentle AdaBoost focuses on these difficult cases.

Forwarding to the tenth iteration, the right panel of Figure I.2d shows the result of the tenth decision stump ($t = 10$) and the subsequent weight update. The left panel illustrates the frontier drawn by the committee of ten stumps. A notch has been added to the bottom-right

"O" region to acheive a perfect classification of the data. However, the complexity of the frontier illustrates how Gentle AdaBoost can overfit when learning from noisy data. Using an early stopping criterion based on a validation dataset could have, for instance, stopped the learning process at the third iteration, thus preventing Gentle AdaBoost from overfitting the data.

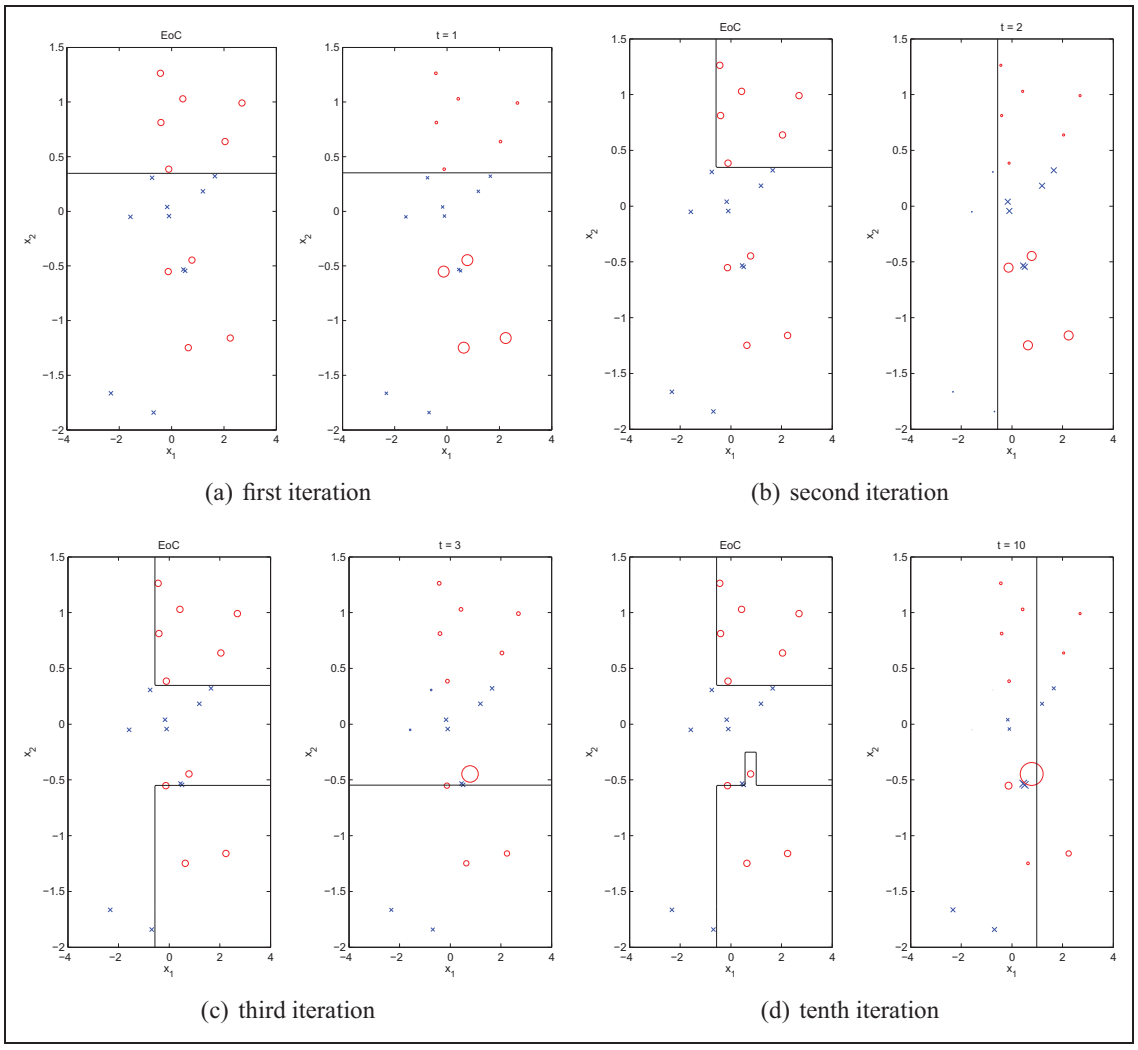

Figure I.2: Three firsts and last iterations of Gentle AdaBoost (a to d, respectively). At each iteration, the left panel shows the classification result from the committee of stumps while the right panel illustrates the current decision stump and the weights to be used for the next iteration.

APPENDIX II

SINGLE SCALE EXTENDED SHADOW CODE SELECTED FEATURES

For each Extended Shadow Code representation (Figures II.1 to II.5), the selected features are shown with continous lines while the others are made up of dotted lines. The regions of the signature image where information is extracted are colored in grey.

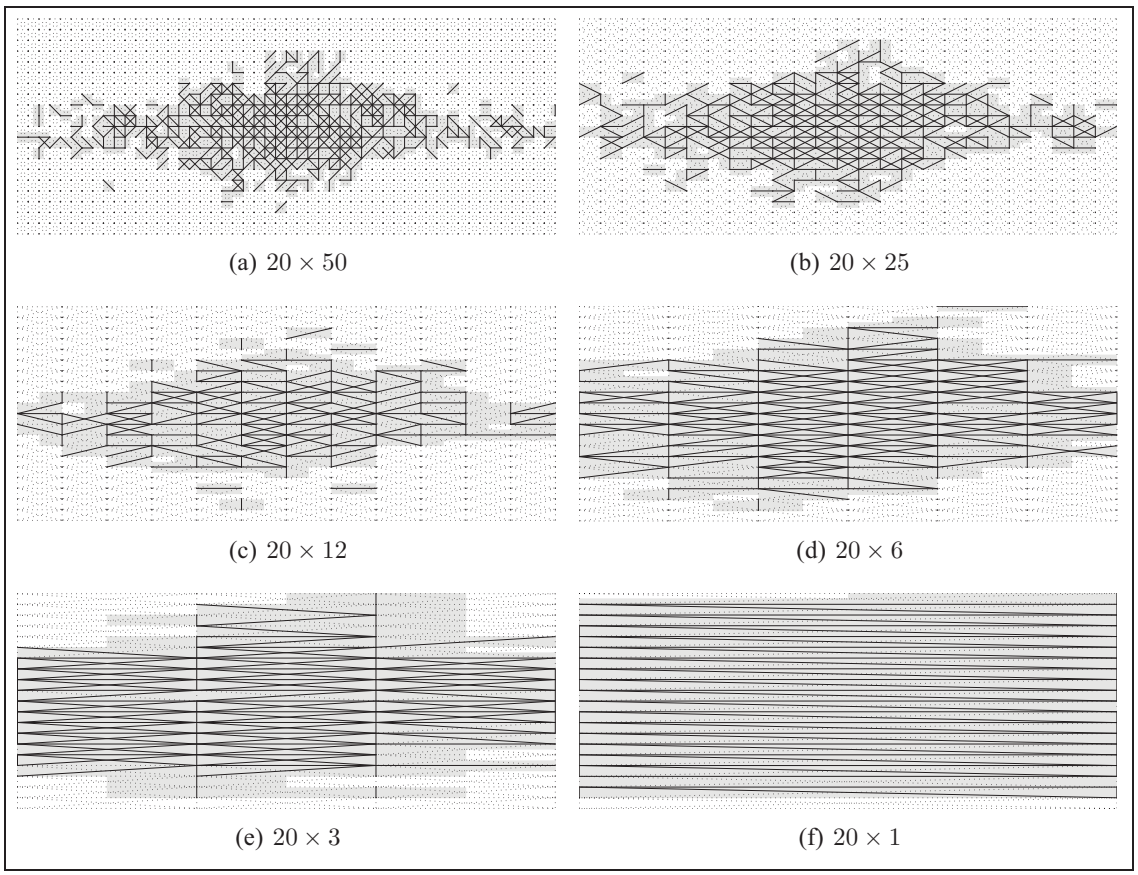

Figure II.1: Extended Shadow Code selected features and their corresponding region of the image for the "20 rows" single scale representations.

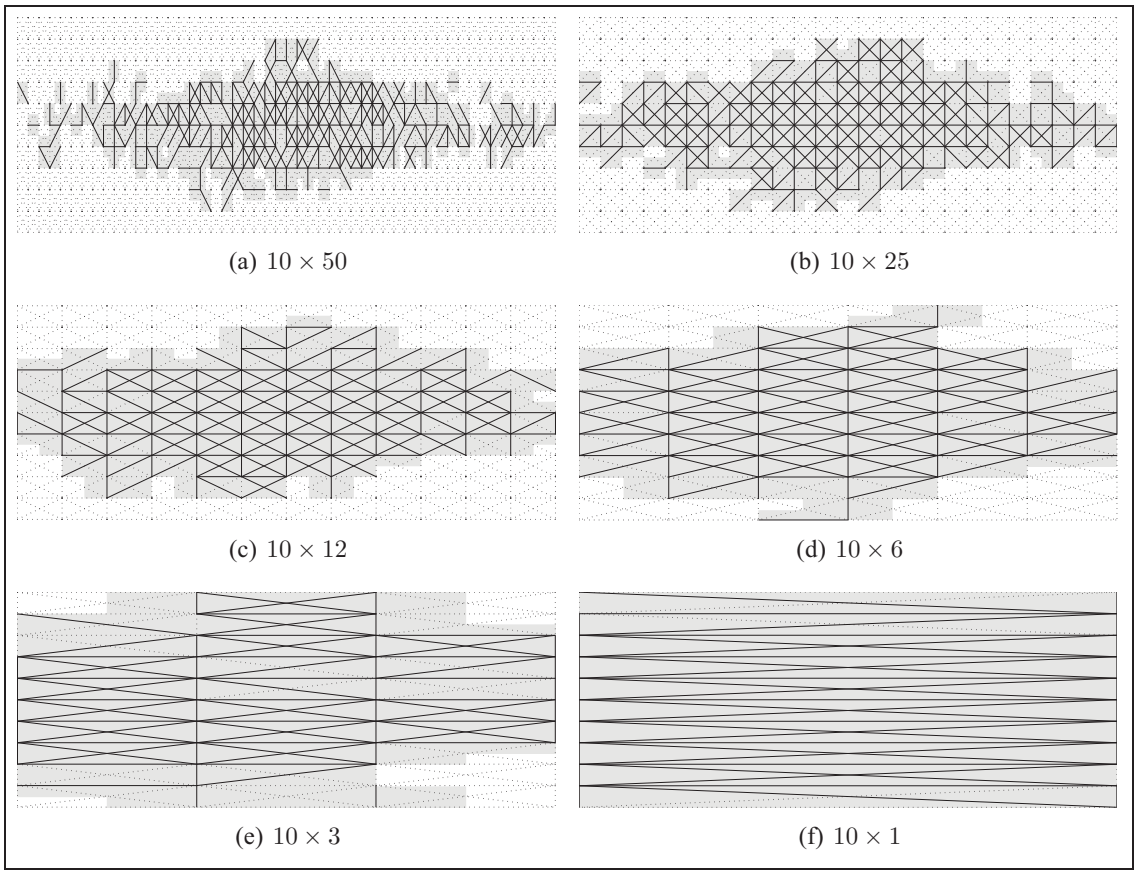

Figure II.2: Extended Shadow Code selected features and their corresponding region of the image for the "10 rows" single scale representations.

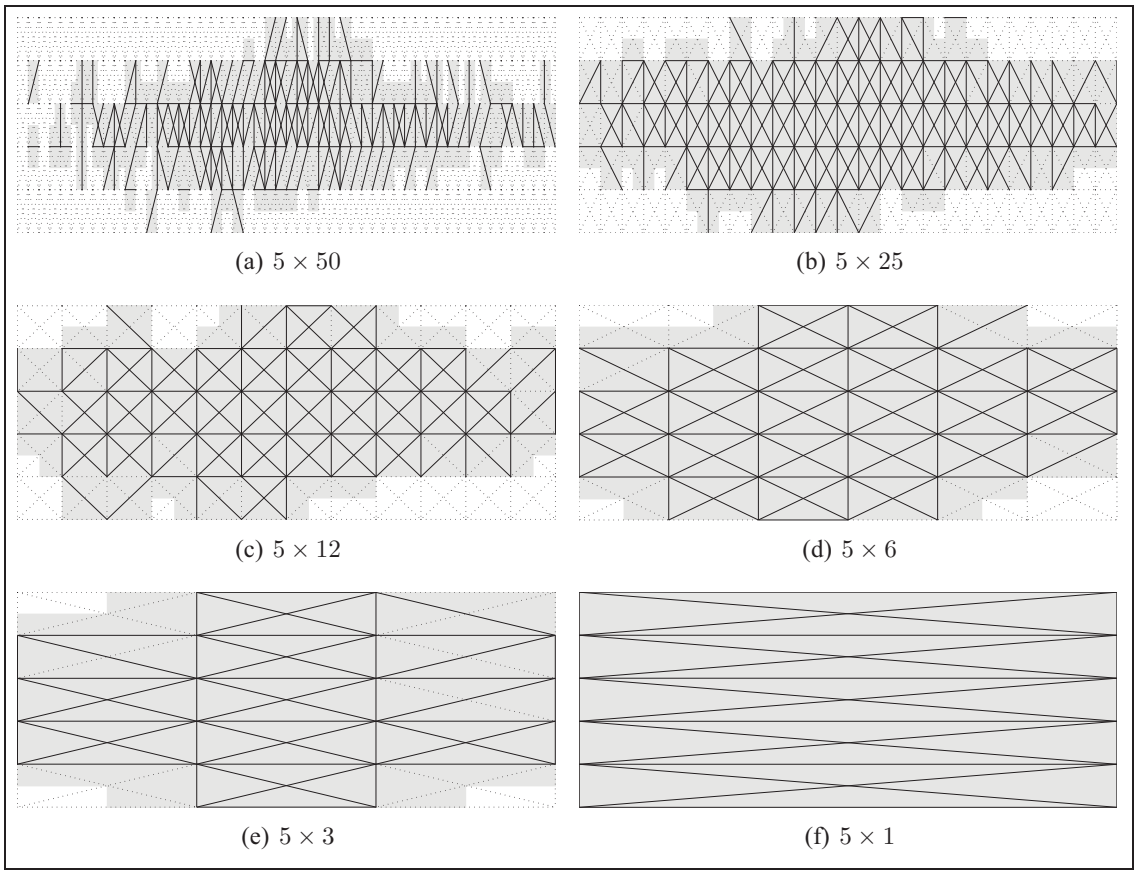

Figure II.3: Extended Shadow Code selected features and their corresponding region of the image for the "5 rows" single scale representations.

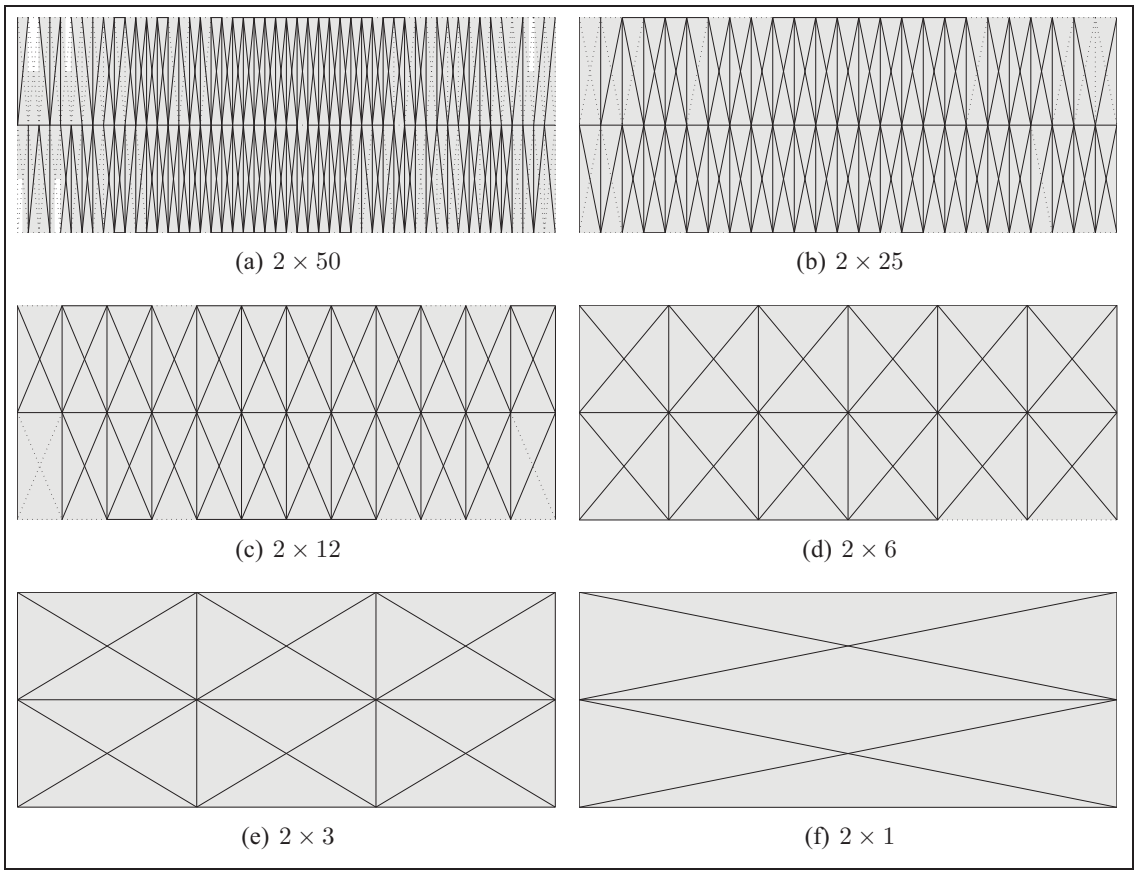

Figure II.4: Extended Shadow Code selected features and their corresponding region of the image for the "2 rows" single scale representations.

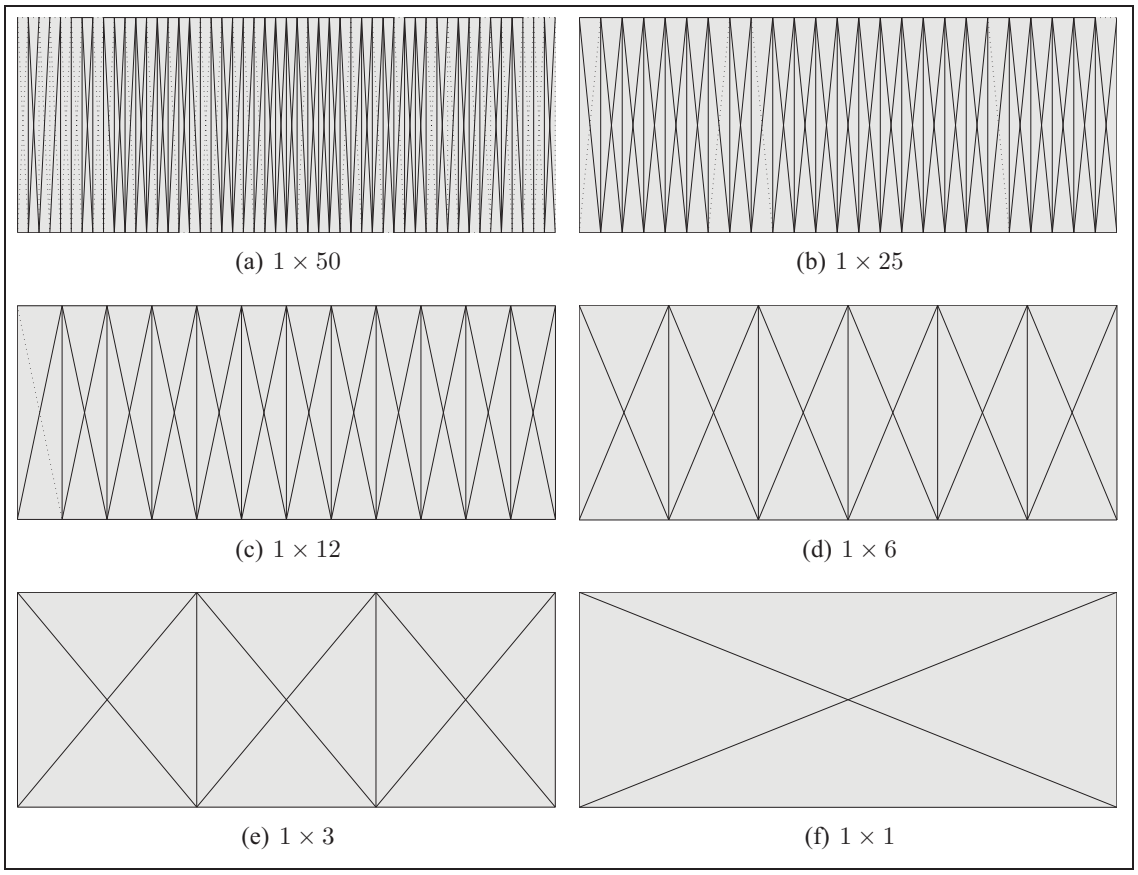

Figure II.5: Extended Shadow Code selected features and their corresponding region of the image for the "1 row" single scale representations.

APPENDIX III

SINGLE SCALE DIRECTIONAL PDF SELECTED FEATURES

For each Directional PDF representation (Figures III.1 to III.5), the selected features of each grid cell are shown using the color code illustrated at Figure 3.9 and white being used to represent unselected features.

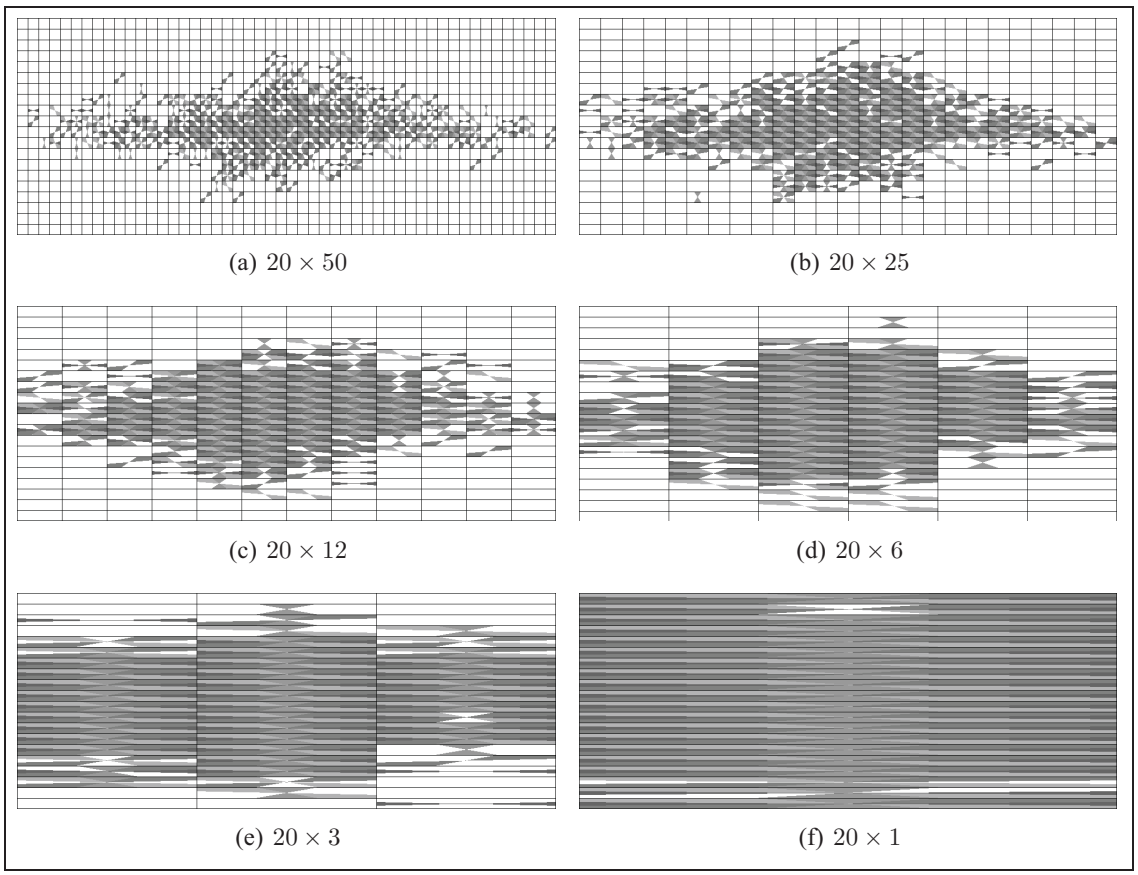

Figure III.1: Directional PDF selected features for the "20 rows" single scale representations.

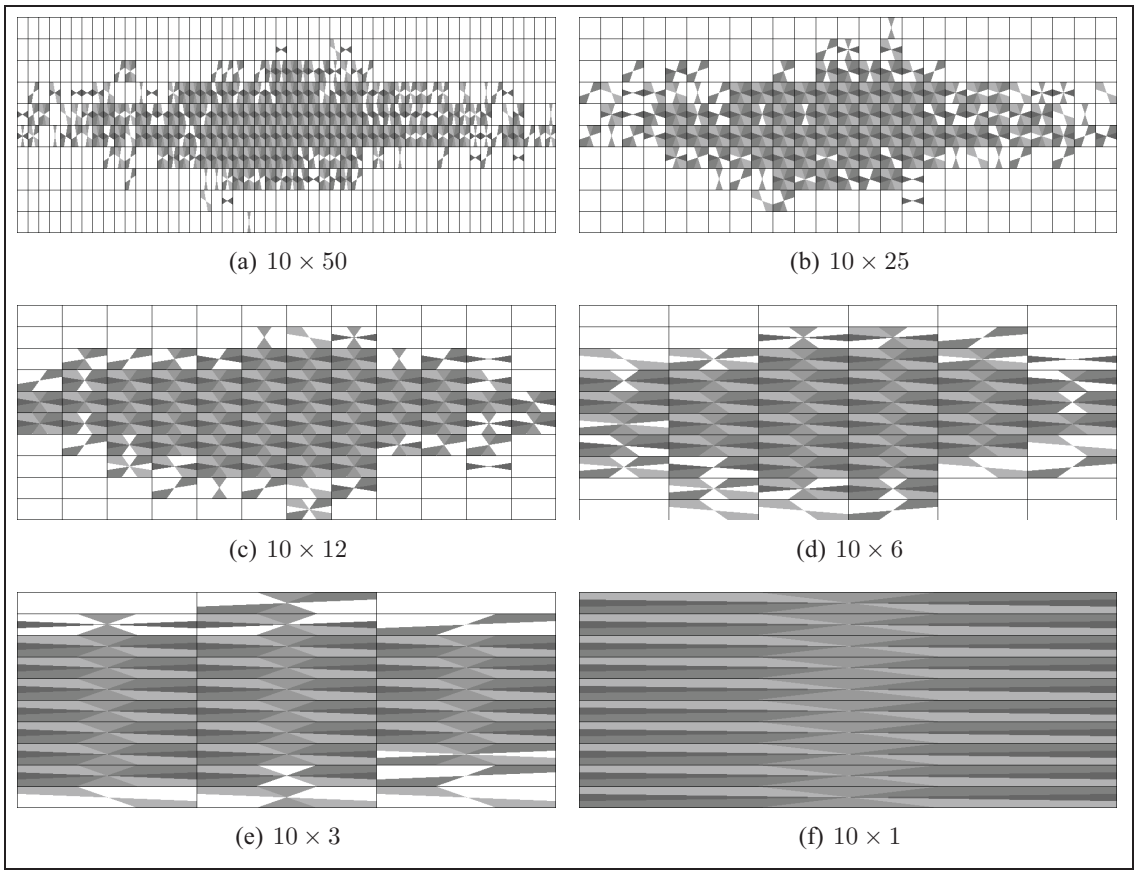

Figure III.2: Directional PDF selected features for the "10 rows" single scale representations.

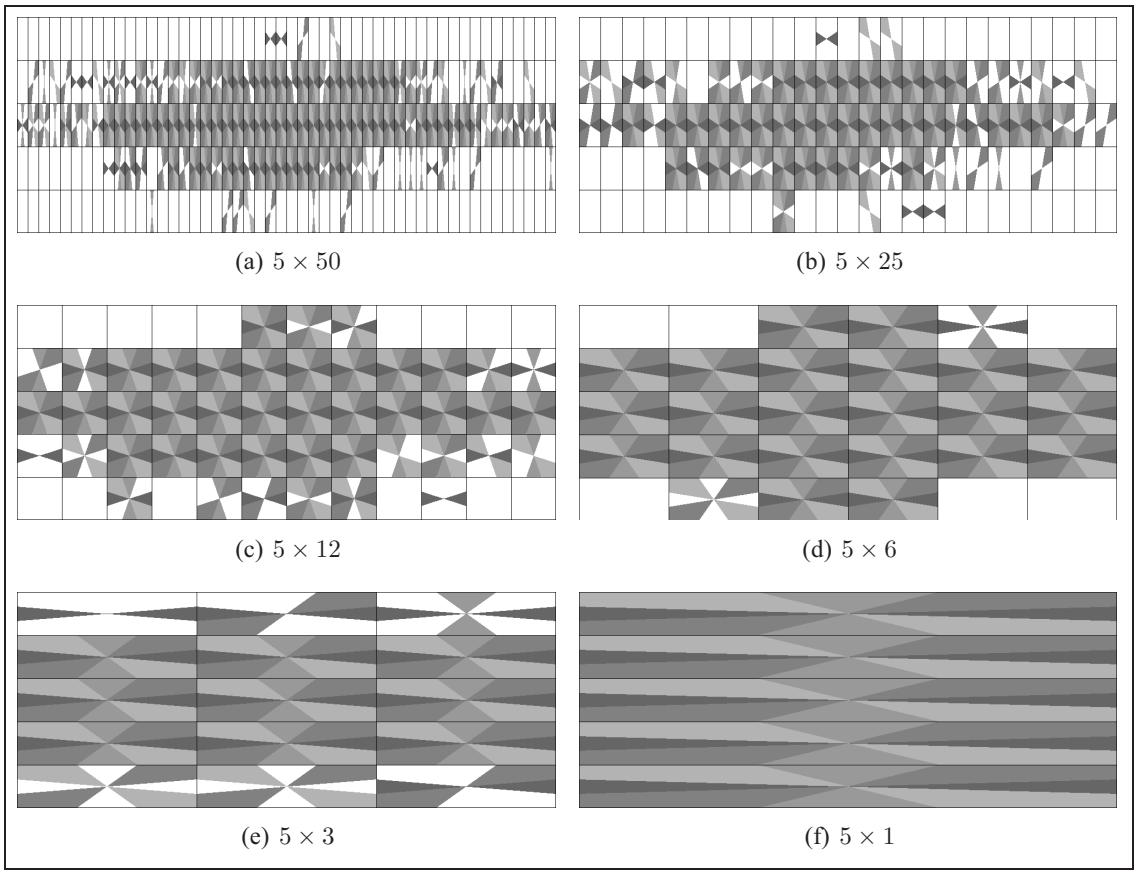

Figure III.3: Directional PDF selected features for the "5 rows" single scale representations.

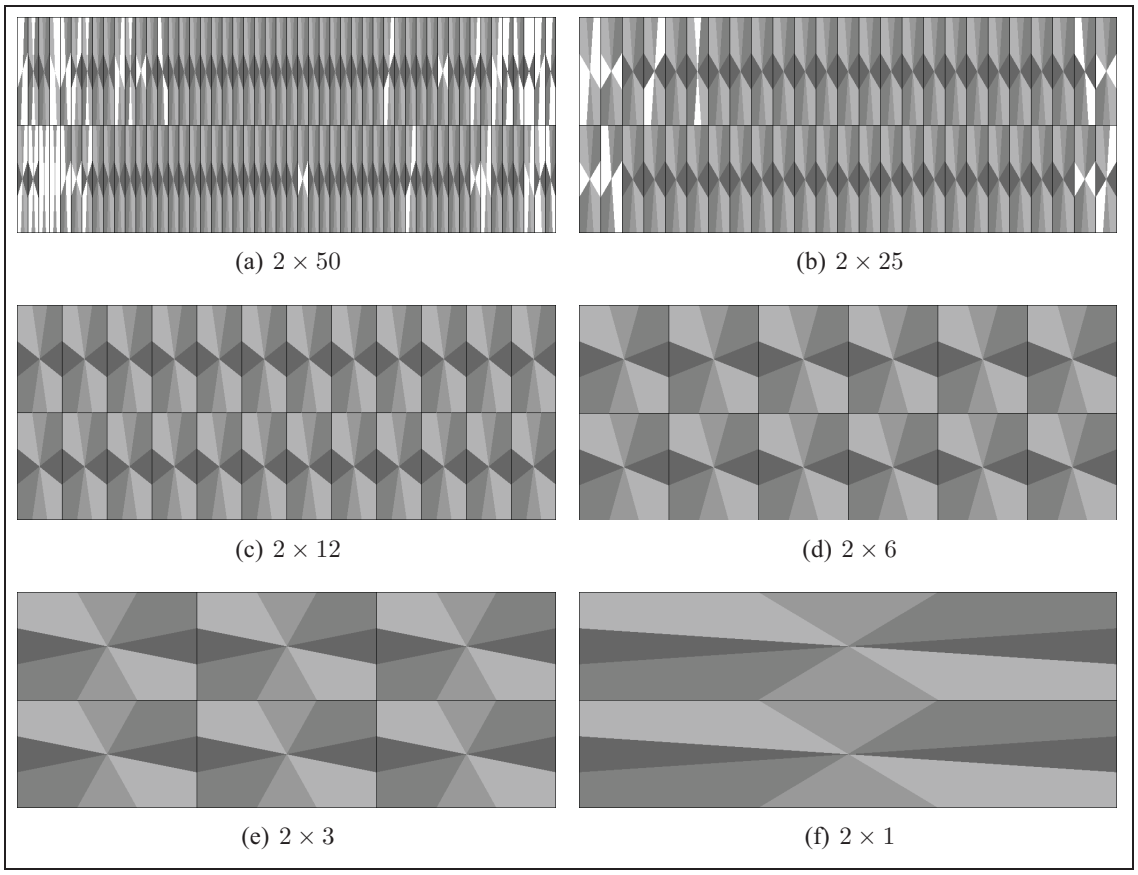

Figure III.4: Directional PDF selected features for the "2 rows" single scale representations.

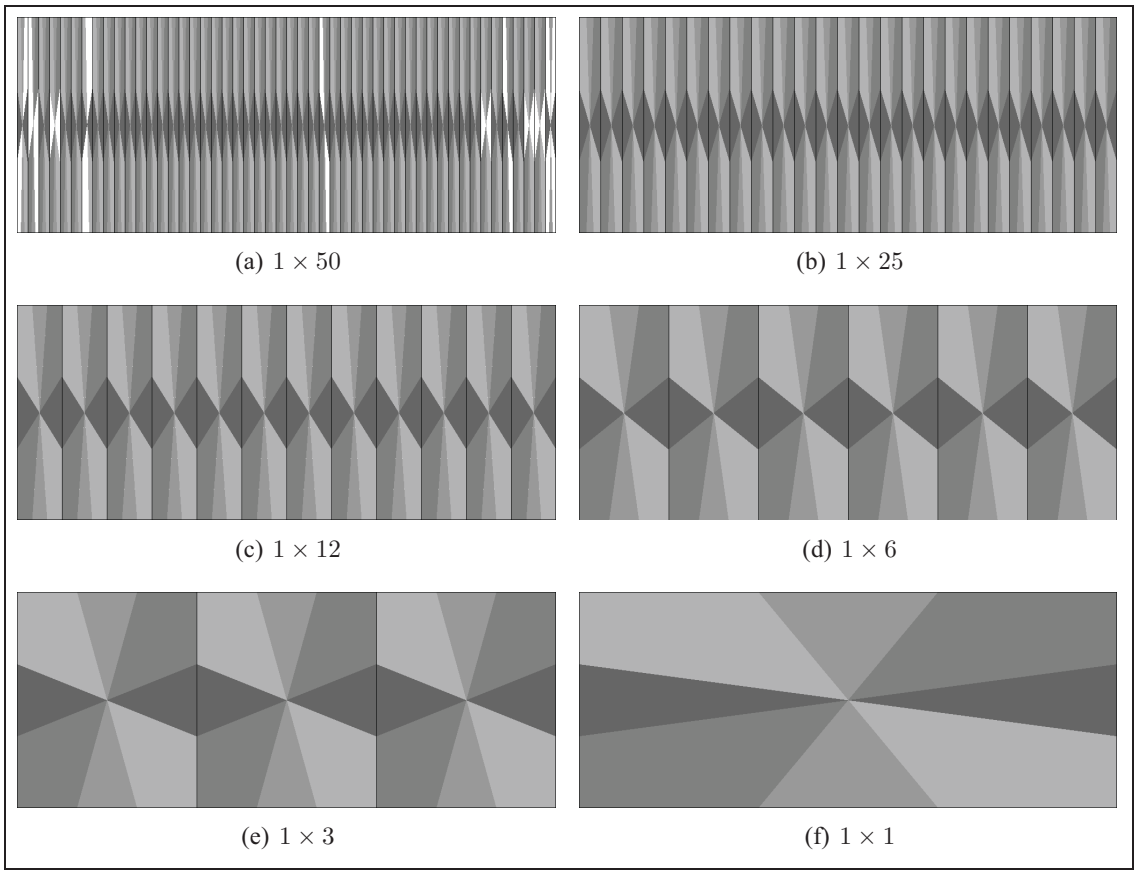

(a) 1×50 (b) 1×25

(c) 1×12 (d) 1×6

(e) 1×3 (f) 1×1

Figure III.5: Directional PDF selected features for the "1 row" single scale representations.

APPENDIX IV

MULTISCALE EXTENDED SHADOW CODE SELECTED FEATURES

For the Extended Shadow Code multiscale representation (Figures IV.1 to IV.5), the features selected at each scale are shown with continous lines while the others are made up of dotted lines. The regions of the signature image where information is extracted are colored in grey.

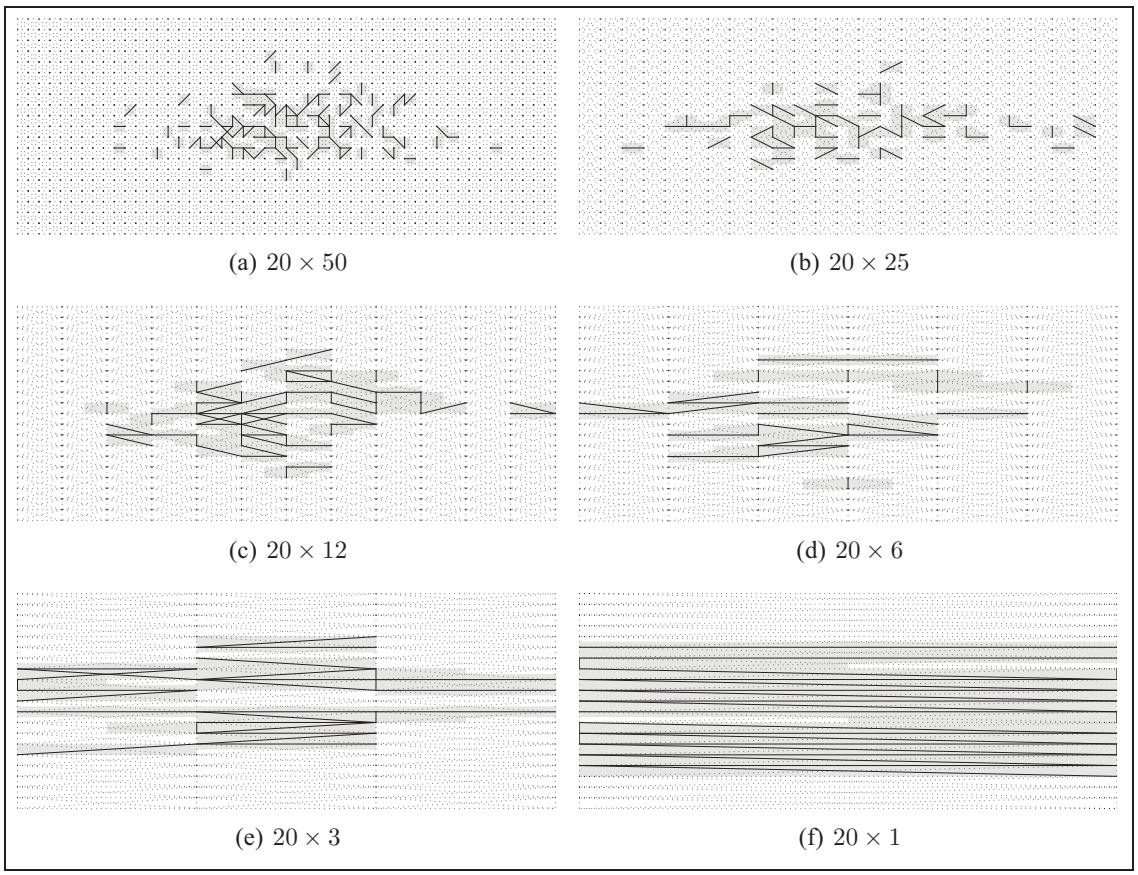

Figure IV.1: Extended Shadow Code selected features and their corresponding region of the image for the "20 rows" aspect of the multiscale representation.

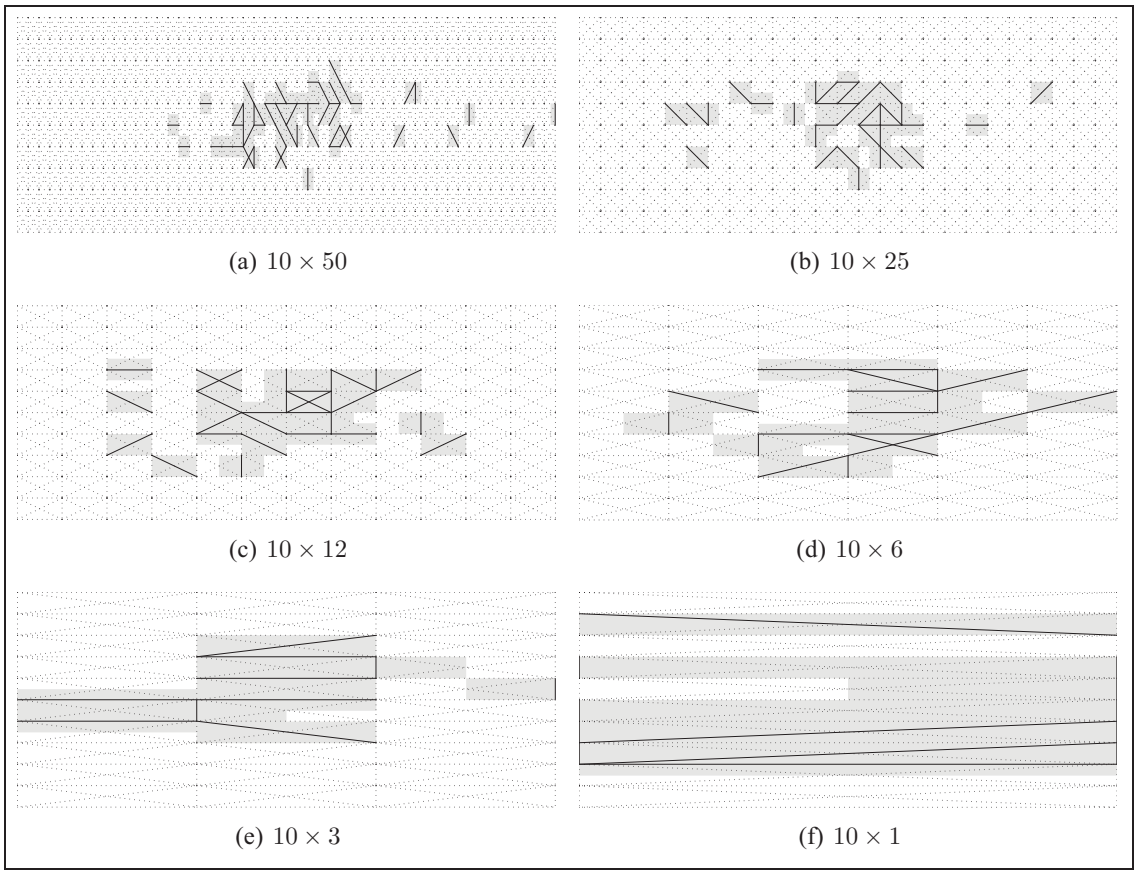

Figure IV.2: Extended Shadow Code selected features and their corresponding region of the image for the "10 rows" aspect of the multiscale representation.

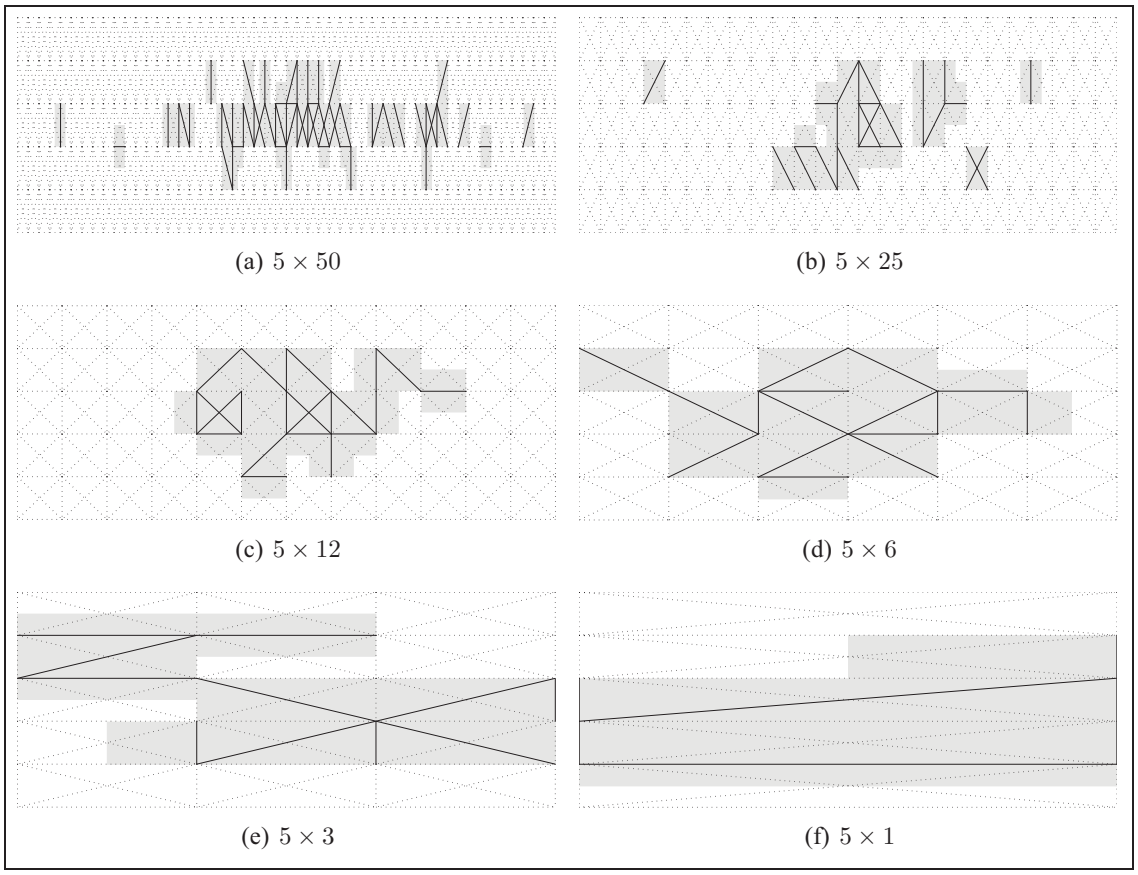

Figure IV.3: Extended Shadow Code selected features and their corresponding region of the image for the "5 rows" aspect of the multiscale representation.

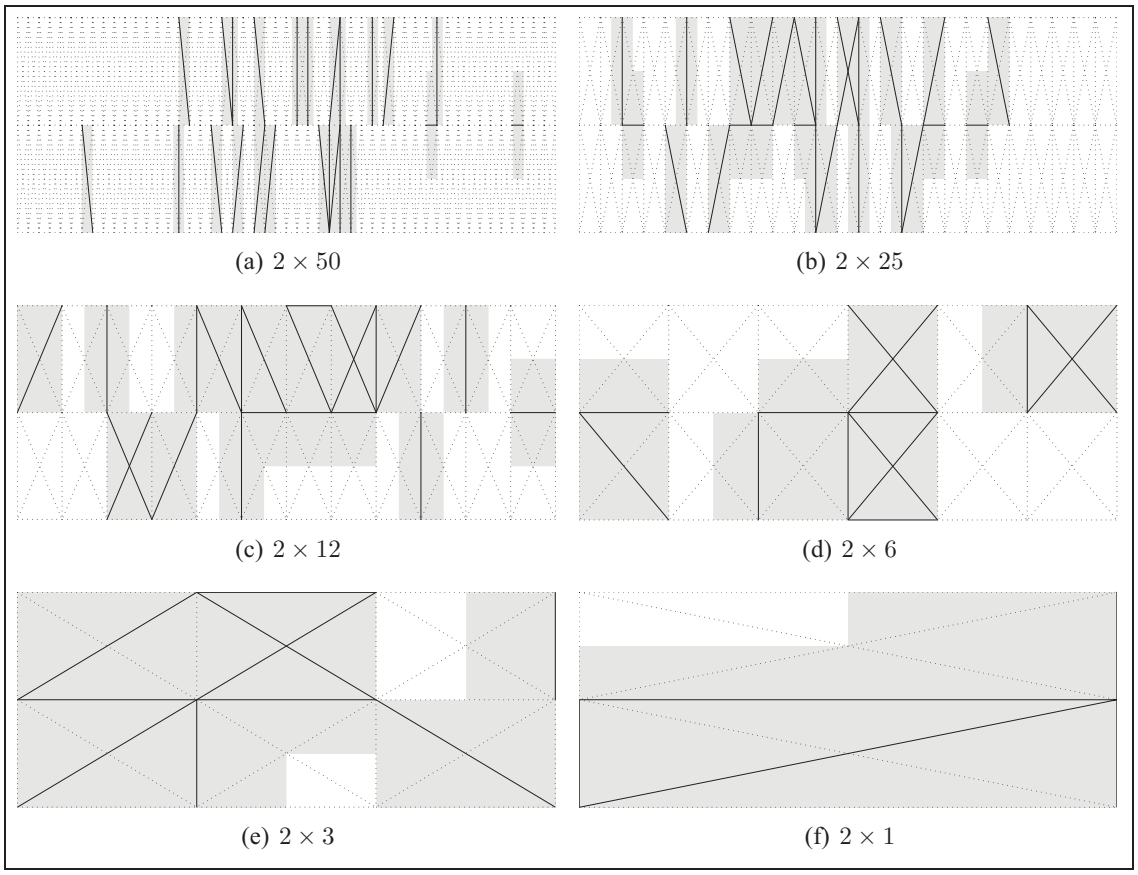

Figure IV.4: Extended Shadow Code selected features and their corresponding region of the image for the "2 rows" aspect of the multiscale representation.

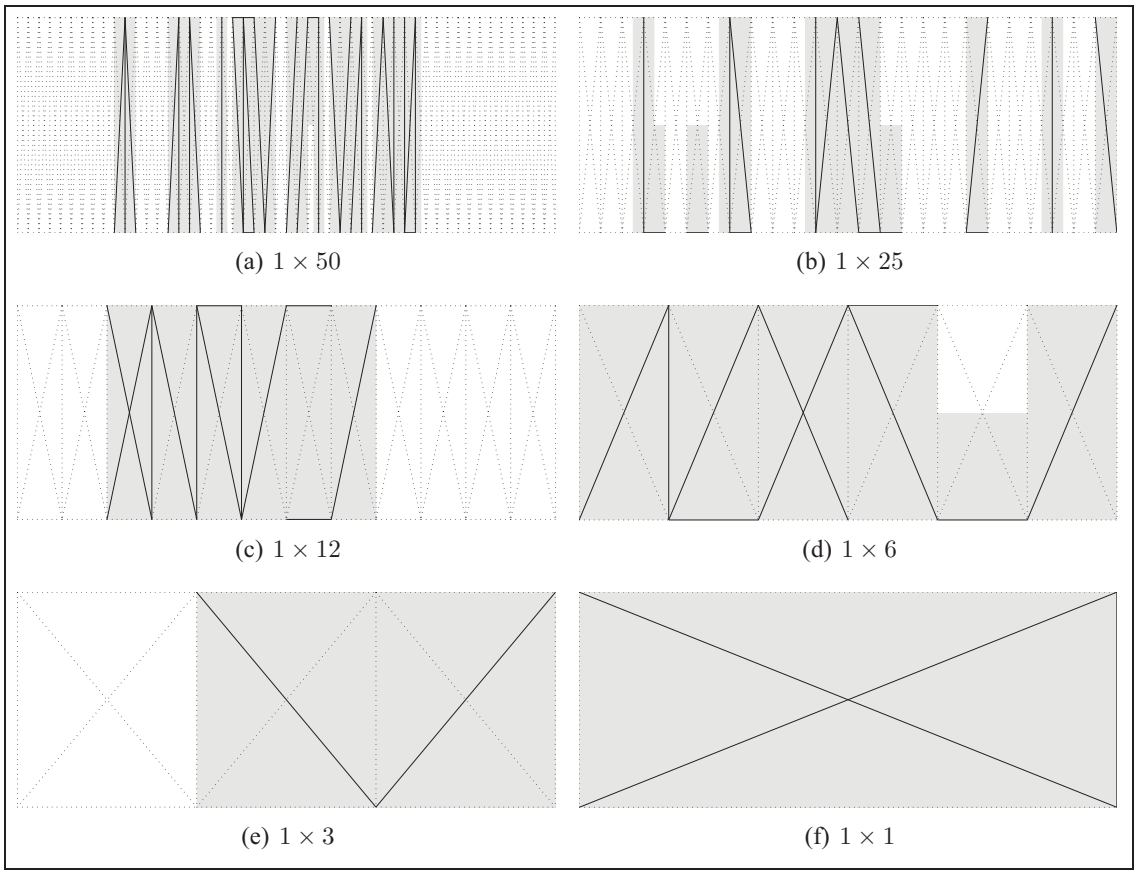

Figure IV.5: Extended Shadow Code selected features and their corresponding region of the image for the "1 row" aspect of the multiscale representation.

APPENDIX V

MULTISCALE DIRECTIONAL PDF SELECTED FEATURES

For the Directional PDF multiscale representation (Figures V.1 to V.5), the features selected at each scale are shown for each grid cell using the color code illustrated at Figure 3.9 and white being used to represent unselected features.

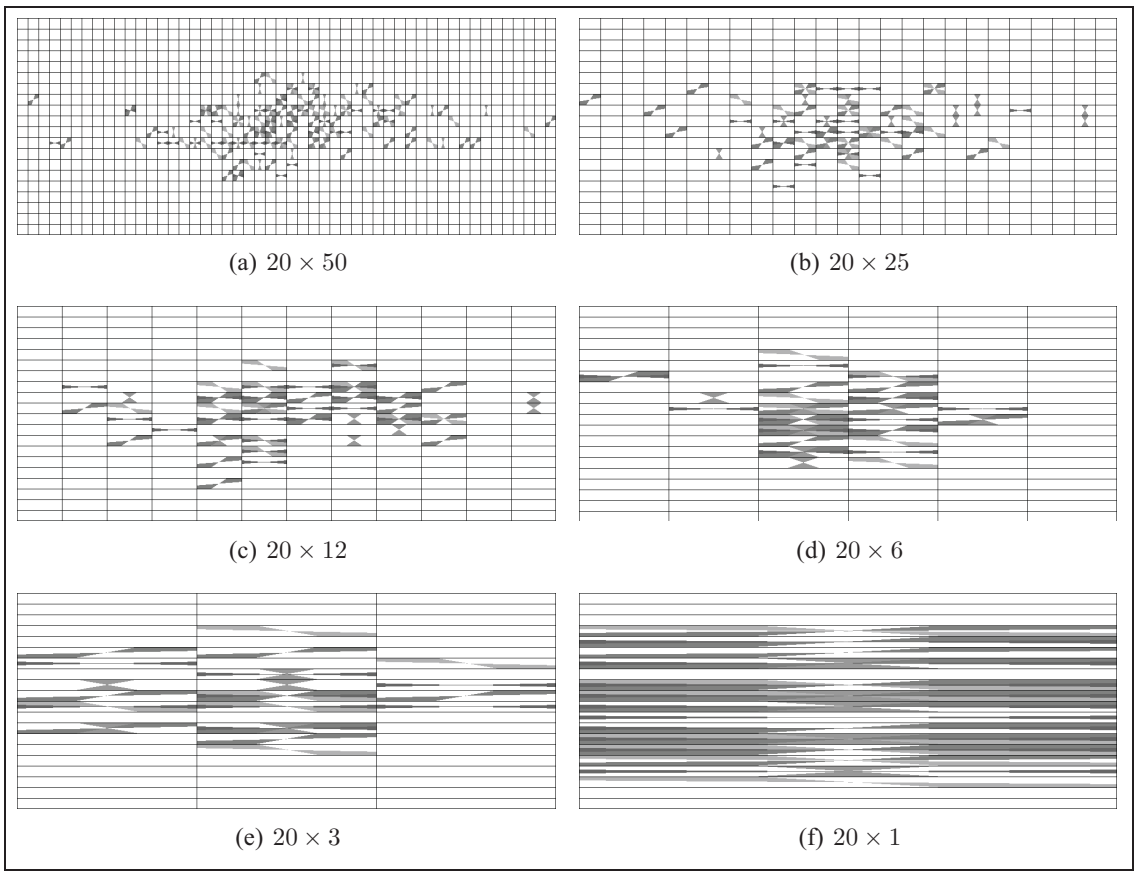

Figure V.1: Directional PDF selected features for the "20 rows" aspect of the multiscale representation.

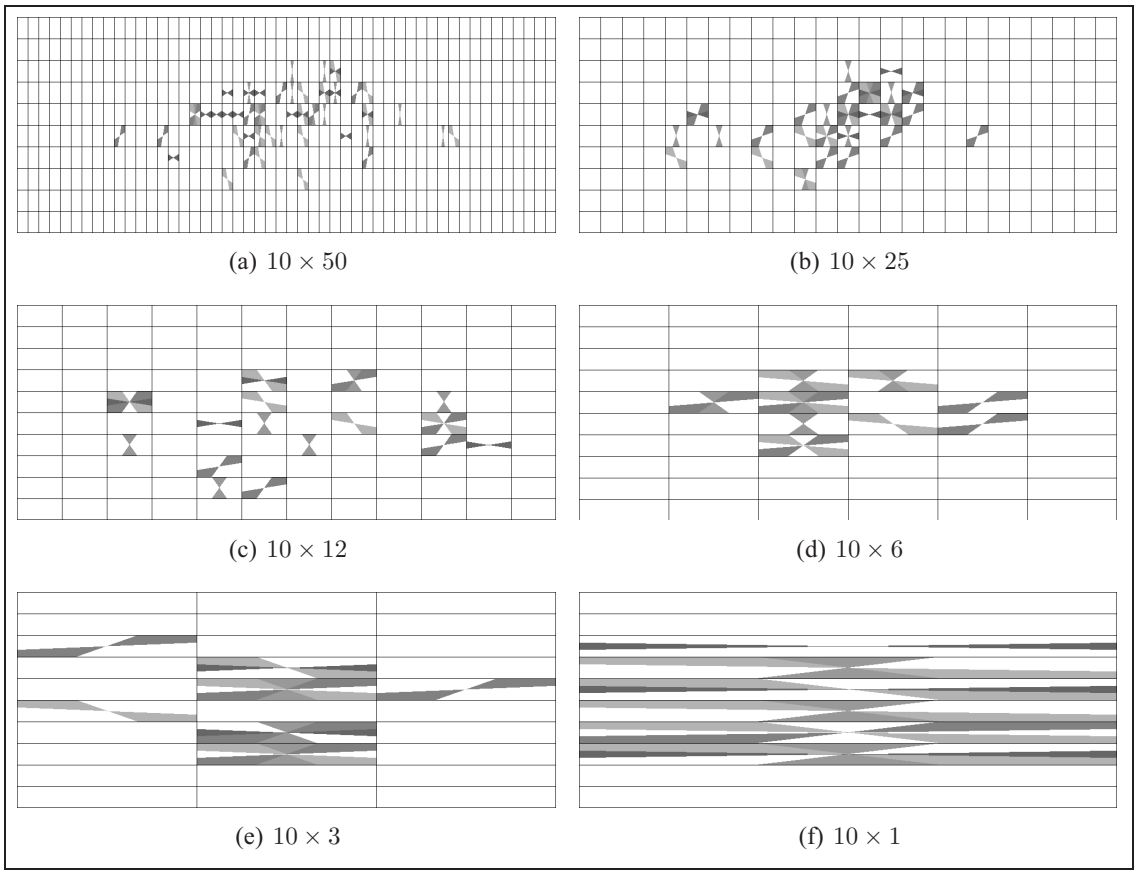

Figure V.2: Directional PDF selected features for the "10 rows" aspect of the multiscale representation.

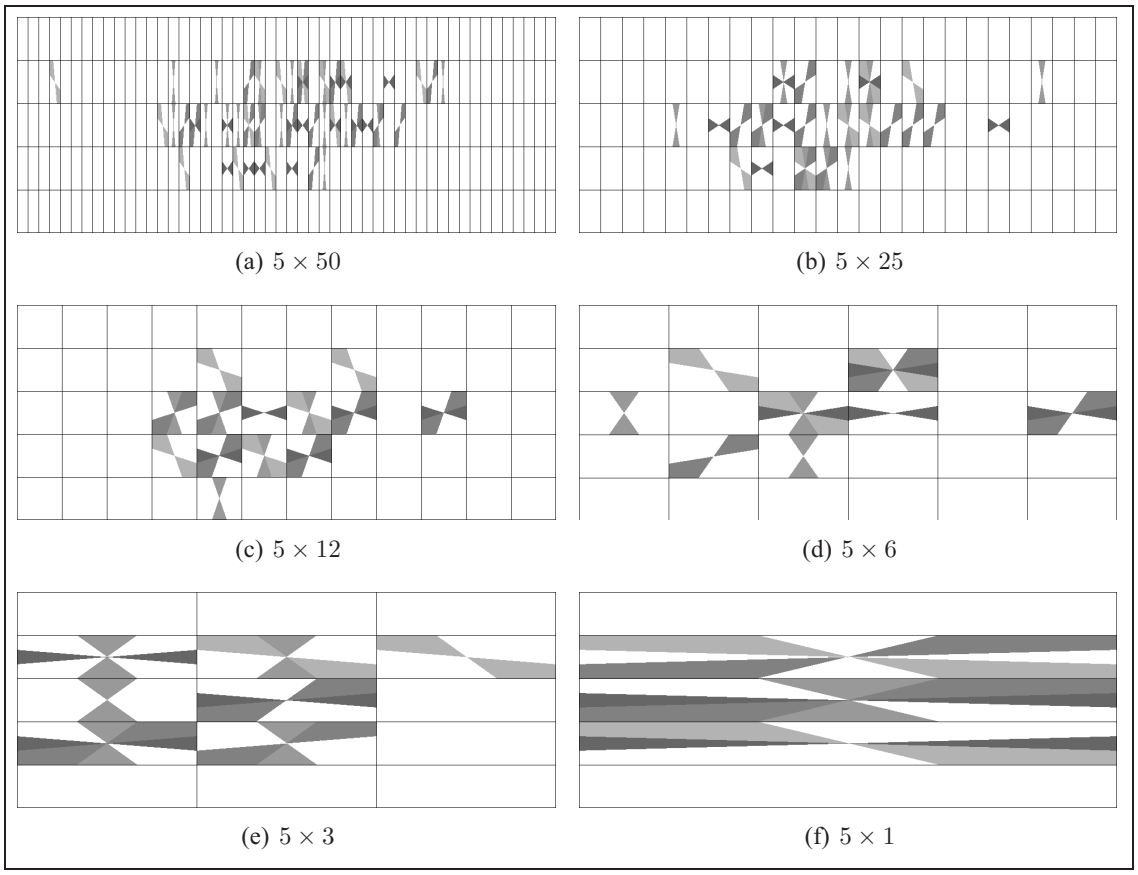

Figure V.3: Directional PDF selected features for the "5 rows" aspect of the multiscale representation.

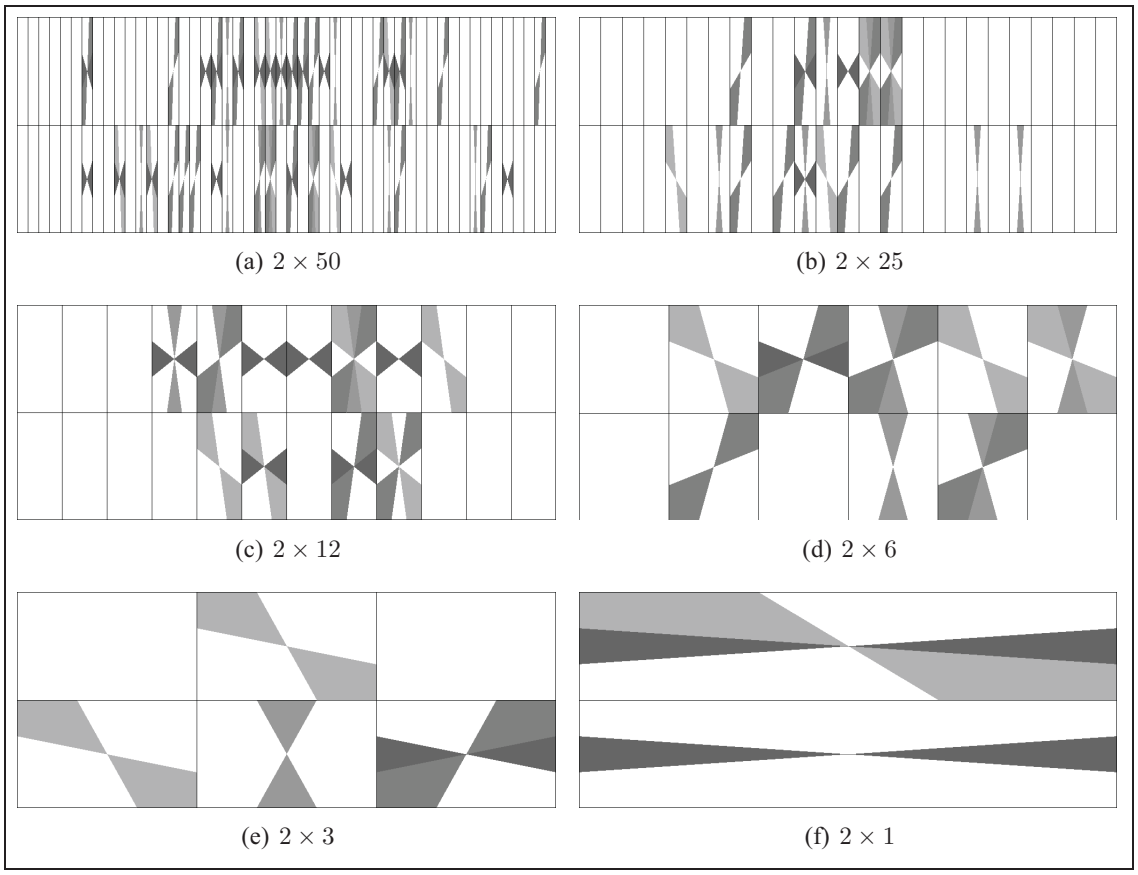

Figure V.4: Directional PDF selected features for the "2 rows" aspect of the multiscale representation.

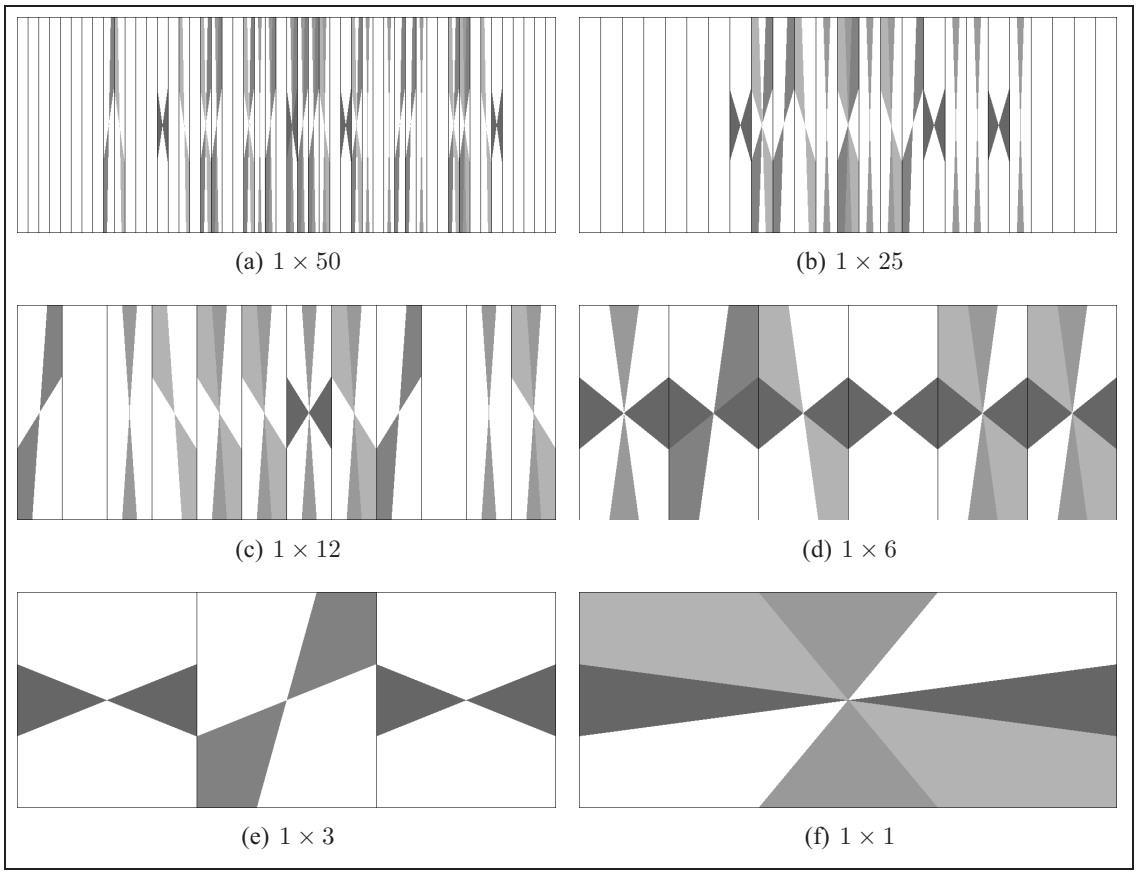

Figure V.5: Directional PDF selected features for the "1 row" aspect of the multiscale representation.

APPENDIX VI

MULTISCALE EXTENDED SHADOW CODE AND DIRECTIONAL PDF SELECTED FEATURES

For the Extended Shadow Code and Directional PDF multiscale representation, the Extended Shadow Code features (Figures VI.1 to VI.5) selected at each scale are shown with continous lines while the others are made up of dotted lines. The regions of the signature image where information is extracted are colored in grey.

Regarding the Directional PDF (Figures VI.6 to VI.10), the features selected at each scale are shown for each grid cell using the color code illustrated at Figure 3.9 and white being used to represent unselected features.

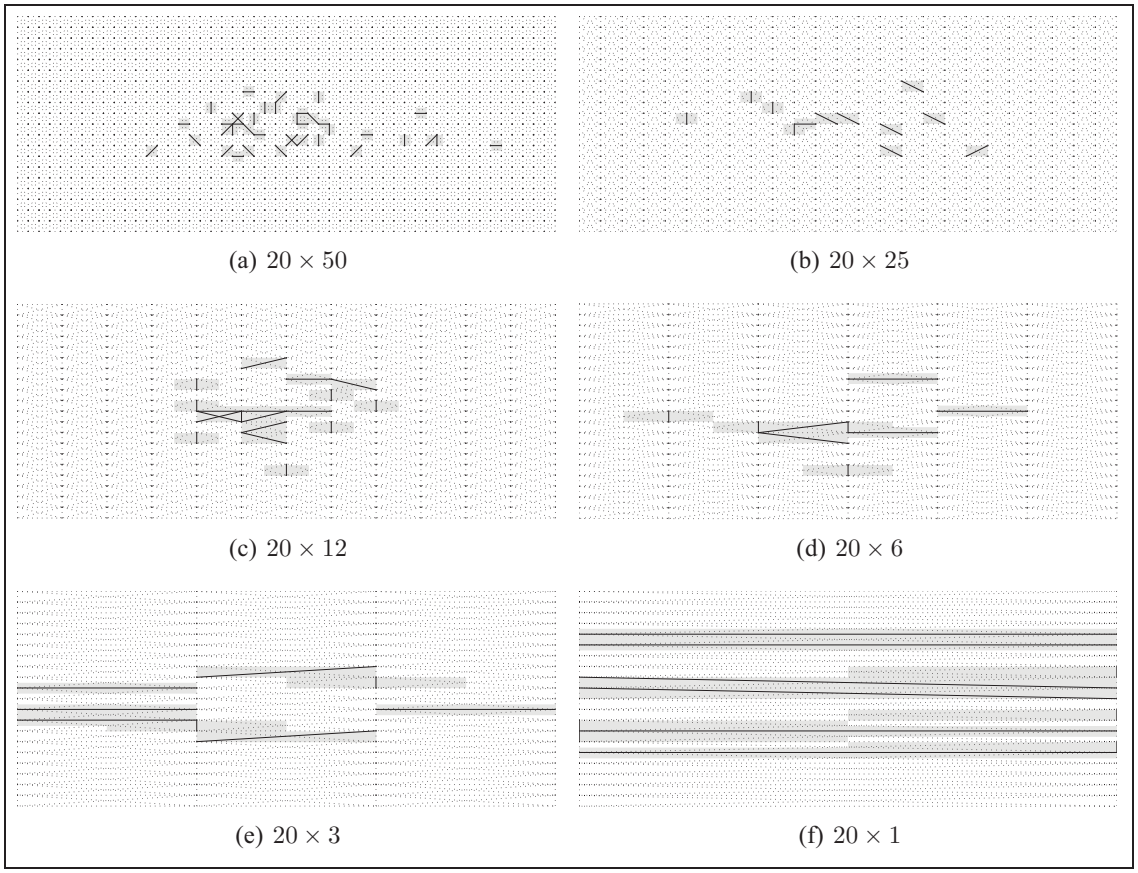

Figure VI.1: Extended Shadow Code selected features and their corresponding region of the image for the "20 rows" aspect of the Extended Shadow Code and Directional PDF multiscale representation.

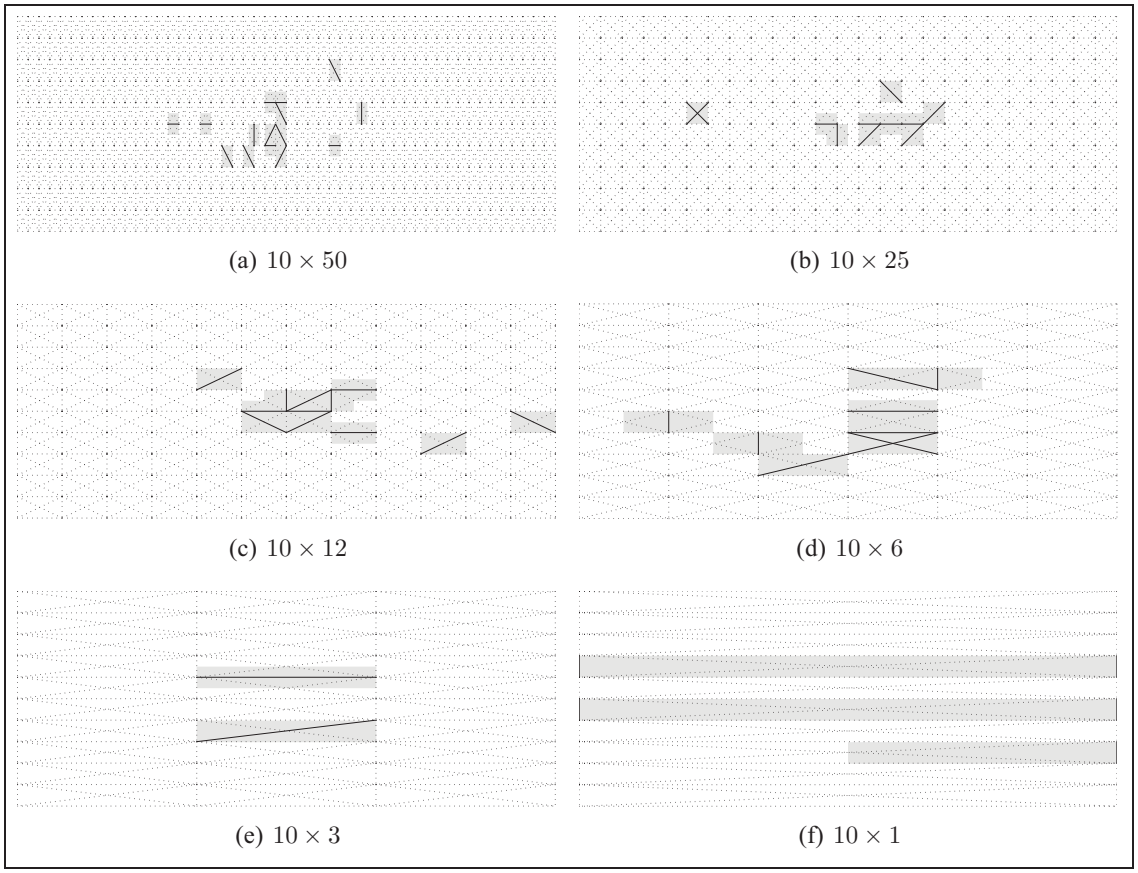

(a) 10×50 (b) 10×25

(c) 10×12 (d) 10×6

(e) 10×3 (f) 10×1

Figure VI.2: Extended Shadow Code selected features and their corresponding region of the image for the "10 rows" aspect of the Extended Shadow Code and Directional PDF multiscale representation.

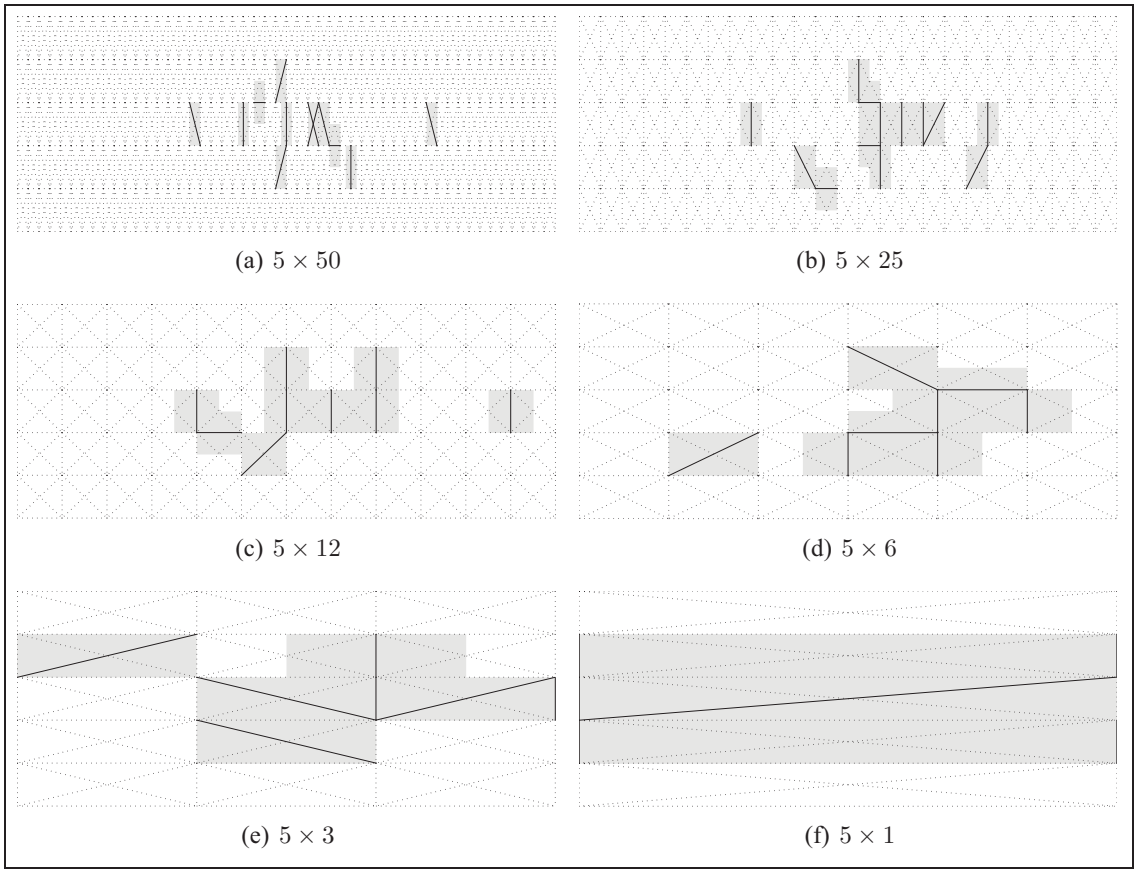

Figure VI.3: Extended Shadow Code selected features and their corresponding region of the image for the "5 rows" aspect of the Extended Shadow Code and Directional PDF multiscale representation.

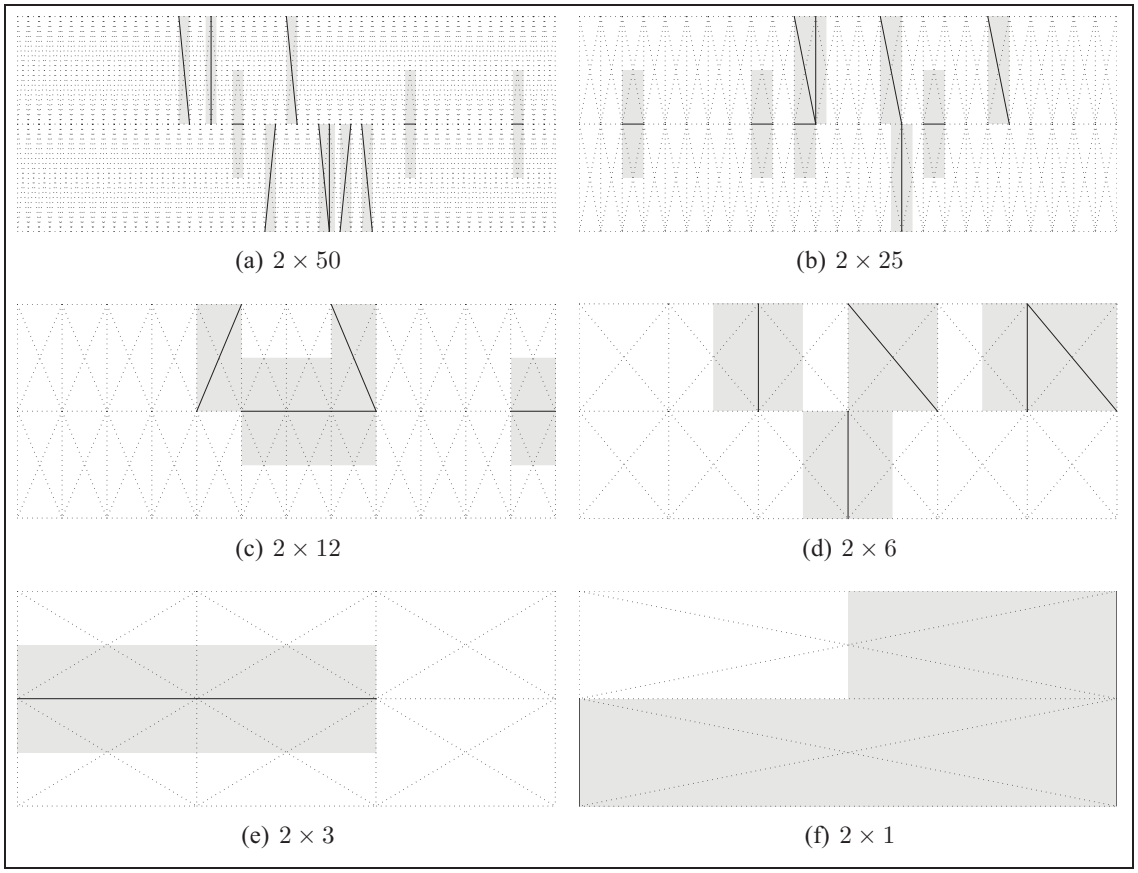

Figure VI.4: Extended Shadow Code selected features and their corresponding region of the image for the "2 rows" aspect of the Extended Shadow Code and Directional PDF multiscale representation.

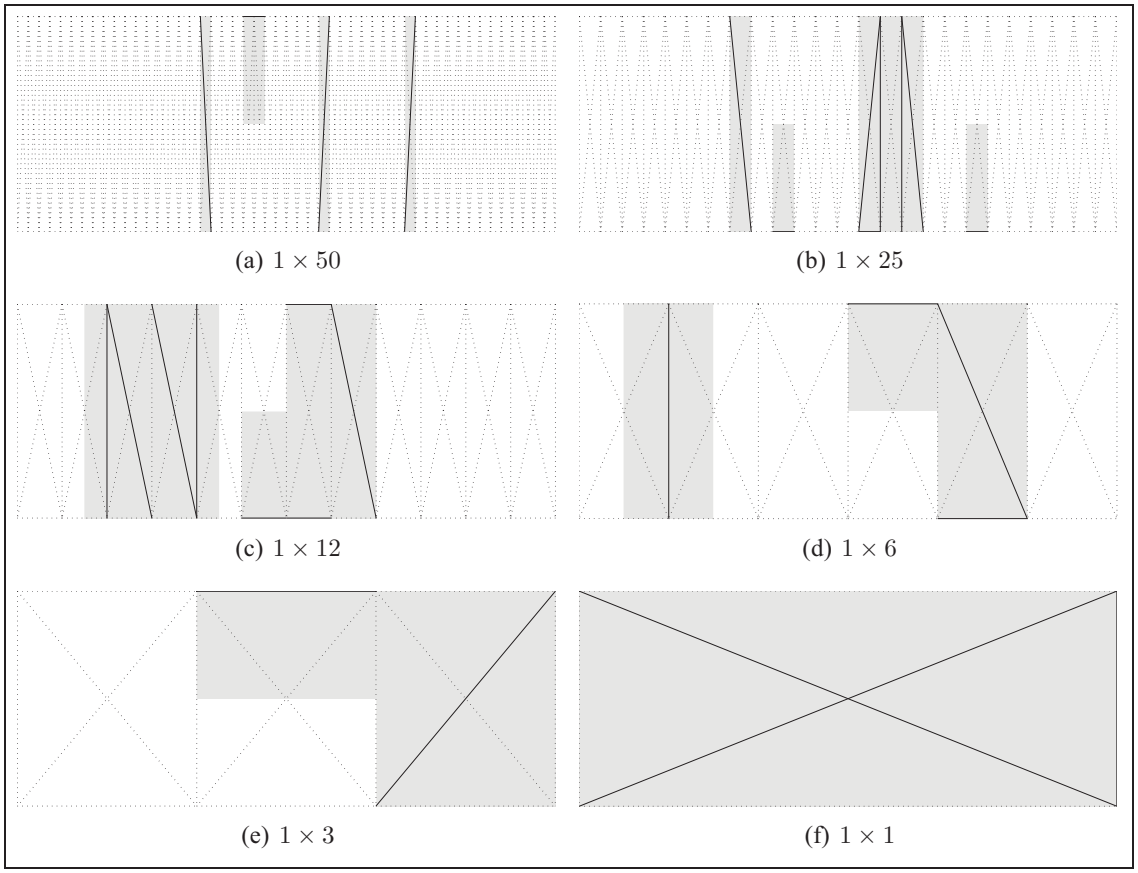

Figure VI.5: Extended Shadow Code selected features and their corresponding region of the image for the "1 row" aspect of the Extended Shadow Code and Directional PDF multiscale representation.

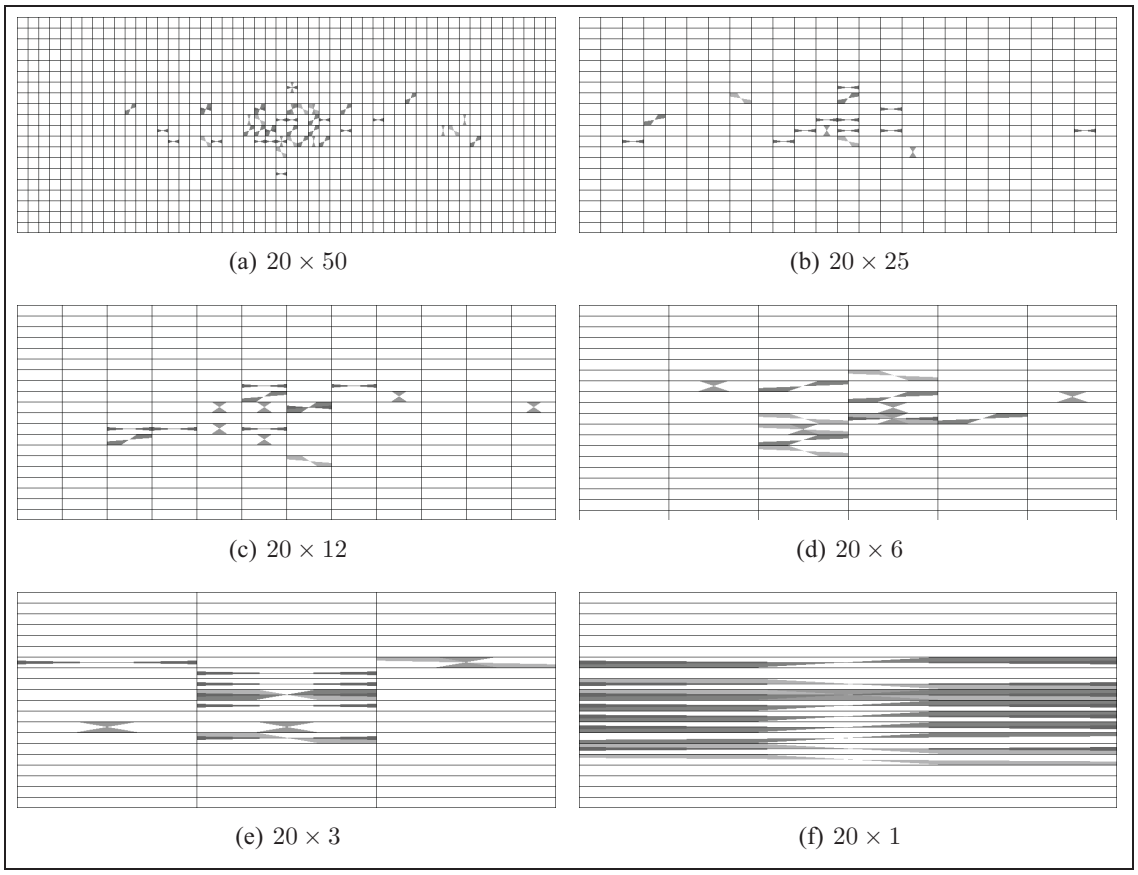

Figure VI.6: Directional PDF selected features for the "20 rows" aspect of the multiscale representation.

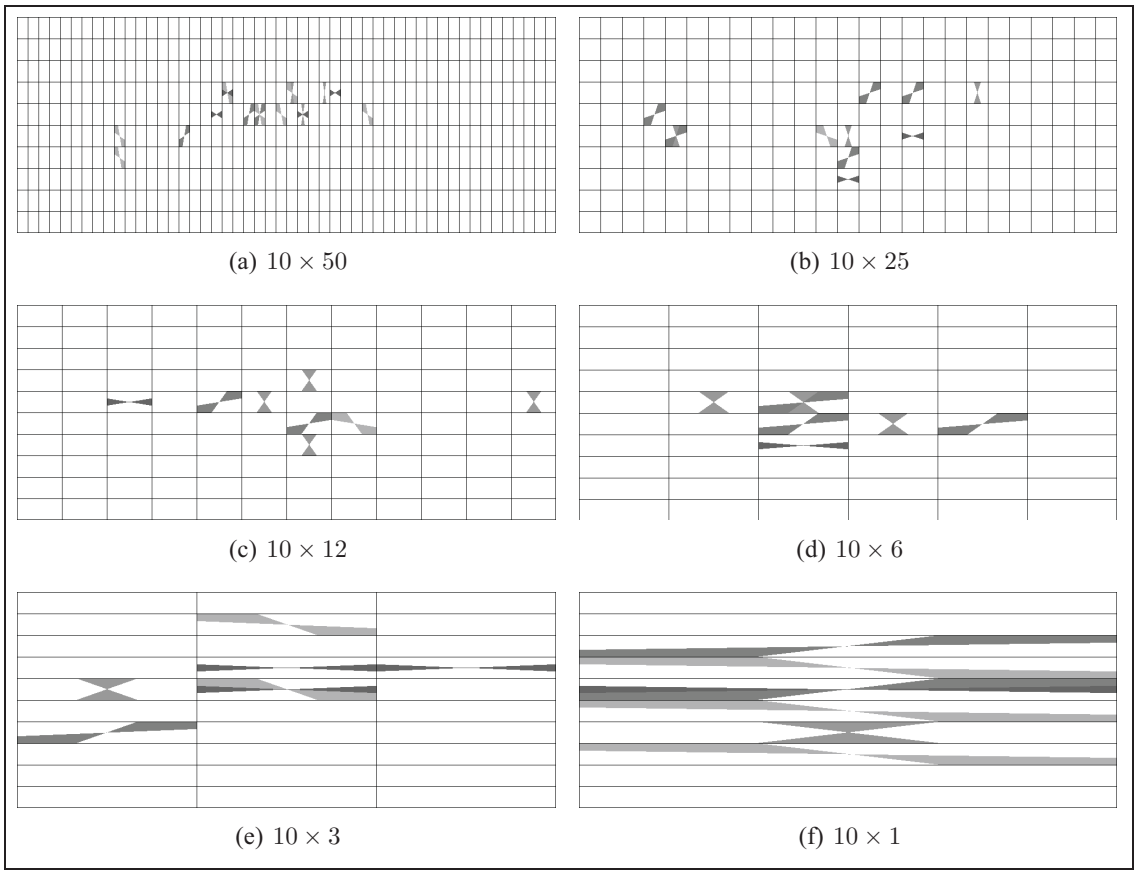

Figure VI.7: Directional PDF selected features for the "10 rows" aspect of the multiscale representation.

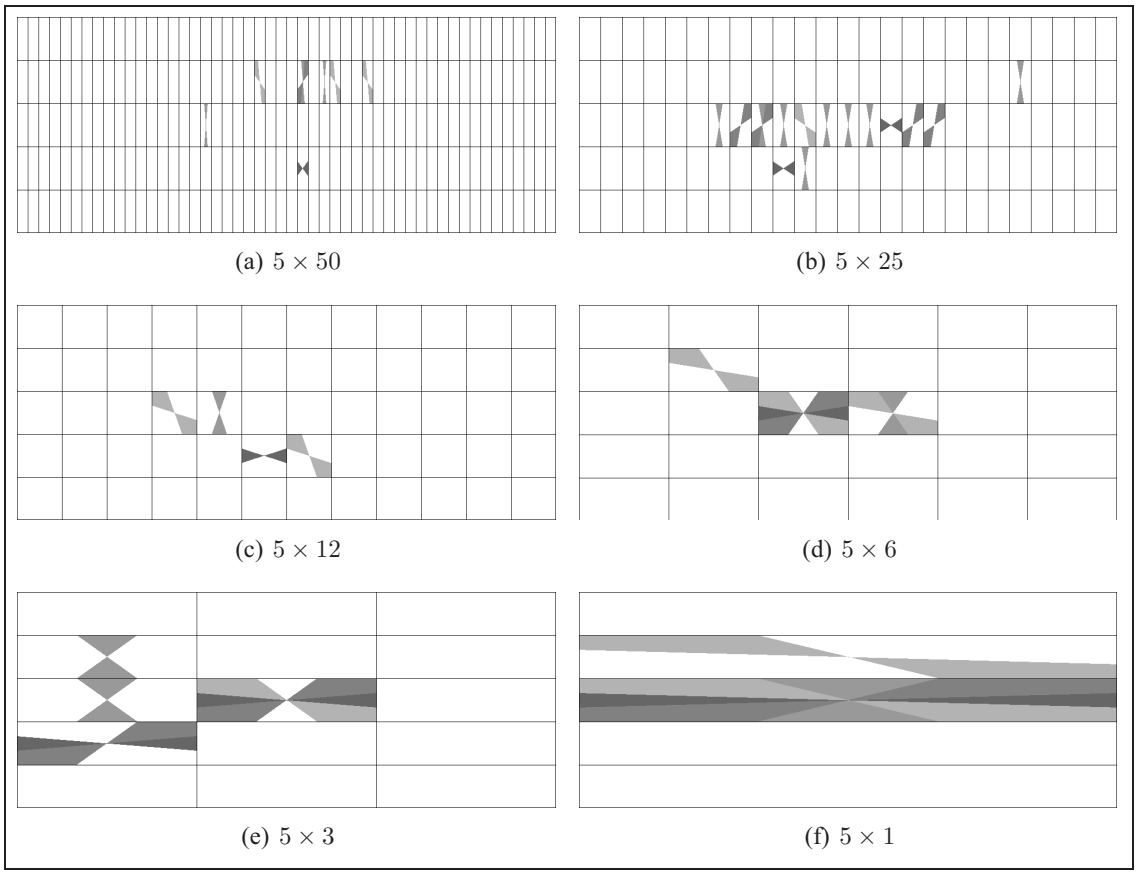

Figure VI.8: Directional PDF selected features for the "5 rows" aspect of the multiscale representation.

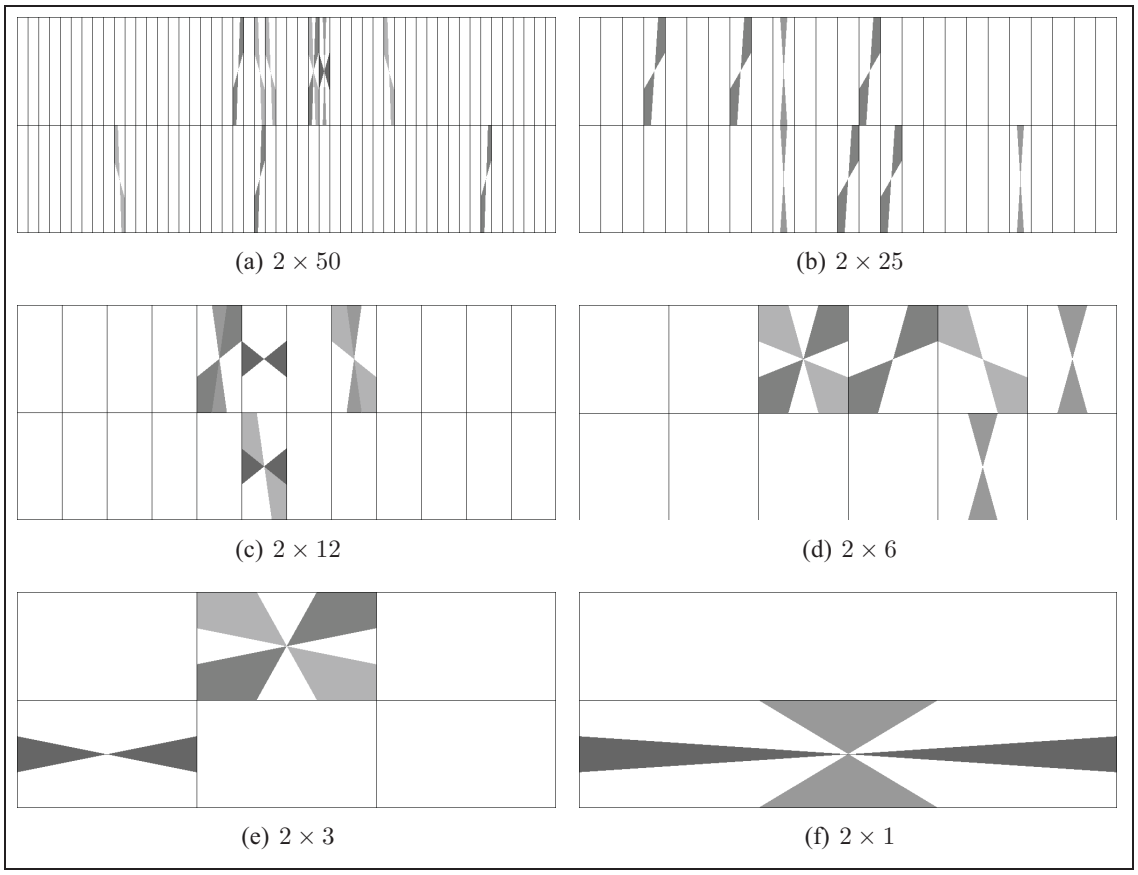

Figure VI.9: Directional PDF selected features for the "2 rows" aspect of the multiscale representation.

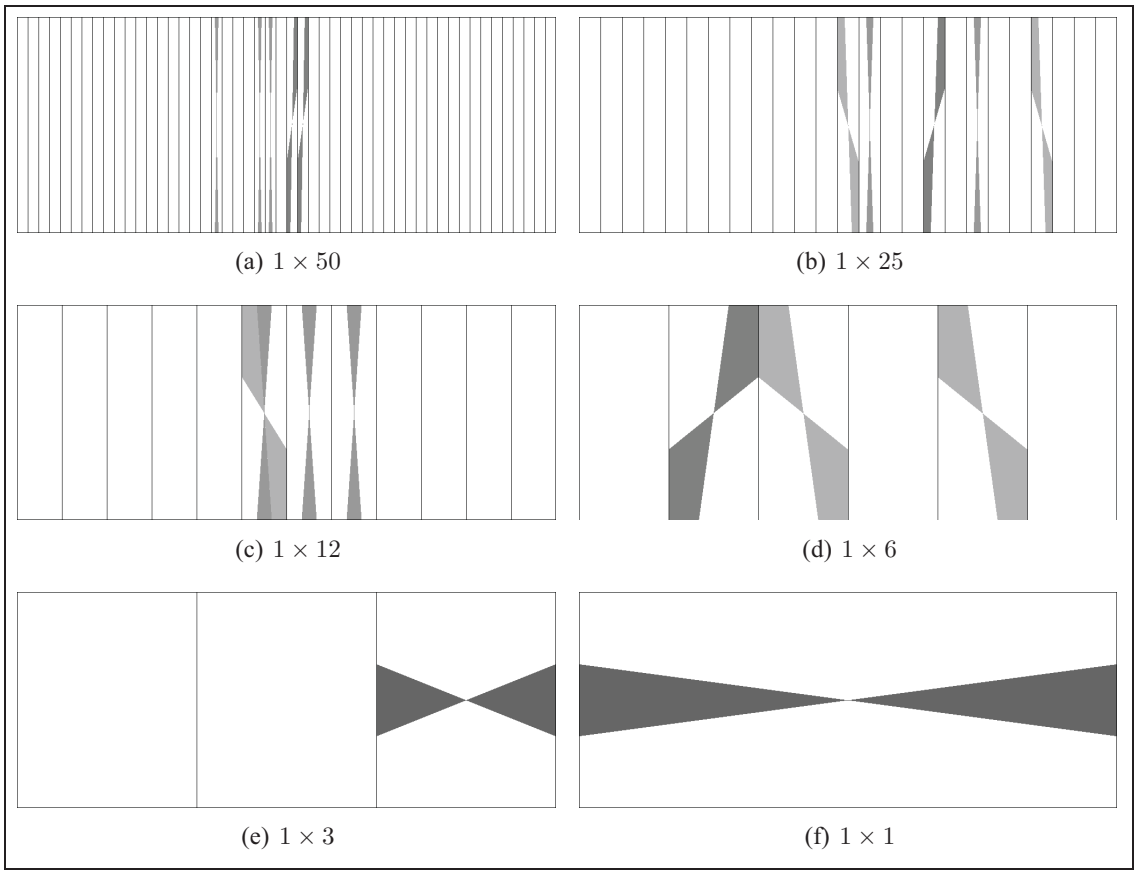

Figure VI.10: Directional PDF selected features for the "1 row" aspect of the multiscale representation.

BIBLIOGRAPHY

Imen A. Abdelghani and Najoua E. Amara. 2006. "Deux approches neuronales pour la vérification hors-ligne de la signature manuscrite". In *15ième congrès francophone sur la reconnaissance de forme et l'intelligence artificielle (RFIA2006)*.

A. I. Al-Shoshan. 2006. "Handwritten signature verification using image invariants and dynamic features". In *2006 International Conference on Computer Graphics, Imaging and Visualisation*, p. 173–176.

M. Ammar. 1991. "Progress in verification of skillfully simulated handwritten signatures". *International Journal of Pattern Recognition and Artificial Intelligence*, vol. 5 no. 1-2, p. 337–351.

M. Ammar, Y. Yoshida, and T. Fukumura. 1985. "Off-line verification of signature based on pressure features". In *Tech. Group Meeting of Pattern Recognition Learn*, p. 134–144.

M. Ammar, Y. Yoshida, and T. Fukumura. 1988. "Off-line pre-processing and verification of signatures". *International Journal of Pattern Recognition and Artificial Intelligence*, vol. 2 no. 4, p. 589–602.

Shingo Ando and Masato Nakajima. 2003. "An active search method for local individual features in off-line signature verification". *Systems and Computers in Japan*, vol. 34 no. 12, p. 64–76.

S. Armand, M. Blumenstein, and V. Muthukkumarasamy. 2006a. "Off-line signature verification based on the modified direction feature". In *18th International Conference on Pattern Recognition (ICPR 2006)*, vol. 4, p. 509–512.

Stephane Armand, Michael Blumenstein, and Vallipuram Muthukkumarasamy. 2006b. "Off-line signature verification using the enhanced modified direction feature and neural-based classification". In *International Joint Conference on Neural Networks*.

Reena Bajaj and Santanu Chaudhury. January 1997. "Signature verification using multiple neural classifiers". *Pattern Recognition*, vol. 30 no. 1, p. 1–7.

H. Baltzakis and N. Papamarkos. 2001. "A new signature verification technique based on a two-stage neural network classifier". *Engineering Applications of Artificial Intelligence*, vol. 14, p. 95–103.

L. Bastos, F. Bortolozzi, R. Sabourin, and C. Kaestner. 1997. "Mathematical modelation of handwritten signatures by conics". *Revista da Sociedade Paranaese de Matemática*, vol. 18, p. 135–146.

L. Batista, D. Rivard, R. Sabourin, E. Granger, and P. Maupin. 2008. "State of the art in off-line signature verification". B. Verma and M. Blumenstein, editors, *Pattern Recognition Technologies and Applications: Recent Advances*, p. 39–62.

D. Bertolini, L. S. Oliveira, E. Justino, and R. Sabourin. January 2010. "Reducing forgeries in writer-independent off-line signature verification through ensemble of classifiers". *Pattern Recognition*, vol. 43 no. 1, p. 387–396.

Christopher J. C. Burges. June 1998. "A tutorial on support vector machines for pattern recognition". *Data Min. Knowl. Discov.*, vol. 2 no. 2, p. 121–167.

H. Cardot, M. Revenu, B. Victorri, and M. Revillet. 1994. "A static signature verification system based on a cooperating neural network architecture". *International Journal on Pattern Recognition and Artificial Intelligence*, vol. 8 no. 3, p. 679–692.

Sung-Hyuk Cha and Sargur Srihari. 2000. "Writer identification: Statistical analysis and dichotomizer". *Advances in Pattern Recognition*, p. 123–132.

A. Chalechale, G. Naghdy, P. Premaratne, and A. Mertins. 2004. "Document image analysis and verification using cursive signature". In *2004 IEEE International Conference on Multimedia and Expo (ICME'04)*, vol. 2, p. 887–890.

Siyuan Chen and Sargur Srihari. 2006. "Combining one- and two-dimensional signal recognition approaches to off-line signature verification". In Kazem Taghva and Xiaofan Lin, editors, *Document Recognition and Retrieval XIII*, vol. 6067. SPIE.

P.C. Chuang. 1977. "Machine verification of handwritten signature image". In *1977 International Conference on Crime Countermeasures–Science and Engineering*, p. 105–109.

J. Coetzer. 2005. "Off-line signature verification". PhD thesis, University of Stellenbosch.

J. Coetzer, B. M. Herbst, and J. A. du Preez. 2004. "Offline signature verification using the discrete radon transform and a hidden markov model". *EURASIP Journal on Applied Signal Processing*, vol. 2004 no. 4, p. 559–571.

Peter S. Deng, Hong-Yuan M. Liao, Chin W. Ho, and Hsiao-Rong Tyan. December 1999. "Wavelet-based off-line handwritten signature verification". *Computer Vision and Image Understanding*, vol. 76 no. 3, p. 173–190.

Peter S. Deng, Li-Jing Jaw, Jau-Hwang Wang, and Cheng-Tan Tung. 2003. "Trace copy forgery detection for handwritten signature verification". In *IEEE 37th Annual 2003 International Carnahan Conference on Security Technology*, p. 450–455.

T. G. Dietterich. June 2000. "Ensemble methods in machine learning". In *First International Workshop on Multiple Classifier Systems*, p. 1–15, Berlin, Germany, June 2000. Springer-Verlag.

C. Domingo and O. Watanabe. December 1999. "Madaboost: a modification of adaboost". *Research Reports on Mathematical and Computing Sciences Series C (Computer Science)*, vol. no. C-138, p. 1–26.

J. Drouhard, R. Sabourin, and M. Godbout. March 1996. "A neural network approach to off-line signature verification using directional pdf". *Pattern Recognition*, vol. 29 no. 3, p. 415–424.

Richard O. Duda, Peter E. Hart, and David G. Stork, 2001. *Pattern Classification*. John Wiley & Sons, Inc.

A. El-Yacoubi, E. J. R. Justino, R. Sabourin, and F. Bortolozzi. 2000. "Off-line signature verification using hmms and cross-validation". In *Proceedings of the 2000 IEEE Signal Processing Society Workshop Neural Networks for Signal Processing X*, vol. 2, p. 859–868 vol.2.

E. Fadhel and P. Bhattacharyya. 1999. "Application of a steerable wavelet transform using neural network for signature verification". *Pattern Analysis and Applications*, vol. 2, p. 184–195.

M. C. Fairhurst. 1997. "Signature verification revisited: promoting practical exploitation of biometric technology". *Electronics & Communication Engineering Journal*, vol. 9 no. 6, p. 273–280.

B. Fang, Y. Wang, C. Leung, and K. Tse. 2001. "Off-line signature verification by the analysis of cursive strokes". *International Journal of Pattern Recognition and Artificial Intelligence*, vol. 15 no. 4, p. 659–673.

B. Fang, C. H. Leung, Y. Y. Tang, P. C. K. Kwok, K. W. Tse, and Y. K. Wong. 2002. "Off-fline signature verification with generated training samples". *IEE Proceedings of Vision, Image and Signal Processing*, vol. 149 no. 2, p. 85–90.

B. Fang, C. Leung, Y. Tang, K. Tse, P. Kwok, and Y. Wong. January 2003. "Off-line signature verification by the tracking of feature and stroke positions". *Pattern Recognition*, vol. 36 no. 1, p. 91–101.

Bin Fang and Yuan Y. Tang. 2005. "Improved class statistics estimation for sparse data problems in offline signature verification". *IEEE Transactions on Systems, Man and Cybernetics, Part C*, vol. 35 no. 3, p. 276–286.

J. B. Fasquel and M. Bruynooghe. March 2004. "A hybrid opto-electronic method for fast off-line handwritten signature verification". *International Journal on Document Analysis and Recognition (IJDAR)*, vol. 7 no. 1, p. 56–68.

Tom Fawcett. June 2006. “An introduction to roc analysis”. *Pattern Recognition Letters*, vol. 27 no. 8, p. 861–874.

M. Ferrer, J. Alonso, and C. Travieso. 2005. “Offline geometric parameters for automatic signature verification using fixed-point arithmetic”. *IEEE Transactions on Pattern Analysis and Machine Intelligence*, vol. 27 no. 6, p. 993–997.

J. Fierrez-Aguilar, N. Alonso-Hermira, G. Moreno-Marquez, and J. Ortega-Garcia. 2004. “An off-line signature verification system based on fusion of local and global information”. In D. Maltoni and A. K. Jain, editors, *Biometric Authentication, Proceedings Lecture Notes In Computer Science 3087: 295-306 2004*, p. 295–306. Springer-Verlag Berlin, Heidelberger Platz 3, D-14197 Berlin, Germany.

Katrin Franke, Yu-Nong Zhang, and Mario Koppen. 2002. “Static signature verification employing a kosko-neuro-fuzzy approach”. In *Proceedings International Conference on Fuzzy Systems - Advances in Soft Computing (AFSS 2002)*, vol. 2275, p. 185–190. Springer Berlin / Heidelberg.

Y. Freund and R. E. Schapire. July 1996. “Experiments with a new boosting algorithm”. In *Proceedings of Thirteenth International Conference on Machine Learning*, San Francisco, CA, USA, July 1996. Eur. Coordinating Committee for Artificial Intelligence; Italian Assoc. Artificial Intelligence, Morgan Kaufmann Publishers.

Yoav Freund. June 2001. “An adaptive version of the boost by majority algorithm”. *Machine Learning*, vol. 43 no. 3, p. 293–318.

Yoav Freund and Robert E. Schapire. August 1997. “A decision-theoretic generalization of on-line learning and an application to boosting,”. *Journal of Computer and System Sciences*, vol. 55 no. 1, p. 119–139.

E. Frias-Martinez, A. Sanchez, and J. Velez. September 2006. “Support vector machines versus multi-layer perceptrons for efficient off-line signature recognition”. *Engineering Applications of Artificial Intelligence*, vol. 19 no. 6, p. 693–704.

Jerome Friedman, Trevor Hastie, and Robert Tibshirani. 2000. "Additive logistic regression: a statistical view of boosting (with discussion and a rejoinder by the authors)". *Annals of Statistics*, vol. 28 no. 2, p. 337–407.

R. Gonzalez and R. Woods, editors, 2002. *Digital Image Processing*. Prentice Hall, 2nd edition.

F. Griess and A. Jain. 2002. "On-line signature verification". *Pattern Recognition*, vol. 35, p. 2963–2972.

J. K. Guo, D. Doermann, and A. Rosenfeld. 2000. "Off-line skilled forgery detection using stroke and sub-stroke properties". In *15th International Conference on Pattern Recognition*, vol. 2, p. 355–358 vol.2.

Madasu Hanmandlu, Mohd Yusof, and Vamsi K. Madasu. March 2005. "Off-line signature verification and forgery detection using fuzzy modeling". *Pattern Recognition*, vol. 38 no. 3, p. 341–356.

W. R. Harrison, 1981. *Suspect Documents, Their Scientific Examination*. Nelso-Hall publishers, Chicago.

S. Haykin, 1998. *Neural Networks: A Comprehensive Foundation*. Prentice Hall, 2 edition.

C. A. R. Hoare, 1989. *Essays in computing science*. Prentice-Hall, Inc., Upper Saddle River, NJ, USA. ISBN 0-13-284027-8.

K. Huang and H. Yan. 2002. "Off-line signature verification using structural feature correspondence". *Pattern Recognition*, vol. 35, p. 2467–2477.

Kai Huang and Hong Yan. January 1997. "Off-line signature verification based on geometric feature extraction and neural network classification". *Pattern Recognition*, vol. 30 no. 1, p. 9–17.

W. Iba and P. Langley. 1992. "Induction of one-level decision trees". In *Proceedings of the Ninth International Machine Learning Conference*. Morgan Kaufmann.

Juan J. Igarza, Inmaculada Hernaez, and Inaki Goirizelaia. 2005. “Static signature recognition based on left-to-right hidden markov models”. *Journal of Electronic Imaging*, vol. 14 no. 4.

D. Impedovo and G. Pirlo. 2008. “Automatic signature verification: The state of the art”. *IEEE Transactions on Systems, Man, and Cybernetics, Part C: Applications and Reviews*, vol. 38 no. 5, p. 609–635.

A. K. Jain, A. Ross, and S. Prabhakar. 2004. “An introduction to biometric recognition”. *IEEE Transactions on Circuits and Systems for Video Technology*, vol. 14 no. 1, p. 4–20.

A. K. Jain, A. Ross, and S. Pankanti. 2006. “Biometrics: a tool for information security”. *IEEE Transactions on Information Forensics and Security*, vol. 1 no. 2, p. 125–143.

E. Justino. 2001. “O grafismo e os modelos escondidos de markov na verificação automática de assinaturas”. PhD thesis, PUC-PR, Brasil.

Edson Justino, Flavio Bortolozzi, and Robert Sabourin. July 2005. “A comparison of svm and hmm classifiers in the off-line signature verification”. *Pattern Recognition Letters*, vol. 26 no. 9, p. 1377–1385.

Meenakshi K. Kalera, Sargur Srihari, and Aihua Xu. 2004a. “Offline signature verification and identification using distance statistics”. *International Journal of Pattern Recognition and Artificial Intelligence*, vol. 18 no. 7, p. 1339–1360.

Meenakshi K. Kalera, Sargur Srihari, and Aihua Xu. 2004b. “Offline signature verification and identification using distance statistics”. *International Journal of Pattern Recognition and Artificial Intelligence*, vol. 18 no. 7, p. 1339–1360.

Alisher A. Kholmatov, 2003. “Biometric identity verification using on-line and off-line signature verification”. Master’s thesis, Sabanci University, Istanbul, Turkey.

M. Kudo. January 2000. “Comparison of algorithms that select features for pattern classifiers”. *Pattern Recognition*, vol. 33 no. 1, p. 25–41.

Kai K. Lau, Pong C. Yuen, and Yuan Y. Tang. 2005. "Universal writing model for recovery of writing sequence of static handwriting images". *International Journal of Pattern Recognition and Artificial Intelligence*, vol. 19 no. 5, p. 603–630.

F. Leclerc and R. Plamondon. 1994. "Automatic signature verification: the state of the art - 1989-1993". *International Journal of Pattern Recognition and Artificial Intelligence*, vol. 8 no. 3, p. 643–660.

Luan L. Lee and M. G. Lizarraga. 1996. "An off-line method for human signature verification". In *13th International Conference on Pattern Recognition*, vol. 3, p. 195–198 vol.3.

Hairong Lv, Wenyuan Wang, Chong Wang, and Qing Zhuo. November 2005. "Off-line chinese signature verification based on support vector machines". *Pattern Recognition Letters*, vol. 26 no. 15, p. 2390–2399.

V. K. Madasu. April 2004. "Off-line signature verification and bank cheque processing". PhD thesis, University of Queensland.

Vamsi K. Madasu, Madasu Hanmandlu, and Shweta Madasu. 2003. "Neuro-fuzzy approaches to signature verification". In *2nd National Conference on Document Analysis and Recognition (NCDAR-2003)*.

L. E. Martinez, C. M. Travieso, J. B. Alonso, and M. A. Ferrer. 2004. "Parameterization of a forgery handwritten signature verification system using svm". In *Security Technology, 2004. 38th Annual 2004 International Carnahan Conference on*, p. 193–196.

D. Mighell, T. Wilkinson, and J. Goodman, 1989. *Advances in Neural Information Processing Systems I.* Morgan Kaufmann, San Mateo, CA.

N. Murshed, F. Bortolozzi, and R. Sabourin. 1995. "Off-line signature verification using fuzzy artmap neural networks". In *IEEE International Conference on Neural Networks*, p. 2179–2184.

R. Nagel and A. Rosenfeld. 1977. "Computer detection of freehand forgeries". *IEEE Transactions on Computers*, vol. 26, p. 895–905.

Masayuki Nakamura, Hiroki Nomiya, and Kuniaki Uehara. May 2004. "Improvement of boosting algorithm by modifying the weighting rule". *Annals of Mathematics and Artificial Intelligence*, vol. 41 no. 1, p. 95–109.

E. M. Nel, J. A. du Preez, and B. M. Herbst. 2005. "Estimating the pen trajectories of static signatures using hidden markov models". *IEEE Transactions on Pattern Analysis and Machine Intelligence*, vol. 27 no. 11, p. 1733–1746.

W. Nemcek and W. Lin. 1974. "Experimental investigation of automatic signature verification". *IEEE Transactions on Pattern Analysis and Machine Intelligence*, vol. 4, p. 121–126.

L. Oliveira, E. J. R. Justino, C. O. A. Freitas, and R. Sabourin. 2005. "The graphology applied to signature verification". In *12th Conference of the International Graphonomics Society (IGS2005)*, p. 178–182.

Luiz S. Oliveira, Edson Justino, and Robert Sabourin. 2007. "Off-line signature verification using writer-independent approach". In *International Joint Conference on Neural Networks*.

N. Otsu. January 1979. "A threshold selection method from gray-level histograms". *IEEE Transactions on Systems, Man and Cybernetics*, vol. 9 no. 1, p. 62–66.

Cemil Oz. 2005. "Signature recognition and verification with artificial neural network using moment invariant method". In *Advances in Neural Networks - ISNN 2005. Second International Symposium on Neural Networks. Proceedings, Part II*, vol. 3497 of *Lecture Notes in Computer Science*, p. 195–202. Springer Berlin / Heidelberg.

E. Ozgunduz, T. Senturk, and M. E. Karsligil. September 2005. "Off-line signature verification and recognition by support vector machine". In *13th European Signal Processing Conference (EUSIPCO 2005)*.

A. Perez-Hernandez, A. Sanchez, and J. F. Velez. 2004. "Simplified stroke-based approach for off-line signature recognition". In *2nd COST Workshop on Biometrics on the Internet:*

Fundamentals, Advances and Applications, p. 89–94, Ed. Univ. Vigo, 2004. C. Garcia et al.

R. Plamondon, 1994. *Progress in Automatic Signature Verification*. Word Scientific, Singapore.

R. Plamondon and G. Lorette. 1989. "Automatic signature verification and writer identification - the state of the art". *Pattern Recognition*, vol. 22, p. 107–131.

Salil Prabhakar, Josef Kittler, Davide Maltoni, Lawrence O'Gorman, and Tieniu Tan. 2007. "Introduction to the special issue on biometrics: Progress and directions". *IEEE Transactions on Pattern Analysis and Machine Intelligence*, vol. 29 no. 4, p. 513–516.

Y. Qi and B. Hunt. 1994. "Signature verification using global and grid features". *Pattern Recognition*, vol. 27 no. 12, p. 1621–1629.

C. Quek and R. Zhou. 2002. "Antiforgery: A novel pseudo product based fuzzy neural network driven signature verification system". *Pattern Recognition Letters*, vol. 23, p. 1795–1816.

L. Rabiner. 1989. "A tutorial on hidden markov models and selected applications in speech recognition". *IEEE*, vol. 77 no. 2, p. 257–286.

V. Ramesh and M. Murty. February 1999. "Off-line signature verification using genetically optimized weighted features". *Pattern Recognition*, vol. 32 no. 2, p. 217–233.

G. Rätsch, T. Onoda, and K. R. Müller. March 2001. "Soft margins for adaboost". *Machine Learning*, vol. 42 no. 3, p. 287–320.

Gunnar Rätsch and Manfred K. Warmuth. December 2005. "Efficient margin maximizing with boosting". *Journal of Machine Learning Research*, vol. 6, p. 2131–2152.

D. B. Redpath and K. Lebart. 2005. "Observations on boosting feature selection". In *6th International Workshop on Multiple Classifier Systems, MCS 2005*, p. 32–41.

G. Rigoll and A. Kosmala. 1998. “A systematic comparison between on-line and off-line methods for signature verification with hidden markov models”. In *International Conference on Pattern Recognition*, vol. 2, p. 1755–1757.

D. Rumelhart, G. Hinton, and R. William, 1986. *Learning Internal Representations by Error Propagation*, vol. 1. MIT Press.

R. Sabourin and J. Drouhard. 1992. “Off-line signature verification using directional pdf and neural networks”. In *International Conference on Pattern Recognition*, p. 321–325.

R. Sabourin and G. Genest. 1994. “An extended-shadow-code based approach for off-line signature verification. i. evaluation of the bar mask definition”. In *12th IAPR International Conference on Pattern Recognition*, vol. 2, p. 450–453 vol.2.

R. Sabourin and G. Genest. 1995. “An extended-shadow-code based approach for off-line signature verification. ii. evaluation of several multi-classifier combination strategies”. In *Third International Conference on Document Analysis and Recognition*, vol. 1, p. 197–201 vol.1.

R. Sabourin and R. Plamondon. 1986. “Preprocessing of handwritten signatures form image gradient analysis”. In *8th International Conference on Pattern Recognition*, p. 576–579.

R. Sabourin, M. Cheriet, and G. Genest. 1993. “An extended-shadow-code based approach for off-line signature verification”. In *Second International Conference on Document Analysis and Recognition*, p. 1–5.

R. Sabourin, R. Plamondon, and L. Beaumier. 1994. “Structural interpretation of handwritten signature images”. *International Journal of Pattern Recognition and Artificial Intelligence*, vol. 8 no. 3, p. 709–748.

R. Sabourin, G. Genest, and F. Preteux. 1996. “Pattern spectrum as a local shape factor for off-line signature verification”. In *Pattern Recognition, 1996., Proceedings of the 13th International Conference on*, vol. 3, p. 43–48 vol.3.

R. Sabourin, J. P. Drouhard, and E. S. Wah. 1997a. "Shape matrices as a mixed shape factor for off-line signature verification". In *Fourth International Conference on Document Analysis and Recognition*, vol. 2, p. 661–665 vol.2.

R. Sabourin, G. Genest, and F. J. Preteux. 1997b. "Off-line signature verification by local granulometric size distributions". *IEEE Transactions on Pattern Analysis and Machine Intelligence*, vol. 19 no. 9, p. 976–988.

C. Sansone and M. Vento. 2000. "Signature verification: Increasing performance by a multi-stage system". *Pattern Analysis and Applications*, vol. 3, p. 169–181.

C. Santos, E. J. R. Justino, F. Bortolozzi, and R. Sabourin. 2004. "An off-line signature verification method based on the questioned document expert's approach and a neural network classifier". In *Ninth International Workshop on Frontiers in Handwriting Recognition*, p. 498–502.

Robert E. Schapire. 2003. "The boosting approach to machine learning: An overview.", chapter 8. Springer.

B. Scholkopf, J. Platt, J. Taylor, A. Smola, and R. Williamson. 2001. "Estimating the support of a high dimensional distribution". *Neural Computation*, vol. 13, p. 1443–1471.

Canan Senol and Tulay Yildirim. 2005. "Signature verification using conic section function neural network". In *20th International Symposium on Computer and Information Sciences (ISCIS 2005)*, p. 524–532.

Rocco A. Servedio. September 2003. "Smooth boosting and learning with malicious noise". *Journal of Machine Learning Research*, vol. 4, p. 633–648.

S. N. Srihari, Aihua Xu, and M. K. Kalera. 2004a. "Learning strategies and classification methods for off-line signature verification". In *Ninth International Workshop on Frontiers in Handwriting Recognition*, p. 161–166.

S. N. Srihari, Aihua Xu, and M. K. Kalera. 2004b. “Learning strategies and classification methods for off-line signature verification”. In *Ninth International Workshop on Frontiers in Handwriting Recognition*, p. 161–166.

Yuan Y. Tang, Yu Tao, and Ernest C. Lam. May 2002. “New method for feature extraction based on fractal behavior”. *Pattern Recognition*, vol. 35 no. 5, p. 1071–1081.

Kinh Tieu and Paul Viola. January 2004. “Boosting image retrieval”. *International Journal of Computer Vision*, vol. 56 no. 1, p. 17–36.

V. Vapnik, editor, 1999. *The Nature of Statistical Learning Theory*. Springer-Verlag, New York, 2nd edition.

J. Vélez, Á. Sánchez, and A. Moreno. 2003. “Robust off-line signature verification using compression networks and positional cuttings”. In *IEEE Workshop on Neural Networks for Signal Processing*, p. 627–636.

Zuo Wen-Ming, Li Shao-Fa, and Zeng Xian-Gui. 2004. “A hybrid scheme for off-line chinese signature verification”. In *Cybernetics and Intelligent Systems, 2004 IEEE Conference on*, vol. 2, p. 1402–1405.

T. Wilkinson and J. Goodman. 1990. “Slope histogram detection of forged handwritten signatures”. In *SPIE - International Society for Optical Engineering*, p. 293–304.

Xuhong Xiao and Graham Leedham. May 2002. “Signature verification using a modified bayesian network”. *Pattern Recognition*, vol. 35 no. 5, p. 983–995.

Y. Xuhua, T. Furuhashi, K. Obata, and Y. Uchikawa. 1996. “Selection of features for signature verification using the genetic algorithm”. *Computers & Industrial Engineering*, vol. 30 no. 4, p. 1037–1045.

Xiufen Ye, Weiping Hou, and Weixing Feng. 2005. “Off-line handwritten signature verification with inflections feature”. In *IEEE International Conference on Mechatronics and Automation*, vol. 2, p. 787–792.

Xinge You, Bin Fang, Zhenyu He, and Yuanyan Tang. 2005. "Similarity measurement for off-line signature verification". In *International Conference on Intelligent Computing, ICIC 2005*, p. 272–281.